Loughborough University

Loughborough University
Institutional Repository

Mechanisms of thermoplastics to metal adhesion for applications in electronics manufacture

This item was submitted to Loughborough University's Institutional Repository by the/an author.

Additional Information:

- A Doctoral Thesis. Submitted in partial fulfillment of the requirements for the award of Doctor of Philosophy of Loughborough University.

Metadata Record: https://dspace.lboro.ac.uk/2134/8531

Publisher: © Hrushikesh Abhyankar

Please cite the published version.

Loughborough University

This item was submitted to Loughborough's Institutional Repository (https://dspace.lboro.ac.uk/) by the author and is made available under the following Creative Commons Licence conditions.

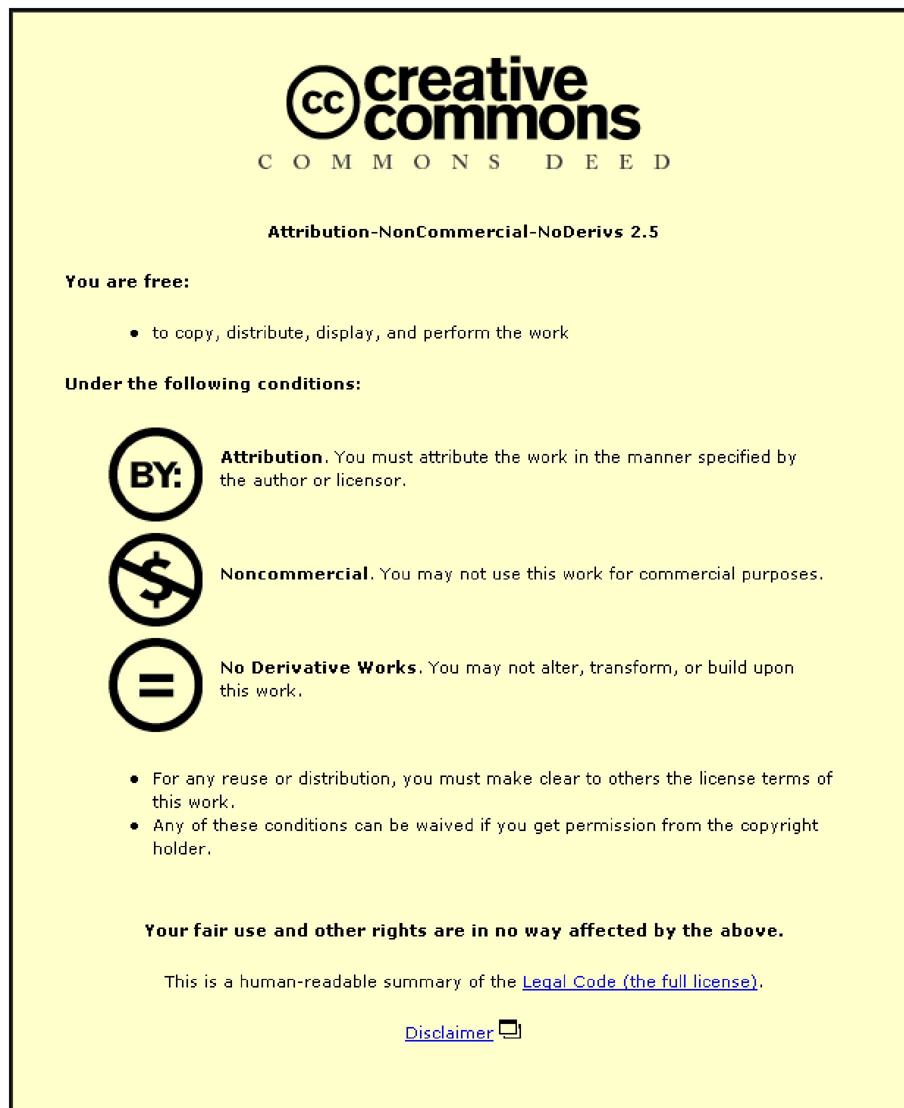

For the full text of this licence, please go to:
http://creativecommons.org/licenses/by-nc-nd/2.5/

TABLE OF CONTENTS

1 INTRODUCTION 1

1.1 End of Life Issues in Electronics 2
1.1.1 End of Life (EOL) and Waste from Electrical and Electronic Equipment (WEEE) Directive 3

1.2 Approaches to Improve the End of Life Profile of PCBs 4

1.3 Manufacturing of Electronics by Overmoulding: Substrateless Packaging 6
1.3.1 Developmental Challenges for Substrateless Packaging 9

1.4 Aim of the Study 10

2 BACKGROUND AND LITERATURE 13

2.1 Forces of Adhesion 13
2.1.1 Primary forces (Short range interactions) 14
2.1.2 Secondary forces (Long range interactions) 14
2.1.3 Hydrogen bonding 15
2.1.4 Van der Waals Forces 15
2.1.5 Surface energy and surface tension 16
2.1.6 Wetting 17
2.1.7 Work of Adhesion 19
2.1.8 Acid-base interactions 20

2.2 Theories of Adhesion 21
2.2.1 Mechanical Interlocking 21
2.2.2 Adsorption theory 22
2.2.3 Chemical Bonding theory 22
2.2.4 Diffusion theory 23
2.2.5 Theory of Weak Boundary layer (WBL) 23
2.2.6 Electronic/Electrostatic theory 25

2.3 Injection Moulding 26
2.3.1 Overview 26
2.3.2 Types of Injection Moulding Machines (IMM) 27
2.3.3 Part descriptions 28
2.3.4 Process description 30
2.3.5 Sequence of Operations 30
2.3.6 Key Parameters Involved in IM 31

2.4 Multi Material Injection Moulding (MMIM) 33
2.4.1 Process Description for Overmoulding/Insert Moulding 35
2.4.2 *Sequence of Operations*: Overmoulding/insert moulding 36
2.4.3 Key parameters 36

2.5 Insert Moulding and Adhesion 38

2.6 Gap in the Literature 38

3 METHODOLOGY 43

3.1 Introduction 43

3.2 Methodology 45

4 MATERIALS AND PROPERTIES 48

4.1 Introduction 48

4.2 Background 49
4.2.1 Electronic Assemblies 49
4.2.2 Material Properties expected from PCBs 50
4.2.3 IPC standard 4101B 51

4.3 Uses of Thermoplastics for Electronic Interconnection 51

4.4 Choice of Materials for This Study 53
4.4.1 Overmould 53
4.4.2 Electronic Component Materials 53

4.5 Selected Thermoplastics and Their Properties 54

4.6 Selected Insert Material 55

5 ATOMIC FORCE MICROSCOPY 57

5.1 The Atomic Force Microscope 58
5.1.1 Imaging Modes 59

5.2 Force-distance Curve 60

5.3 Functionalising the AFM Tip 63

5.4 Study of Adhesion Using Force-distance Curves 64

5.5 Methodology 65
5.5.1 Materials and Experimental Apparatus 67
5.5.1.1 AFM 67
5.5.1.2 Tin Powder 67
5.5.1.3 Polymer Samples 67
5.5.1.4 AFM Probes 68
5.5.1.5 Dual Beam Focussed Ion Beam Microscope 68
5.5.2 Cantilever Deflection Measurements 70
5.5.3 Adhesive Attachment of the Particle to the Tip 71
5.5.3.1 Method 71

5.5.3.2 Results 74
5.5.4 Metallurgical Bonding of the Particle to the Tip 77
5.5.4.1 Method 77
5.5.4.2 Design of Experiment 78

5.6 Results 82

5.7 Discussion 92

5.8 Conclusions 94

6 CONTACT ANGLE ANALYSIS 96

6.1 Introduction 96

6.2 Theory 97

6.3 Review of the Literature 98
6.3.1 Techniques for Contact Angle Measurement at High Temperature 100
6.3.1.1 Immersion - Emersion 100
6.3.1.2 Wetting Balance Test 101

6.4 Methodology 102
6.4.1 Materials and Experiment apparatus 102
6.4.1.1 Tin Foil 102
6.4.1.2 Thermoplastics 102
6.4.1.3 Contact angle measurement 103
6.4.1.4 Wetting Balance tester 103
6.4.2 Immersion-Emersion 103
6.4.3 Wetting Balance Technique 104
6.4.3.1 Description of the Set-up 105
6.4.3.2 Experimental procedure 105
6.4.4 Sessile Drop Analysis on Heated Substrate 107
6.4.4.1 Description of the Set-up 107
6.4.4.2 Experimental Procedure 107
6.4.5 Experimental Technique Adopted 108
6.4.5.1 Description of the Set-up 108
6.4.5.2 Experimental details 109

6.5 Results 110

6.6 Discussion 115

6.7 Conclusions 120

7 MECHANICAL STRENGTH TEST: PULL OUT TEST 122

7.1 Introduction 122

7.2 Mechanical Strength Tests for Adhesion 123

7.2.1 Shear Tests 123
7.2.2 Peel Tests 124
7.2.3 Tensile Pull Tests 125

7.3 Mechanical Strength Testing of Adhesion in Insert Moulding 128

7.4 Methodology 129
7.4.1 Materials and experimental Apparatus 130
7.4.1.1 Thermoplastics 130
7.4.1.2 Insert materials 130
7.4.1.3 Injection Moulding Machine and Mould Tool Manufacture 130
7.4.2 Lap Shear Test Method 132
7.4.3 Block Shear Test / Peel Test 135
7.4.4 Shear Pull Test 136
7.4.4.1 Insert Temperature 138
7.4.4.2 Experimental Procedure 140

7.5 Results 141

7.6 Discussion 145

7.7 Conclusions 151

8 MOLDFLOW ANALYSIS 152

8.1 Introduction 152

8.2 Reports of Use of FEA for Insert Moulding Analysis 153

8.3 Moldflow 154
8.3.1 Workflow Sequence for Moldflow Analysis 154

8.4 Experimental Method 157
8.4.1 Meshing Procedure in Moldflow for Insert Moulding Analysis 157
8.4.2 Selection of Model Parameters 162

8.5 Results 165
8.5.1 Temperature at the Flow Front 165
8.5.1.1 Discussion 169
8.5.2 Injection Pressure and Temperature 169
8.5.2.1 Discussion 172
8.5.3 Volumetric Shrinkage 173
8.5.3.1 Discussion 174

8.6 Conclusions 178

9 DISCUSSION 179

9.1 Introduction 179

9.2 AFM Force-Distance and Pull Test 180

9.3 Wetting and Pull Test 182

9.4 Moldflow Analysis and Pull Test 184

9.5 General Discussion 185

9.6 Selection of Materials 187

9.7 Selection of Materials for Substrateless Packaging 188

10 CONCLUSIONS 190

10.1 Future Work 195

11 REFERENCES 197

12 APPENDIX-1 203

13 APPENDIX – 2 206

Table of Figures

FIGURE 1: MOUNTING OF ELECTRONIC COMPONENTS ON ADHESIVE FILM 8

FIGURE 2: PLACEMENT OF LOADED CARRIER FILM IN MOULD TOOL. OVERMOULDING OF FILM AND COMPONENTS WITH POLYMERS 8

FIGURE 3: REMOVAL OF MOULDING FROM MOULD TOOL 8

FIGURE 4: REMOVAL OF CARRIER FILM, REVEALING COMPONENT METALLISATION ON UNDERSIDE OF MOULDING. 8

FIGURE 5: DEPOSITION OF INTERCONNECTION PATTERN ON UNDERSIDE OF MOULDING 8

FIGURE 6: A DEMONSTRATOR REPRESENTING STAGE D OF THE PROCESS 9

FIGURE 7: GAPS OBSERVED IN INJECTION MOULDING TRIALS OF THE SUBSTRATELESS PACKAGING PROCESS 10

FIGURE 8: WETTING AND DE-WETTING 18

FIGURE 9: TYPICAL CAUSES OF WEAK BOUNDARY LAYER [12] 25

FIGURE 10: BASIC STAGES OF IM PROCESS 26

FIGURE 11: PART DESCRIPTION WITH GENERAL LOCATION ON RECIPROCATING SCREW IM MACHINE [16] 29

FIGURE 12: STAGES INVOLVED IN IM 30

FIGURE 13: INJECTION, COOLING, EJECTION AND OTHER OPERATIONS WITH REFERENCE TO TIMEFRAME 31

FIGURE 14: PROCESSING OF POLYMERS IN IM, VISCOSITY VS. TEMPERATURE. 32

FIGURE 15: MULTI MATERIAL INJECTION MOULDING PROCESSES [19] 33

FIGURE 16: STAGES INVOLVED IN OVERMOULDING 35

FIGURE 17: VARIOUS OPERATIONS WITH REFERENCE TO TIMEFRAME 36

FIGURE 18: SET UP OF THE AFM 58

FIGURE 19: A TYPICAL TIP-SAMPLE SYSTEM 60

FIGURE 20: TYPICAL FORCE CURVE WITH LABELLING CORRESPONDING TO TIP-SAMPLE INTERACTION POINTS 61

FIGURE 21: AFM WITH MANUAL Z AXIS CONTROL USED FOR GLUING PARTICLES TO THE PROBE 72

FIGURE 22: (A) THE HOLDER FOR THE PROBE (B) SCHEMATIC 72

FIGURE 23: THE RELATIVE POSITION OF THE CANTILEVER WITH RESPECT TO THE PARTICLE FOR ATTACHMENT BY GLUE 73

FIGURE 24: THE UV LIGHT CHAMBER 74

FIGURE 25: OUT OF SCALE RESULTS FOR THE DNP-10 TIPS 75

FIGURE 26: ILLUSTRATION OF THE GLUED PARTICLES ON DNP 10 TIP AND TESP TIP 76

FIGURE 27: VACUUM CHAMBER OF THE DUAL BEAM MICROSCOPE 79

FIGURE 28: SHARPENED TIP OF THE MICROMANIPULATOR 79

FIGURE 29: SIZE OF THE SELECTED PARTICLE 79

FIGURE 30: PLATINUM DEPOSITION TO JOIN MICROMANIPULATOR TO THE PARTICLE 79

FIGURE 31: MICROMANIPULATOR WITH PARTICLE ATTACHED MOVING TOWARDS THE TIP OF THE PROBE 79

FIGURE 32: MICROMANIPULATOR DETACHMENT 79

FIGURE 33: CANTILEVER DEFLECTION VS Z DEFLECTION FOR TIN FUNCTIONALISED TESP PROBE AND PA 6 87

FIGURE 34: CANTILEVER DEFLECTION VS Z DEFLECTION SN FUNCTIONALISED TESP AND PS. AXIS SCALES AS FOR FIG. 33 88

FIGURE 35: CANTILEVER DEFLECTION VS Z DEFLECTION SN FUNCTIONALISED TESP PROBE AND PC. AXIS SCALES AS FOR FIG. 33 88

FIGURE 36: CANTILEVER DEFLECTION VS Z DEFLECTION SN FUNCTIONALISED TESP PROBE AND PBT. AXIS SCALES AS FOR FIG. 33 88

FIGURE 37: CANTILEVER DEFLECTION VS Z DEFLECTION SN FUNCTIONALISED TESP PROBE AND ABS. AXIS SCALES AS FOR FIG. 33 88

FIGURE 38: CANTILEVER DEFLECTION VS Z DEFLECTION SN FUNCTIONALISED TESP PROBE AND PMMA. AXIS SCALES AS FOR FIG. 33 88

FIGURE 39: CANTILEVER DEFLECTION RATIO OBTAINED FROM AFM FOR CANTILEVER 1 89

FIGURE 40: CANTILEVER DEFLECTION RATIO OBTAINED FROM AFM FOR CANTILEVER 2 90

FIGURE 41: CANTILEVER DEFLECTION RATIO OBTAINED FROM AFM FOR CANTILEVER 3 91

FIGURE 42: TYPICAL SOLID-LIQUID-VAPOUR SYSTEM. Θ IS THE CONTACT ANGLE. 97

FIGURE 43: TYPICAL IMMERSION EMERSION SET-UP. 101

FIGURE 44: THE IMMERSION-EMERSION TECHNIQUE FOR PMMA. 104

FIGURE 45: SCHEMATIC OF THE MODIFIED WETTING BALANCE TESTER. 105

FIGURE 46: SCHEMATIC OF THE RE-MODIFIED WETTING BALANCE TESTER................................ 106

FIGURE 47: HEATED CHAMBER AND HEATED SYRINGE SET-UP FOR SESSILE DROP EXPERIMENT. 109

FIGURE 48: HEATED CHAMBER SET-UP FOR SESSILE DROP EXPERIMENT.................................... 109

FIGURE 49: CONTACT ANGLE OF PA 6 ON TIN FOIL WITH HEATED CHAMBER AT 210°C............ 113

FIGURE 50: CONTACT ANGLE OF PA 6 ON TIN FOIL WITH HEATED CHAMBER AT 220°C............ 113

FIGURE 51: CONTACT ANGLE OF PA 6 ON TIN FOIL WITH HEATED CHAMBER AT 230°C............ 113

FIGURE 52: CONTACT ANGLE OF PA 6 ON TIN FOIL WITH HEATED CHAMBER AT 240°C............ 113

FIGURE 53: CONTACT ANGLE VS. TEMPERATURE FOR MOLTEN THERMOPLASTIC ON TIN FOIL 114

FIGURE 54: LAP SHEAR TEST 126

FIGURE 55: THICK ADHEREND LAP SHEAR TEST 126

FIGURE 56: DOUBLE LAP SHEAR TEST 126

FIGURE 57: PEEL TEST SET UPS 127

FIGURE 58: TENSILE TEST SET UPS 127

FIGURE 59: VERTICAL INJECTION MOULDING MACHINE SET UP 131

FIGURE 60: MOULD PLATE SIDE A WITH CAVITY FOR THE INSERT AND PROTRUSION............... 133

FIGURE 61: MOULD PLATE SIDE B WITH RUNNER, GATE AND CAVITY 133

FIGURE 62: EXPLODED VIEW OF SUBSTRATE AND MOULD PLATES' ASSEMBLY 134

FIGURE 63: CAD DRAWING OF THE MOULD MANUFACTURED FOR LAP SHEAR JOINT SAMPLES (CLOSED). 134

FIGURE 64: REPRESENTATION OF THE DIRECTIONS OF FORCES ON THE ADHESIVE JOINT PRODUCED DURING EJECTION FROM THE MOULD, AND DURING TESTING.......................... 135

FIGURE 65: REPRESENTATIVE SAMPLE OF THE EFFECT OF EJECTION ON THE LAP SHEAR JOINT 135

FIGURE 66: REPRESENTATION OF THE DIRECTIONS OF FORCES ON THE ADHESIVE JOINT PRODUCED.. 136

FIGURE 67: CONFIGURATION OF A PULL TEST SAMPLE... 137

FIGURE 68: CAD IMAGE OF THE JIG PRODUCED FOR THE PULL TEST 138

FIGURE 69: TYPICAL LOAD VS EXTENSION CURVE FOR PMMA, INSERT AT ROOM TEMPERATURE 142

FIGURE 70: TYPICAL LOAD VS EXTENSION CURVE FOR ABS @ INSERT TEMPERATURE 60°C ... 142
FIGURE 71: TYPICAL LOAD VS EXTENSION CURVE FOR PBT, INSERT AT ROOM TEMPERATURE. ... 142
FIGURE 72: TYPICAL LOAD VS EXTENSION CURVE FOR PA 6 INSERT TEMPERATURE 80°C ... 142
FIGURE 73: COMPILATION OF DATA: AVERAGED BREAKING LOAD VS TEMPERATURE ... 144
FIGURE 74: PVT DATA FOR PBT ... 149
FIGURE 75: PVT DATA FOR PS ... 149
FIGURE 76: TYPICAL MOLDFLOW ANALYSIS WORKFLOW SEQUENCE ... 156
FIGURE 77: CAD IMAGES ... 158
FIGURE 78: DUAL DOMAIN MESH ... 158
FIGURE 79: ‘ADDING’ INSERT TO OVERMOULD STUDY ... 159
FIGURE 80: ISOLATION OF INTERFACE AREA MESH ... 160
FIGURE 81: MIS-MATCH OF THE MESH AT INTERFACE ... 160
FIGURE 82: ISOLATION OF OVERLAPPED INTERFACE MESH ... 161
FIGURE 83: RESULT OF DELETING OVERLAPPED MESH ELEMENTS ... 161
FIGURE 84: MESH-MATCH AT INSERT INTERFACE ... 162
FIGURE 85: GATE LOCATION ... 163
FIGURE 86: CUTTING PLANES FOR SECTION VIEWS ... 165
FIGURE 87: TEMPERATURE AT MELT FLOW FRONT FOR PMMA (X-Y SECTION VIEW) ... 167
FIGURE 88 AND FIGURE 89: PRESSURE AND TEMPERATURE PROFILE FOR PS (Y-Z SECTION VIEW) ... 172
FIGURE 90: VOLUMETRIC SHRINKAGE DISTRIBUTION FOR PC (CUTTING PLANE Y-Z) ... 175
FIGURE I: FORMATION OF WELD LINE FOR PA 6 WITH INSERT AT ROOM TEMPERATURE ... 204
FIGURE II: PROBABLE AIR TRAPS (SHADED BLUE AREAS) FOR PBT WITH INSERT AT 100°C ... 205

List of Tables

TABLE 1 TYPICAL FORMULATIONS USED FOR PCBS 3

TABLE 2: TARGET FOR WEEE COMPLIANCE 4

TABLE 3: CLASSIFICATION OF VAN DER WAALS FORCES 16

TABLE 4: CLASSIFICATION OF VAN DER WAALS FORCES 16

TABLE 5: MATERIALS USED IN MIDS 52

TABLE 6: THERMOPLASTICS USED FOR ENCAPSULATION 52

TABLE 7: KEY PROPERTIES OF THERMOPLASTICS USED 56

TABLE 8: PROPERTIES OF THE DNP 10 CANTILEVERS USED 69

TABLE 9: PROPERTIES OF THE TESP CANTILEVER USED 69

TABLE 10: CANTILEVER DEFLECTION EXPERIMENTS 86

TABLE 11: SURFACE TENSION OF THERMOPLASTICS 116

TABLE 12: WORK OF ADHESION AT 240°C 117

TABLE 13: WORK OF ADHESION FOR PMMA 117

TABLE 14: WORK OF ADHESION FOR PS 118

TABLE 15: DETAILS OF THE VERTICAL INJECTION MOULDING MACHINE 131

TABLE 16: PEAK LOADING INSERT TEMPERATURES AND TG OF THE THERMOPLASTIC. 148

TABLE 17: TENSILE STRESS AT BREAK AND PEAK BREAKING LOADS 150

TABLE 18: MESH STATISTICS 164

TABLE 19: TEMPERATURE AT MELT FLOW FRONT 168

TABLE 20: VOLUMETRIC SHRINKAGE 176

Glossary of Symbols

Description	Symbol (unit)
Cantilever deflection	$\boldsymbol{\delta_c}$ (m)
Change in apparent mass before and after the foil is immersed	$\Delta \boldsymbol{m}$ (g)
Change in enthalpy	$\Delta \mathrm{H}$ (J)
Coefficient of friction	μ
Contact angle	$\boldsymbol{\theta}$ (°)
Crystallisation temperature	**Tc** (°C)
Force	F (N)
Glass transition temperature	**Tg** (°C)
Perimeter of a solid sample	p (m)
Pull off force	$\mathrm{F_{pull\ off}}$ (N)
Shear strength	$\boldsymbol{\tau}$ (N/m^2)
Stiffness of cantilever	k (N/m)
Surface area fraction	$\boldsymbol{n}$ (moles/m^2)
Surface tension	$\boldsymbol{\gamma}$ (N/m)
Work of adhesion	$\boldsymbol{W_a}$ (J/m^2)

1 Introduction

Contents

- *End of Life Issues in Electronics*
- *Approaches to Improve End of life Profile of PCBs*
- *Manufacturing of Electronics by Overmoulding: Substrateless Packaging*
- *Aim of the study*

It is hard to imagine modern day life without electronics. Electronics today, is the cornerstone of modern society pervading most products and services. Life without consumer electronics like TV, refrigerator, mobile phones etc. is unthinkable. In fact the demand for new and innovative electronics has seen an exponential rise in the last few decades. The global market for electronic based equipment has grown at 8% p.a. in recent years and exceeds $1200bn (£ 669 bn) [1]. Over the years the physical size of electronics has gone down while the functions and complexity of electronic products has gone up. The electronics manufacturing industry is constantly evolving and it has kept pace with the rising demands and requirements from new products. Although the process of electronics manufacture has remained fairly constant over the past few decades there have been incremental advances in the technology at every step to continue to deliver smaller, faster devices. In spite of the advances in manufacturing technology, there is an inherent problem regarding the lack of recyclability and end of life disposal issues that has come to the fore, especially with the explosion in the use of electronics.

1.1 End of Life Issues in Electronics

One of the major constituents of electronic products is the printed circuit board (PCB). A PCB is a composite of organic and inorganic materials with external and internal wiring, allowing electronic components to be electrically interconnected and mechanically supported [2]. The three key components of a standard PCB are:

- Organic resin
- Inorganic filler
- Copper conductor

Table 1 lists some of the typical formulations used for PCBs.

FR-4 is the most widely used formulation, because of its low cost and suitable performance. It can be seen from Table 1 that most of the materials used for manufacturing PCBs are thermoset plastics which are not recyclable. In addition, these formulations have inorganic fillers like glass etc. which make recycling even more difficult.

The PCB technology to manufacture electronics has been well researched over the years and has been the cornerstone of the electronics manufacturing industry. However the inherent lack of recyclability of the PCBs has led to end of life disposal problems. The world's annual volume of "e-waste" was expected to exceed 40m tonnes by 2007 [3]. Various laws have been passed to control this ever increasing problem of electronic waste, one of the most important in recent years is the European Union WEEE directive.

Table 1 Typical formulations used for PCBs

Sr. No.	Material	Matrix-Fibre
1.	FR-2	Flame retardant phenolic resin with cotton paper
2.	FR-3	Phenolic resin with cotton fibre
3.	FR-4	Epoxy resin with woven glass
4.	FR-5	Epoxy (polyfunctional) resin with woven glass
5.	G-10	Epoxy resin with woven glass (high temperature)

1.1.1 End of Life (EOL) and Waste from Electrical and Electronic Equipment (WEEE) Directive

The major effect of the WEEE directive is to make electronics producers and importers responsible for ensuring that a large proportion of the materials in electronic products are recycled or reused at end of life. Salient features of the directive are summarised below:

- Aims to reduce the amount of WEEE going to landfill, by requiring all manufacturers and producers to take “end of life” responsibility for the products they sell.
- March 2007 – deadline for producers/schemes to register (already enforced).

- July 2007 – full producer responsibility (already enforced).
- Producers are financially responsible for collecting, treating, recovering and disposing of an equivalent amount of WEEE that is calculated according to the amount of EEE that they produce.

By the end of any relevant compliance period, each operator of a scheme shall meet the targets (Table 2) for WEEE sent for treatment:

Table 2: Target for WEEE compliance

	Recovery by the average weight	**Reuse and recycling of components, materials and substances**
• Large household appliances • Auto dispensers	80%	75%
• IT and telecoms equipment • Consumer equipment	75%	65%

1.2 Approaches to Improve the End of Life Profile of PCBs

The directive discourages production of non-recyclable waste. It also has provisions for financial penalties for non-compliance. The electronics manufacturers in Europe face a major problem. They are required by the WEEE directive to take

back e-waste, and to re-use or recycle a major portion of it. At the same time one of the major constituents of electronics waste, PCBs are not recyclable. It is very clear that the root cause of this problem are the constituents that make up the PCBs and hence the alternatives to conventional electronics would be to manufacture recyclable electronics by using recyclable PCBs or PCB-less electronic circuits. Some attempts have been made in this direction. They are as follows:

A) **Thermoplastic boards**: A natural alternative to non-recyclable thermoset PCBs is to use thermoplastics to manufacture PCBs. Polyethylene terephthalate (PET) and Polyether imide (PEI), Polyether Ether Ether Ketone (PEEK) are some of the thermoplastics which have been tried to manufacture PCBs [4]. The success of these and other thermoplastic materials is subject to on-going evaluation and research.

B) **Moulded Interconnect Devices (MIDs)**: MIDs have been explored as an alternative option to PCBs for more than two decades now. They have been defined as, ‘an injection moulded plastic substrate that incorporates a conductive circuit pattern, integrating both mechanical and electrical features’ [5]. There are many examples where MIDs are being explored such as electrical connectors, 3D moulded antenna etc. [6-8].

C) **Overmoulding of electronic components by thermoplastics**: This technique has received attention in recent years. There are two approaches in manufacturing electronics circuits through overmoulding.

   a. Encapsulation of the PCB with all the components: This would in-turn facilitate incorporation of electronics in automobiles etc. [5] While this does not help recycling, it has led to alternative technologies.

b. Overmoulding of electronic components: In this case, the overmoulded polymer forms a 'board' in a ''PCB-less'' or substrateless manufacturing process. The Occam process and the process that formed the basis of this research are based on this principle [9-10].

1.3 Manufacturing of Electronics by Overmoulding: Substrateless Packaging

Although contemporary PCB technology has been a clear winner amongst the technologies used for electronics manufacture, the future demands of the electronics industry may result in one of the many alternatives coming to the fore. The process that is most likely to win the race is the one with maximum product recyclability at end of life. Considering this, Loughborough University developed a process called 'substrateless packaging' as an alternative to both conventional PCBs and the above listed methods of electronic circuit manufacture.

The process is termed 'substrateless packaging' since no PCB is involved. Substrateless packaging involves the use of thermoplastics to overmould the individual electronic components and hold them in their placement positions. A circuit pattern is then created on the moulding by either plating or printing of a conductive ink. The route thus reverses the normal order of surface mount technology (SMT) assembly steps i.e. components are assembled before the interconnection pattern is created. A detailed description of the process and the current state of development are given in Webb *et.al.* [9]. The process is as follows (Fig. 1-5)

a) Conventional pick and place machines are used to position components onto an adhesive carrier film.

b) The carrier film with components is overmoulded with a thermoplastic polymer using an injection moulding process.

c) The moulding is removed from the mould tool.

d) The carrier film is removed from the moulding, revealing the undersides of the component leads. The component leads are set flush with the surface of the moulding, facilitating the electrical interconnection step.

e) A conductive circuit pattern is then produced using established processes such as plating or printing of a conductive ink. The circuit pattern acts to interconnect the components directly, without requiring soldering.

The major advantage of the process is that the components can be easily separated from the overmoulded thermoplastic at end of life. This could be done by simply melting the overmould in the case of a commodity thermoplastic. Other approaches would be to use a biodegradable plastic and break it down in an industrial composter, or to use a soluble thermoplastic that could be dissolved away by a suitable solvent.

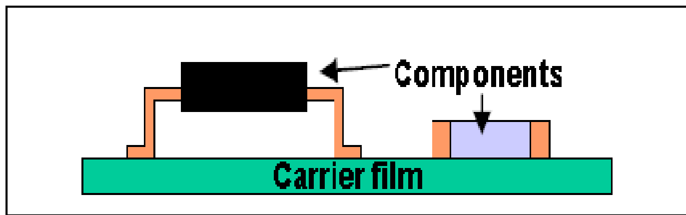

Figure 1: Mounting of electronic components on adhesive film

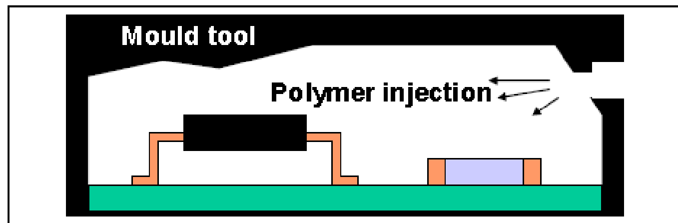

Figure 2: Placement of loaded carrier film in mould tool.

Overmoulding of film and components with polymers

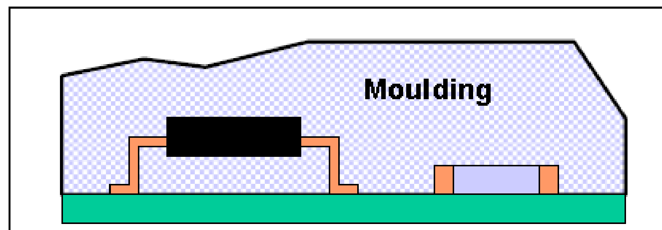

Figure 3: Removal of moulding from mould tool

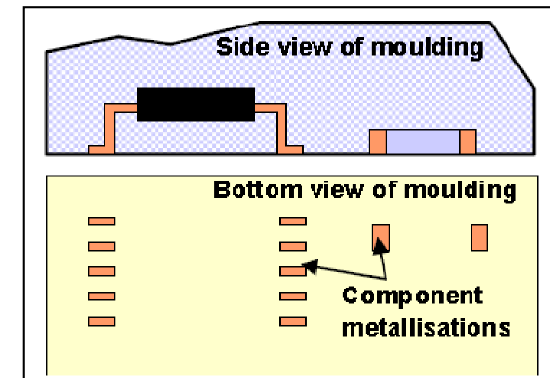

Figure 4: Removal of carrier film, revealing component metallisation on underside of moulding.

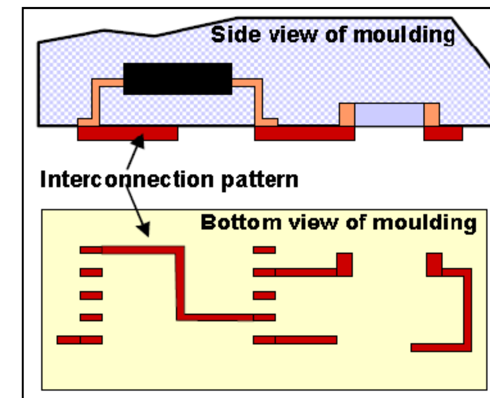

Figure 5: Deposition of interconnection pattern on underside of moulding

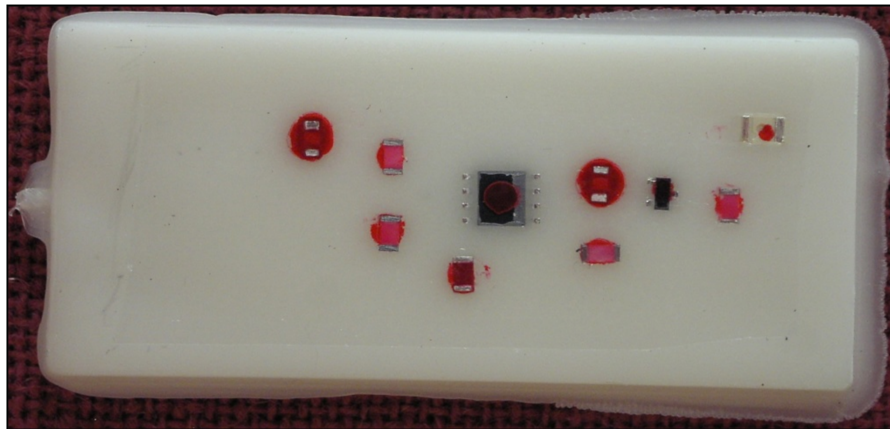

Figure 6: A demonstrator representing stage d of the process

Figure 6 shows a demonstrator manufactured at Loughborough without the metallised interconnects, representing the process at the end of stage d. However, there are a number of developmental challenges for substrateless packaging that must be overcome.

1.3.1 Developmental Challenges for Substrateless Packaging

- Development of a tape and adhesive system that both withstands the process temperatures and pressures and yet can be peeled off easily from the moulding.
- Development of processes and materials for high quality and high adhesion interconnection patterns.
- In order for the system to work, the electronic components should be perfectly embedded into the thermoplastic polymer. Any sort of relative movement between the electronics and the overmoulded casing will be a potential reliability issue with the manufactured assembly.

- A fully finished product will also carry conductor paths to interconnect the components and thus form an electronic circuit. It is therefore crucial, that there are no gaps between the 'legs' of the electronic components and the thermoplastic casing (Fig. 7). Such gaps were observed in the prototypes developed by Webb *et.al.* [9] Any gaps will result in plating errors, and hence an 'open circuit'.

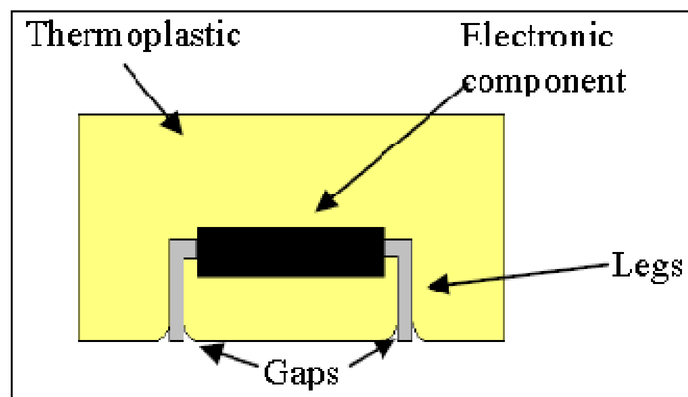

Figure 7: Gaps observed in injection moulding trials of the substrateless packaging process

- Thermal management is another area of concern. Thermal implications of a similar packaging system (an overmoulded PCB) have been studied by Sarvar *et.al.* and it was concluded that any gap or lack of adhesion between the polymer and the electronic components will create stress on the interconnections [11]

1.4 Aim of the Study

For substrateless packaging to be the technology of choice for electronics manufacture it has to compete with the quality and reliability offered by PCBs. The PCB technology today is the result of grass root level research on materials and manufacturing processes. For substrateless packaging to be a reliable manufacturing

technique, similar research on material interactions and manufacturing process has to be done in order to overcome all the developmental challenges. The areas of research that come to the fore based on the problems mentioned above are very wide and not all of them formed a part of this research project.

In substrateless packaging intimate contact between the overmoulded thermoplastic resin and the legs of the electronic components is crucial for the integrity of the electrical interconnection. If small gaps open up around the embedded components after solidification these will either act as weak points in the electrical interconnect pattern, or prevent electrical interconnect being achieved at all. The question of what material-material interactions, and process conditions, promote adhesion between insert and overmould is therefore a crucial one to address to enable production of high quality and reliable circuits. The aim of this study was therefore to improve the reliability of substrateless packaging by studying the reasons for gap formation at the interface of the electronic component and the thermoplastic overmould.

The objectives of this study were

1. *To understand adhesion between the legs of electronic components and the thermoplastic overmould at the material level*
2. *To understand the effects of the insert injection moulding process conditions on interfacial adhesion, i.e. adhesion at the interface between the legs of the electronic components and thermoplastic overmould*
3. *To identify thermoplastic polymers that may be used for overmoulding electronic components.*

To fully comprehend the adhesion at the interface during insert moulding, it is necessary to study the theories of adhesion and the process of injection moulding. In Chapter 2 the classic theories of adhesion and injection moulding methods were reviewed. In Chapter 3 the methodology of the study, i.e. the reason for choice of experimental methods used is described. In chapter 4, a detailed description of the material selection and the adaptation of the generic techniques described in Chapter 3 to the particular requirements of this project are given. Each results Chapter, Chapters 5-8, describes the practical difficulties encountered during initial trial experiments and the processes of selecting specific techniques for substantive experiments. The results from the individual areas for investigation are discussed in the appropriate experimental Chapter, and the overall results of all the experiments are discussed in Chapter 9. Finally, the major conclusions from the study are summarised and recommendations for further work are made in Chapter 10.

2 Background and Literature

Contents

- *Forces of Adhesion*
- *Theories of Adhesion*
- *Injection Moulding*
- *Multi Material Injection Moulding (MMIM)*
- *Insert Moulding and Adhesion*
- *Gap in the Literature*

One of the aims of this project was to understand the interfacial adhesion between materials used in electronics and injection overmoulded thermoplastics. Interfacial adhesion in injection overmoulding is the result of interactions that take place between the substrate and the thermoplastic melt. Understanding of the inter-atomic forces is essential to gauge the likelihood of adhesion (or repulsion) between materials. Various theories have been put forward to explain the mechanisms of adhesion based on the inter-atomic interactions.

In this section, the current understanding of the inter-atomic forces contributing to adhesion is given, followed by brief summaries of the theories of adhesion. Finally the theories of adhesion are discussed with reference to the current study.

2.1 Forces of Adhesion

Two types of forces are commonly referred to in the study of adhesion, *adhesive forces* and *cohesive forces*. Two surfaces are held in contact by the adhesive forces while the bulk of the material is held together by the cohesive forces.

Both these forces contribute towards the bond strength of a joint. In this work discussion will be limited to the *adhesive forces*.

Adhesive forces (and cohesive) are dependent on the interactions between different atoms and molecules. They can broadly be grouped as *primary* and *secondary forces*. These terms originate from the relative bond energy of each type of interaction.

2.1.1 Primary forces (Short range interactions)

There are typically three types of primary bonding forces

1. Ionic bonding (bond energy 600 to 1000 kJ/mol)
2. Covalent bonding (bond energy 60 to 700 kJ/mol)
3. Metallic bonding (bond energy 100 to 350 kJ/mol)

Covalent forces result from chemical reactions that happen across the interface while metallic bonds are formed across metals during processes like welding, soldering etc. However, for general adhesive applications at the metal-polymer interface, these forces are generally not at work [12].

2.1.2 Secondary forces (Long range interactions)

Secondary forces of attraction like Van der Waals forces, Hydrogen bonding etc are important forces in adhesion studies. Their origin lies in physical adsorption or strong polar attraction. Their exact nature and effect on adhesive/cohesive strength is

very hard to determine, however awareness of their origin and characteristics assists in understanding bond formation.

2.1.3 Hydrogen bonding

Hydrogen bonding is due to the strong interaction of hydrogen attached to another atom by a polar covalent bond with the bonded atom of high electronegativity (such as O, N and halogens). Liquids and polymer surfaces have one of the following three types of hydrogen-bonding capabilities:

- Proton acceptor (electron donor or basic) such as esters, ketones, ethers or aromatics, which include such polymers as polymethylmethacrylate (PMMA), polystyrene (PS), ethylene–vinyl acetate copolymers and polycarbonate (PC).
- Proton donor (electron acceptor or acidic) such as partially halogenated molecules, including polymers such as poly(vinyl chloride), chlorinated polyethylenes or polypropylenes, poly(vinyl-idene fluoride) and ethylene–acrylic acid copolymers;
- both proton acceptor and proton donor molecules such as amides, amines and alcohols where the polyamides, polyimides and poly(vinyl alcohol) are included.

2.1.4 Van der Waals Forces

The terms ‘dispersion’, ‘polar’ and ‘Van der Waals forces’ are widely used in the literature of adhesion. Van der Waals forces describe dipolar interactions between the atoms and molecules. They can be further sub divided into London,

Debye and Keesom forces depending on the types of interactions viz. dispersion, induction and orientation respectively (Table 3). Two popular ways of classifying Van der Waals forces are shown in Tables 3 and 4 [13]. It must be noted that the dipolar interactions due to orientation of interacting species are permanent while those on account of induction can be induced.

Table 3: Classification of Van der Waals Forces

		Dipolar Interaction
Van der Waals	*London Dispersion*	*Transient/transient*
	Debye Induction	*Permanent/induced*
	Keesom Orientation	*Permanent/permanent*

Table 4: Classification of Van der Waals Forces

		Dipolar Interaction
Van der Waals	*London Dispersion*	*Transient/transient*
Polar Forces	*Debye Induction*	*Permanent/induced*
	Keesom Orientation	*Permanent/permanent*

2.1.5 Surface energy and surface tension

Surface energy is the algebraic sum of the energy required to break the bonds to form the surface *in vacuo* and is the same as that released when any new bonds are formed on the surface when it is brought in contact with the second phase. Thus, surface energy can be referred to as the energy required to maintain the cohesive integrity of a solid or to hold an adhesive to a substrate [12][13]. The study of surface energy forms a vital part of adhesion studies and references to surface energy

comparisons between the bonding surfaces are common. The reason for this is fairly obvious though, as theoretically, it is surface energy difference between the liquid adhesive and the bonding surface that determines the extent of contact, and hence the bond strength.

'Surface tension and surface energy are interchangeable definitions with the same units' [12-13]. Surface tension and surface energy are especially used interchangeably in liquid systems as both represent forces required to maintain the cohesive integrity.

Young's equation gives us the dependence of contact angle of the adhesive on the bonding surface on the surface energies:

$$\boldsymbol{\gamma_{sv} = \gamma_{sl} + \gamma_{lv} * cos\theta} \qquad \text{.............................} \; [1]$$

where, θ: contact angle

γ: Surface/interfacial energy with subscripts referring to:

v: vapour in equilibrium

s: solid in equilibrium

l: liquid in equilibrium

2.1.6 Wetting

There is almost unanimous agreement amongst all researchers (very rare in any study of adhesion) that good wetting is one of the essential factors responsible for adhesion. The process of establishing continuous contact between the adhesive

and adherend is called 'Wetting'. Wetting and surface energy/surface tension is interdependent. Young's equation (Eqn. 1) gives the exact relationship between them.

From Young's equation, it is observed that wetting occurs when the contact angle is 0 degrees (spreading) or a finite value (usually less than 90 degree) (Fig 8 a and b) i.e.

When, cosθ=1 $$\gamma_{sv} = \gamma_{sl} + \gamma_{lv}$$

or

when, θ > 0 $$\gamma_{sv} > \gamma_{sl} + \gamma_{lv}$$

Thus in the case of a liquid adhesive on a substrate, adhesion is favoured when

$$\gamma_{\text{substrate}} >> \gamma_{\text{adhesive}} \text{ (good wetting)}$$

Also, adhesion is not favoured when

$$\gamma_{\text{substrate}} << \gamma_{\text{adhesive}} \text{ (de-wetting)}$$

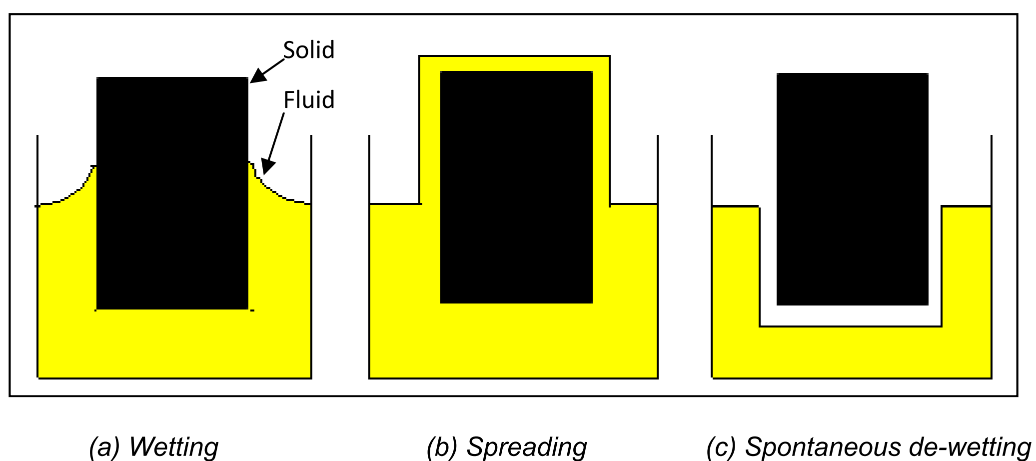

(a) Wetting *(b) Spreading* *(c) Spontaneous de-wetting*

Figure 8: Wetting and de-wetting

The popular and widely accepted school of thought is that wetting is absolutely necessary, followed by one or more of the adhesion mechanisms (explained later) for a good adhesive bond to be formed.

2.1.7 Work of Adhesion

Work of adhesion is a thermodynamic quantity is defined as the energy required to separate an adhesive from an adherend. The energy expended in the formation of the new surfaces must be the sum of the surface energies γ_{lv} and γ_{sv}. Also, as the surfaces were in contact with each other intermolecular forces must also be accounted for (γ_{sl}). The work of adhesion, therefore, can be defined as

$$W_a = \gamma_{lv} + \gamma_{sv} - \gamma_{sl} \qquad \text{.............................[2]}$$

This is known as Dupre's equation.

Substituting Young's equation into Dupre's equation

$$W_a = \gamma_{lv} * (1 + cos\theta) \qquad \text{..........................[3]}$$

Where,

θ= angle of contact at the solid to liquid interface

This is known as the Young-Dupre equation. The thermodynamic parameter W_a is expressed in two measurable quantities viz. contact angle and surface energy (tension) of the liquid.

2.1.8 Acid-base interactions

As an alternative to the inter-atomic interactions listed in Tables 3 and 4, some authors treat adhesion in terms of acid-base interactions. Acid–Base interactions can be explained using quantum mechanics and the concept of Lewis Acids and Lewis Bases. According to quantum mechanics, each atom has electrons in orbitals around the nuclei in discrete energy levels, also referred to as shells. An atom is supposed to be in the lowest energy state and hence stable when it has completely filled orbitals. Thus, atoms like fluorine, oxygen etc. require electrons to complete their outermost orbital and so are electronegative (Lewis Acids). Conversely alkali and alkali earth metals empty their last orbitals and hence are electropositive (Lewis Bases). The interactions between them results in ionic and covalent bonds of varying proportions.

Drago *et.al.* and Fowkes investigated the analytical work of adhesion in acid base interactions [14]. According to Drago, the acid-base interactions contribution to the work of adhesion is

$$\boldsymbol{W_A^{A-B} = -f * n^{A-B} * \Delta H^{A-B}} \qquad \textbf{\textit{.......................... [4]}}$$

where,

f: free energy to enthalpy correction factor.

n: Surface area fraction of acid base interaction (moles/area)

$\Delta H^{A\text{-}B}$: Change in enthalpy of acid base interaction on account of the ionic (E_A, E_B) and covalent (C_A, C_B) parameters

On the other hand Fowkes proposed that the work of adhesion can be approximated to the geometric mean of the dispersion contributions to surface energies γ_1^d and γ_2^d:

$$W_A^{vdw} = \sqrt{\gamma_1^d * \gamma_2^d} \quad \text{...[5]}$$

The work of adhesion between surfaces is the given by:

$$W_A = W_A^{A-B} + W_A^{vdw} \quad \text{...[6]}$$

2.2 Theories of Adhesion

Theories of adhesion have been formed over a period of 70 years. They have been well documented and detailed accounts can be obtained through various books [12-14]. A brief account summarising the literature is provided here.

2.2.1 Mechanical Interlocking

The theory of mechanical interlock represents the ‘common sense’ based explanation. It was one of the first attempts to explain the science of adhesion. Early work of McBain and Hopkins established the fundamentals of this theory [14]. Liquid adhesive entering into the porous surface of the adherend and hardening was the basis of this theory. Thus, surface roughness was one of the most important factors in assessing adhesion. There is an increase in surface area of the adherend due to roughening which also increases the area of interactions. Venables concluded that porosity and microscopic roughness enabled polymers to penetrate the surface and form interlocks rendering higher adhesion to the joint [14]. Due to the advent of

instruments like scanning electron microscope and other surface scanning techniques the interrelation of rough surface and joint strength can be easily established. The mechanical interlock theory is now widely accepted. Surface roughness and wetting of the surface by adhesive are deemed essential for obtaining good mechanical interlock.

2.2.2 Adsorption theory

The adsorption theory states that the adhesive will adhere to the substrate because of interatomic and intermolecular forces established at the interface, provided that an intimate contact is achieved. Thus, the secondary forces (Van der Waals forces, Hydrogen bonding etc.) are responsible for adhesion. Intimate molecular contact (distance of 5 Angstroms or less) between the surfaces is necessary for the attractive forces to be generated between the two surfaces. Thus, ‘wetting’ of the adherend by the adhesive is very important as it ensures that the two surfaces are in close contact.

2.2.3 Chemical Bonding theory

The theory of chemical bonding treats adhesion completely as a surface phenomenon based entirely on the chemical interactions between the two reacting surfaces. Chemical bonds across the two adhering interface (materials) seems to be widely accepted as the ‘best’ recipe for good adhesion. Primary bonds may result due to the functional (bi, tri etc.) atoms in the material. When such materials come into contact under favourable conditions, chemical bonds (covalent/ ionic) may result

across the interface, thus creating a strong force of attraction between the two adherends.

2.2.4 Diffusion theory

Diffusion theory applies to the specific case of polymer-polymer adhesive substrate interaction. The key to 'adhesion' in this case is the miscibility of the interacting polymers and the chemical compatibility of the polymeric chains into each other. The theory was put forward by Voyutskii who was concerned with explaining the autohesion phenomenon in un-vulcanized rubber adhesion [14]. He reasoned that the polymeric chains at one surface diffused into the other surface, and thus the two masses slowly became one through the entanglement of the chains. One must however note that for this to happen, the chains must be highly mobile and hence should be well above the glass transition temperature (Tg) of the polymer.

This concept was further extended to inter-diffusion of dissimilar miscible polymers. Recently, some work has suggested the idea of interpenetration of the adhesive in the microstructure of the substrate, hinting at a mechanism similar to this theory [14]. This theory, however, has had its fair share of detractors and is not very popular.

2.2.5 Theory of Weak Boundary layer (WBL)

The origins of this theory lie in the observations of the failure of an adhesive joint. Bikermann postulated the existence of a finite interface (having a molecular thickness) (Fig. 9) [12]. The properties of such a layer vary from those of the bulk of the material forming it. Thus, in an adhesive joint the WBL forms the weakest link of

the joint. On application of sufficient force, the rupture passes through the weak boundary layer, and the joint fails. Many reasons for the formation of this interphase have been cited by several researchers. [12-14].

- The orientation of chemical groups or the over-concentration of chain ends to minimize the free energy of the interface.
- Migration toward the interface of additives or low-molecular-weight fraction.
- The growth of a trans-crystalline structure, for example, when the substrate acts as a nucleating agent
- Formation of a pseudo-glassy zone resulting from a reduction in chain mobility through strong interactions with the substrate.
- Modification of the thermodynamics and/or kinetics of the polymerization or cross-linking reaction at the interface through preferential adsorption of reaction species or catalytic effects.
- Cohesively weak oxide layer at the interface.

According to the proponents of this theory, the presence of the boundary layer significantly (and in some cases completely) alters the adhesion strength of the joint. WBL over the years has had its fair share of criticisms. The presence of a WBL itself has been questioned, as pure interfacial failure does occur in many adhesive systems.

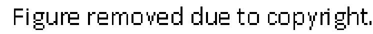

Figure 9: Typical causes of Weak Boundary Layer [12]

2.2.6 Electronic/Electrostatic theory

The electrostatic theory states that electrostatic forces in the form of an electrical double layer are formed at the adhesive-adherend interface. These forces account for resistance to separation. There are a few instances where this theory holds its ground. It is an accepted theory for biological cell adhesion. A simple form of adhesion can also arise from direct contact electrification. This has been demonstrated for thin films of metal sputtered onto polymeric surfaces. This theory, also gathers support from the fact that electrical discharges have been noticed when an adhesive is peeled from a substrate. The presence of an electrical double layer may contribute to the overall adhesion of the system; however, according to some research by Von Harrach and Chapman, the contribution can be termed as negligible [14]. Moreover, the electrical phenomenon is considered as an after effect of bond failure rather than cause of the high bond strength [12-14].

2.3 Injection Moulding

In this section a brief overview of the injection moulding process is given, followed by a description of the key parameters that affect the process. Then injection overmoulding and other forms of multi-material injection moulding (MMIM), and the factors affecting them are discussed. At the end, adhesion in MMIM and its relevance to the current study is described.

2.3.1 Overview

Injection moulding (IM) in principle is similar to metal casting. The process follows the same basic fundamentals explained schematically in Fig. 10

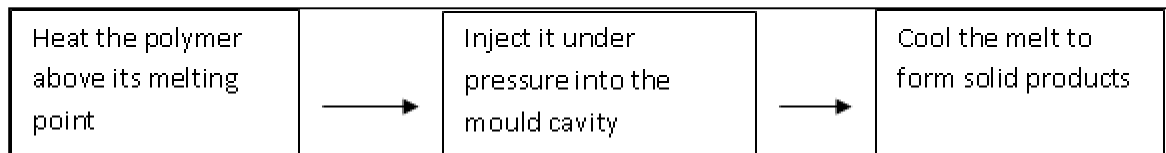

Figure 10: Basic stages of IM process

The IM machines have many variations in the methods of production. However most machines have the three basic units in the given order

- Injection unit: It generally comprises of a feed hopper, heated injection barrel with a plunger/screw and an injection nozzle. Polymer is melted and injected into the mould under pressure.
- Mould: It generally comprises of core and cavity. The mould decides the shape of the product. It may be heated.

- Clamping Unit: It holds the mould together while the polymer melt is being injected into it under pressure.

2.3.2 Types of Injection Moulding Machines (IMM)

Over the years, many variations on injection moulding depending on the feasibility and requirements of particular applications were developed. However, the basic types of machines that define the process are as follows [15]:

- *Plunger IMM*: It is a derivative of the 'transfer moulding' process. The material is heated in a barrel and then a reciprocating plunger pressurises the melt into the mould.

- *Reciprocating Screw*: This is the most commonly used injection moulding machine. Unlike a plunger IMM it has a reciprocating screw which is used to melt the polymer by the shearing action. The screw then reciprocates (like the plunger) to pressurise the melt into the mould.

- *Multiple barrel/screw injection moulding*: These machines have the same working principle as the reciprocating screw injection moulding machine. However, they use multiple barrels for products with multiple materials (co-injection). Barrels with multiple screws (generally 2) are used for better mixing of the polymer melt.

2.3.3 Part descriptions

Although there are variations in the injection moulding machines the basic elements that constitute the injection moulding machine and their functions are similar.

- **Screw**: It generally consists of three zones Feed, Compression and Metering. The diameter of the screw increases towards the metering zone (Fig 11). This helps shearing of the polymer melt and thus ensures good mixing. The reciprocating action of the screw forces the melt into the cavity under pressure. The length to diameter ratio (L/D) of the screw is important for the quality of the product. Higher L/D means better mixing of melt and hence higher quality of product.

- **Plunger**: In the plunger IMM, the reciprocating screw in Fig 11 is replaced by a plunger. Unlike the screw, the plunger only forces the polymer melt into the mould under pressure. The melting of the polymer is normally achieved using band heaters around the barrel.

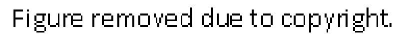

Figure 11: Part description with general location on reciprocating screw IM machine [16]

- Barrel heater/coolers: They are also known as band heaters. They are situated on the barrel near the metering zone of the screw (Fig.11). They ensure that the melt is at the right temperature when it leaves the metering section of the screw.

- Nozzle: The melt leaves the barrel and enters the mould (sprue/runners) through the nozzle. They may or may not be heated / cooled.

- Mould: It consists of the stationary and the moving half. Generally the moving half is the 'core' and the stationary half is the 'cavity', as this arrangement facilitates ejection of the product. The mould can be heated/ cooled with the help of ducts that are drilled into it. (Fig.11).

More details about types of IM machines and part description are given elsewhere and hence are not discussed in detail [15-17].

2.3.4 Process description

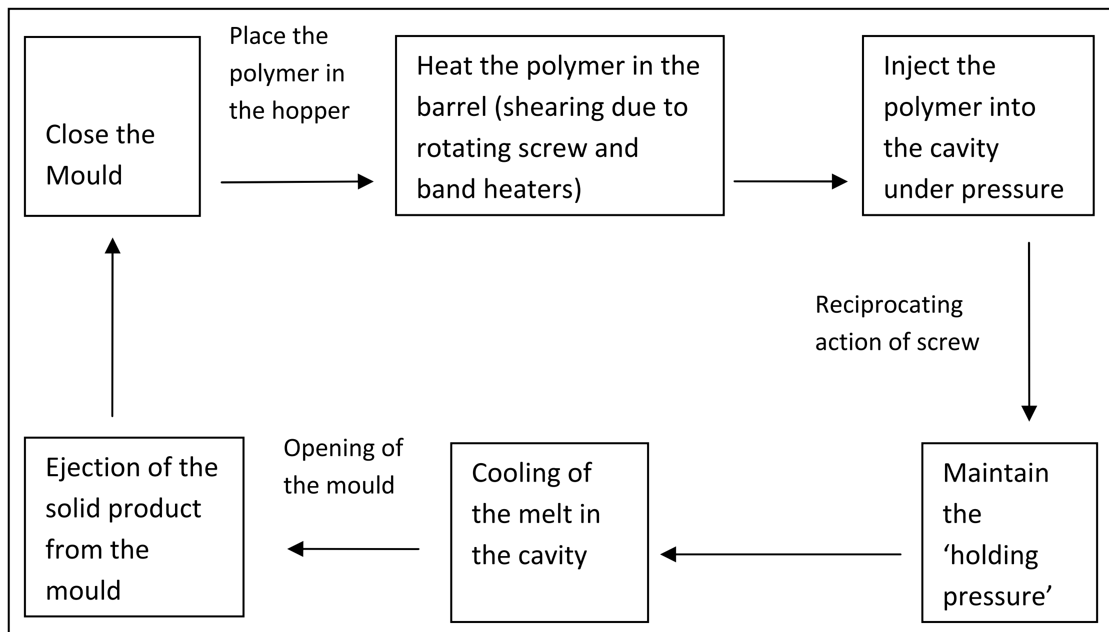

Figure 12: Stages involved in IM

Fig. 12 shows the various stages involved in injection moulding. A typical sequence starts with the closing of the mould. The polymer is melted in the barrel and then pumped under pressure into a cavity, where it cools. The solid part is then ejected and the cycle continues.

2.3.5 Sequence of Operations

Fig.13 shows the sequence of operations (left to right) that take place during an injection cycle. The diagram is based on time (x-axis) and hence shows the various operations that go on in series and parallel.

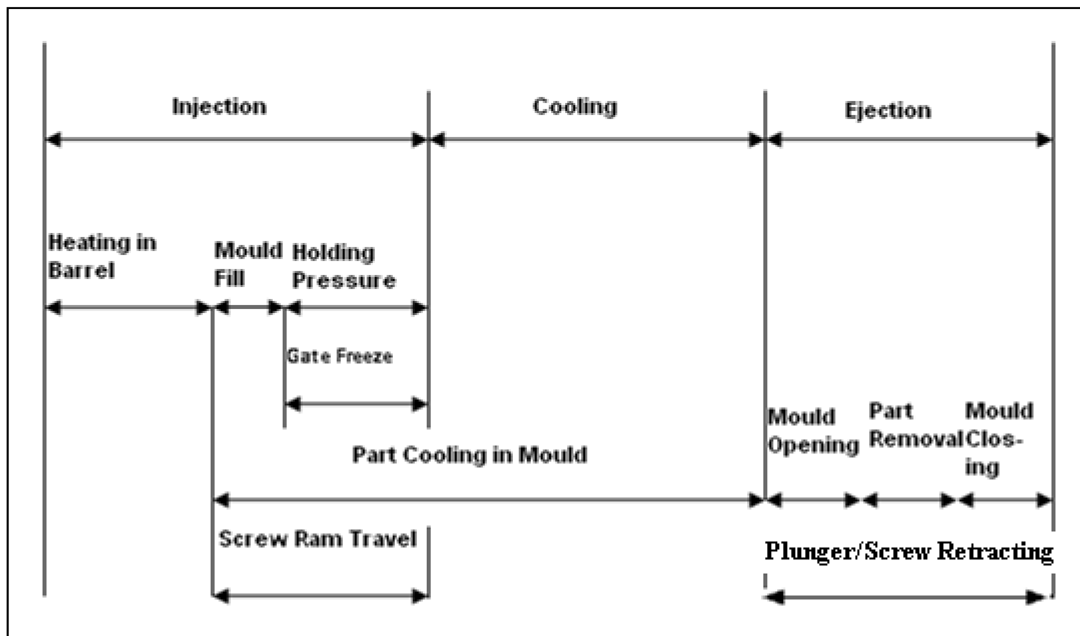

Figure 13: Injection, Cooling, Ejection and other operations with reference to timeframe.

2.3.6 Key Parameters Involved in IM

From the process and part description given above, it is clear that IM is a complex operation depending on many variables. Some of the key variables and the stage at which they can affect the process are listed below.

a. Polymer-melt temperature and viscosity: It is very important that the polymer melt is uniformly heated in the barrel (i.e. no hot spots etc). Both high and low melt temperatures are not desired. High temperatures generally result in degrading of the polymer, thus reducing the mechanical properties of the product. Low temperatures result in excess shear and will lead to surface defects on the products. Viscosity is inversely dependent (although not inversely linear) on melt temperature. (Fig.14)

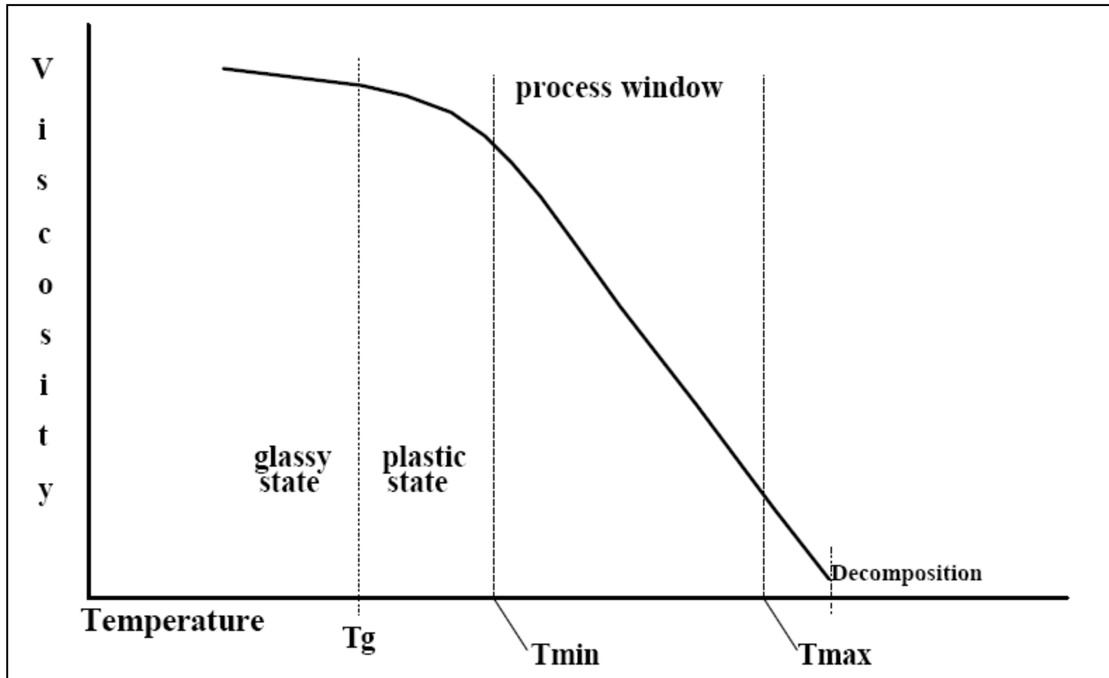

Figure 14: Processing of polymers in IM, Viscosity vs. temperature.

b. Injection pressure: This is the pressure generated in the barrel at the point of injection (Pa or Nm^{-2}). If injection pressure is too low, it can result in short shots i.e. the thermoplastic melt may not fill the mould completely.

c. Injection velocity: This is the time frame required to fill the cavity. The narrower the cavity thickness, the higher should be the injection velocity.

d. Holding pressure / packing pressure: Polymers (like most other materials) shrink when they undergo phase change from liquid to solid. Hence a packing/holding pressure is maintained at the end of the injection cycle to ensure no short shots occur. This process may also influence the mechanical properties of the product.

e. Mould temperature: When the product is cooled in the mould, due to the sudden temperature change, the skin of the melt front in contact with the mould may

freeze instantly causing a ‘shark skin effect’ on the surface of the component. In the case of thin cavities, this might lead to blocking of the flow front resulting in short shots. If the mould is at a higher temperature than the ambient, it helps in controlling the rate of polymer melt temperature drop. This helps to reduce frozen in stresses (due to sudden temperature drop) and gives relatively warpage free product.

2.4 Multi Material Injection Moulding (MMIM)

The substrateless packaging process can be classified as a type of multi material injection moulding (MIMM) and in particular insert / overmoulding. Over the years, the product requirements have changed, and accordingly many new technologies have been developed. Although the primary fundamentals of the injection moulding activity remain the same, many significant changes have taken place. To decrease the downtime on an assembly line, new techniques like (MMIM) were developed [18].

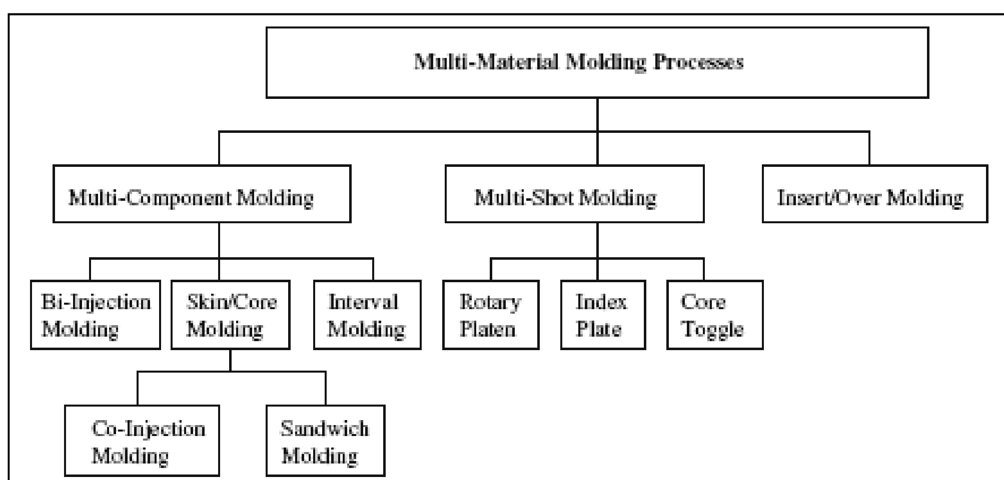

Figure 15: Multi material injection moulding processes [19]

In this technique more than one material is pumped/placed in the mould to obtain a macro composite or just an article with more than one colour. The family of MMIM processes are shown in Fig.15. All the processes have the same end result i.e. the article formed is a composite having one or more interphase or simply different colours, density etc. However, each process has small variations which are as follows

- Multi-component: Two polymers are injected sequentially or simultaneously into the mould. For simultaneous injection, cored screw, sequential gating, double barrels etc. are used. For sequential injection the feed in the hopper is adjusted so that one polymer is followed by the other.

- Multi-shot: In this technique, generally, one part is already injection moulded and placed in the mould before the second/consequent shot of polymer is injected.

- Over-Moulding: There is a thin line of distinction (if any) between the multi-shot and over-moulding processes. Over-moulding generally refers to *'insert overmoulding*'. In this process the insert is placed in the mould and the polymer is injected all around it so that an integrated article is obtained.

Advantages of using MMIM are as follows:

- multicolour appearance,

- skin/core configurations and properties,

- in-mould assembly,

- selective compliance,
- soft touch portions, etc.

The process of overmoulding is explored in more detail in the following sections as it forms the basis of this study.

2.4.1 Process Description for Overmoulding/Insert Moulding

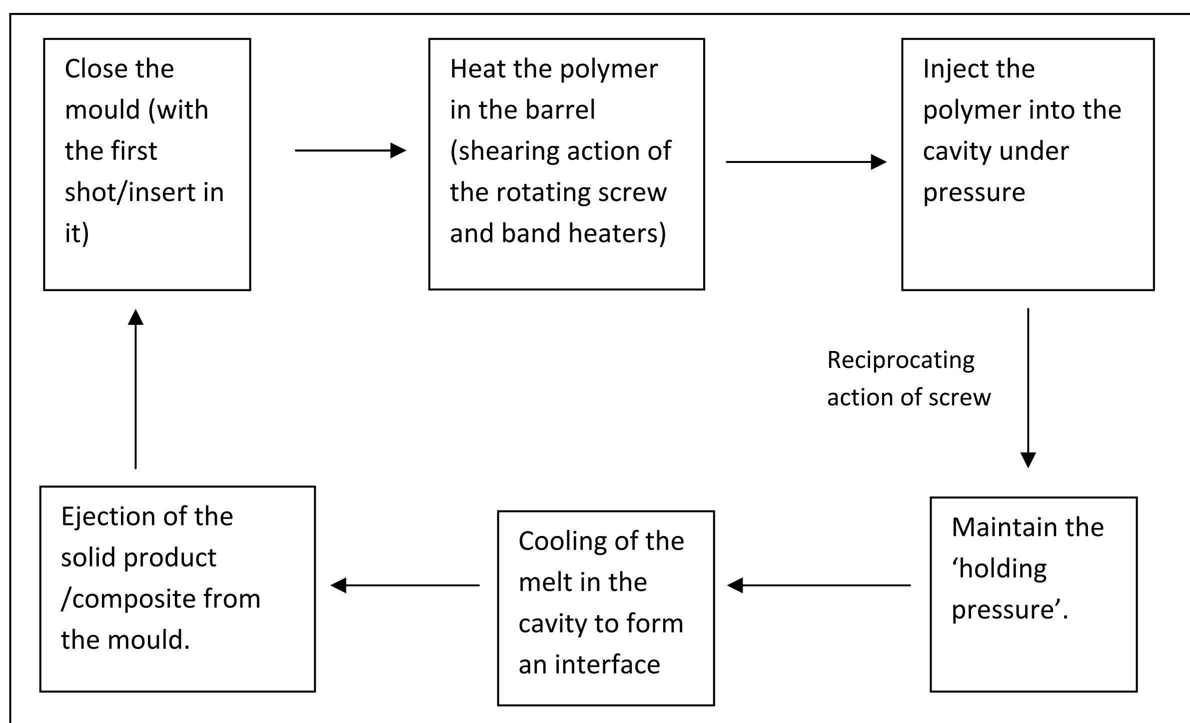

Figure 16: Stages involved in overmoulding

Fig 16 describes the stages involved in overmoulding. This process involves placing the insert in the mould. Care has to be taken so that the insert maintains its position in the mould.

2.4.2 *Sequence of Operations*: Overmoulding/insert moulding

Notice that there is a slight change in the sequence of operation from conventional IM (Fig 16 and 17). In the ejection cycle, after part removal, an insert is placed in the mould and then the mould is closed. This may increase the cycle time. When the mould closes for the next shot, the melt injected into the mould flows around the insert and takes the shape of the cavity with the insert in it.

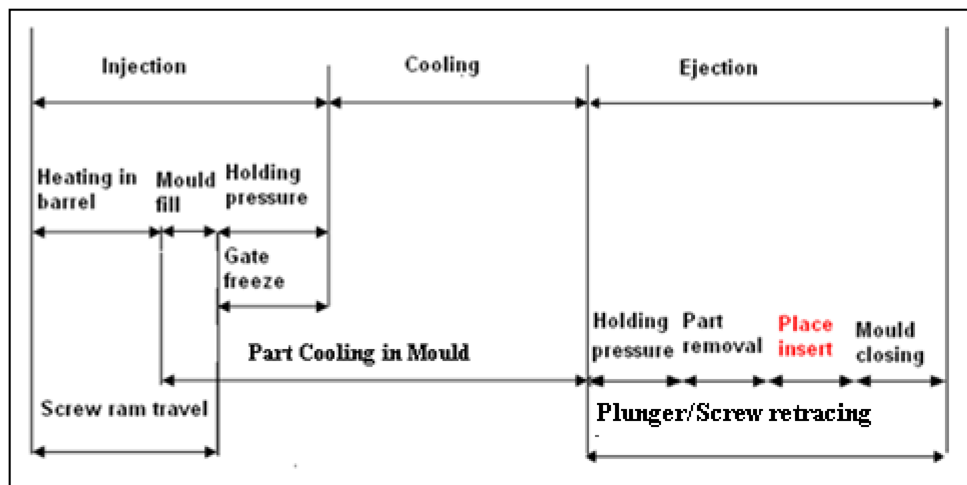

Figure 17: Various operations with reference to timeframe

In sequential / simultaneous injection moulding, the Injection and cooling cycles are repeated for the second shot. And then the ejection cycle follows.

2.4.3 Key parameters

As MMIM is essentially an injection moulding process, all the key parameters that govern the parent process affect this process too.

a. Melt temperature: Like IM, it is important that the melt temperature is not too high, so that the melt degrades nor too low so that there is excess shearing, resulting in poor product quality. However, in MMIM melt temperature

assumes additional importance as the bond strength of the macro-composite may depend on the temperature at the interface.

b. Injection pressure: Similar to the IM process, lower injection pressure may result in short shots.

c. Injection velocity: Generally higher velocities are preferred as they lower cycle time. In the case of co-injection moulding, injection velocity can control the material composition of the product.

d. Holding pressure/ packing pressure: Packing/holding pressure may influence the mechanical properties of the material injected. Packing/holding pressure therefore can influence the properties at the bond interface.

e. Mould temperature: Warpage of the product can be controlled to a great extent by maintaining the mould temperature higher than the ambient. In multi-shot/insert moulding, it can be used to control the insert temperature and influence thermo-mechanical properties at the insert interface.

f. Differential shrinkage: The difference in coefficient of thermal expansion of the materials at the interface in MMIM can result in moulded-in stresses which may have a bearing on the bond strength.

g. Wetting/ surface energy: As discussed earlier, good wetting of the substrate by adherend may result in higher bond strength. In MMIM, when the polymer melt comes in contact with the material at the interface, the ability of the melt to wet the material at interface may influence the bond strength.

2.5 Insert Moulding and Adhesion

Interfacial adhesion in MMIM, as highlighted in the section above, is dependent on the process parameters and the interactions that take place between materials. The open literature available on the interfacial adhesion in MMIM is very limited [20]. It should be noted that designers often use / prefer using shrink fit and undercut geometries to design products due to the availability of empirical knowledge and lack of understanding of the effect and strength of interfacial adhesion [21-22].

As explained earlier, adhesion at the interface of the electronics and thermoplastic overmould is one of the important factors in the future success of the substrateless packaging technology for electronics manufacture. The theories of adhesion have been formed over years of research and explain the scenarios of ‘classical adhesion’ between an adhesive and substrate. However, it must be emphasised here that the high temperature and pressure conditions at which a polymer melt comes in contact with the substrate (i.e. conditions for adhesion across the interface) are unique to insert overmoulding and not observed in the extensive literature that is available on thermoset (e.g. epoxy) and hot melt adhesives. There are a few studies giving details of adhesion at the interface during insert moulding, however given the uniqueness of substrateless packaging there is a gap in the literature as far as insert overmoulding of electronics is concerned.

2.6 Gap in the Literature

MMIM is a relatively new technology and not much literature is available [20]. A few studies on overmoulding in general and insert-overmoulding of metal with

thermoplastic in particular are listed in this section. An overview of the overmoulding technologies (used in the automotive sector) has been done by Grujijic *et.al*. (2008) summarising the material available in the open literature on polymer-to-metal overmoulding [23]. A comprehensive review on joining of polymers and polymer–metal hybrid structures was done by Amancio-Filho *et.al.* (2009) [24]. The papers listed below were found during literature searches prior to the publication of Grujicic *et.al.* and Amancio-Filho *et.al.* reviews. Although some are referenced by Grujijic *et.al*. and cross referenced by Amancio-Filho *et.al.* no other papers relevant to this project are mentioned in both the reviews. This gives some confidence that the literature search was comprehensive and that there is a lack of literature on this topic.

1. Ramani *et.al.* tested in-situ adhesion between injection moulded polycarbonate and aluminium. The aluminium substrates were maintained at 170 and 204°C during injection moulding. They concluded that no adhesion occurs if polymer does not penetrate into the micro-structure (roughness < 5μm in his case) [25].
2. Adhesion of ABS resin to metals like phosphor bronze, brass plates, and electro nickel platings during injection moulding was reported by Sasaki *et.al.* ABS did not adhere to any of the untreated metals. Adhesion at the interface was reported when the metals were treated with triazine trithiol monosodium aqueous solution [26].
3. Grujicic *et.al.* performed computational feasibility analysis of direct-adhesion polymer-to-metal hybrid (PMH) technology for load-bearing body-in-white structural components. They concluded that any modifications done on the

metal components (insert) which affect adhesion at the interface have a profound effect on the distribution and magnitude of residual stresses/distortions in the PMH component and that it must be taken into account when the component and its manufacturing processes are being designed [27].

4. Thermal stresses in an insert injection moulded aluminium 6061 and nylon 66 long fibre thermoplastic (LFT) composite joint in a tailcone were studied by Kulkarni *et.al.* They concluded that co-efficient of thermal expansion (CTE) mismatch between the insert and overmould along with differential cooling cause stresses at the interface affecting the final joint strength [28].

5. In a study by Yamaguchi *et.al.* on the effect of crystallization and interface formation mechanism on the mechanical properties of an insert moulded polypropylene film and polypropylene substrate it was concluded that the crystallinity of the injection moulded polymer is affected by the cooling rate dependent on the heat conducted (temperature) by the substrate [29].

6. Ananthanarayan *et.al.* studied polymer-polymer injection moulded interfaces (thermoplastics), and concluded that the temperature at the interface plays an important role in adhesion. It was suggested that the temperature of the melt should be above the melting temperature of the solid substrate. Poor heat transfer between the melt and the solid may result in the solid surface not melting, thus decreasing or preventing the interdigitation of the liquids, causing poor bonding [30].

7. Adhesion of reaction injection moulded polyurethane (PU) foam and thermoplastics were studied by Mahmood *et.al.* The injection moulding

parameters were kept constant for all the experiments. The thermoplastics used were PC/ABS-SMA, SMA, PC/SAR-GF, PC/ABS and PC/ABS-GF. Mechanical interlocking, diffusion, and chemical linkage between PU and thermoplastic were suggested as causes of adhesion [31].

8. A study of injection moulded thermoplastic elastomers on treated aluminium was done. Etching Al through acid then alkaline solution and further treatment (undisclosed) increased adhesion. Also, thickness of the sample (and hence its heat capacity) was found to affect adhesion as it affects the temperature of the melt at the interface [32].

Each of the above studies suggests some mechanisms (in isolation) for adhesion to occur across the interface of the bonding materials. However, the mechanisms of adhesion at the interface are dependent on the materials interacting at the interface and the processing parameters involved in the injection overmoulding process. Thus, a thorough study of the effects of injection overmoulding parameters as well as an analysis of the material interactions at the interface of the joint for the given thermoplastic-metal combinations relevant to electronics must be done. There are a few research papers suggesting the overmoulding approach for 3D electronics manufacture [33][34][35][36]. However, the author has not identified any study of injection overmoulding for electronic applications describing the adhesion at the metal thermoplastic interface, which can be a crucial step in the success or failure of such a product. Most of the available literature on MMIM deals with polymer-polymer interface or metal inserts that usually have structural applications.

In general, there is a consensus in the literature that in the absence of a chemically modified interface, the adhesion at the interface of the metal-polymer

component in insert injection moulding depends upon material properties, inter atomic interactions across the interface, wetting at the interface, temperature of the insert (consequently temperature at the interface) and insert moulding parameters. This makes the study of adhesion at the interface for each metal-thermoplastic pair unique. Hence, based on eventual applications, the metal-thermoplastic pairs will be selected and the effect of all the above mentioned factors needs to be studied.

3 Methodology

Contents:

- *Introduction*
- *Methodology*

3.1 Introduction

Most studies on adhesion explore one or all the mechanisms of adhesion (viz. wetting of the substrate by the adhesive, mechanical interlocking etc.) and the effect of processing parameters on bond formation (viz. temperature, time etc.). The overriding parameters that may affect adhesion at the metal-thermoplastic interface in an insert injection moulding process are

- Atomic/micro level interactions between the materials (mechanisms of adhesion)
- Injection overmoulding parameters/system level (processing conditions)

Hence, adhesion properties of the interacting materials have to be evaluated at both the micro level and system level. The data can be analysed and linked to identify relations (if any) between the system level (adhesive bond strength of overmoulded samples) and the atomic level interactions. Also, understanding which mechanisms of adhesion are acting at the micro level opens the possibility of enhancing interfacial adhesion by creating favourable conditions.

Injection moulding involves processing of polymers at temperatures above their melting points i.e. in the liquid state, and at high pressures. The expected

interactions of the insert material with molten thermoplastics during moulding consist of first wetting of the insert by the thermoplastics at high temperature. Secondly, thermal flows across the thermoplastic/insert interface will affect the cooling rate of the polymer resulting in change in microstructure and residual stress state. Residual stress will in turn affect the degree of shrinkage of the skin layer i.e. material shrinkage around the insert. Also, as the overmould cools down, the solid state interactions and interfacial adhesion (if any) dictate the reliability of the product. Hence a methodology for this project was devised such that fundamental adhesion (micro level) and practical adhesion (system level) could be taken into consideration.

The magnitude of adhesion in any system containing an adhesive joint can be expressed in terms of the practical adhesion obtained by destructive testing (peel test, lap shear test, fibre pull out etc) or in terms of 'fundamental' adhesion between the adhesive and adherend materials [12-14]. Fundamental adhesion refers to the forces between atoms at a bonding interface. Typically the associated work of adhesion is calculated using theoretical models and measured values of contact angles of test fluids on surfaces. Fundamental and practical adhesions are inter-related. The value of practical adhesion obtained from an experiment is the result of the inter atomic forces, mechanics of materials, joint geometry and variations in test sample preparation. Therefore, in the current work it was intended that measurements of practical adhesion and fundamental techniques be combined to give an overall picture of the factors that affect adhesion at the interface of an insert moulded product.

The study aimed to contribute to the knowledge of adhesion at the interface of thermoplastic overmoulds and metal used to coat the legs of electronic components

and suggest thermoplastics suitable for substrateless packaging. As already mentioned in Chapter 2 there is a consensus in the literature that the adhesion at the metal-thermoplastic interface in insert injection moulding depends upon material properties, interfacial forces between the materials, wetting at the interface, temperature of the insert (consequently temperature at the interface) and insert moulding parameters. Hence, it was decided to investigate each of them in detail.

3.2 Methodology

The choice of experiments to achieve a given aim depends on many factors such as availability of equipment, materials, technical knowhow, and suitability of the experiments in the context of the research. In this section the reasons for the choice of experimental analysis techniques used for each study area listed previously are given.

1. Analysis of interfacial forces between metals used in electronics and thermoplastics

Not many options are available for direct measurement of interatomic interactions between two solid surfaces. The use of the Atomic Force Microscope (AFM) force-distance technique was therefore selected almost by default for this analysis. In this technique a sharp tip attached to a cantilever is brought into the vicinity of the sample surface. The deflection of the cantilever varies depending on the interaction force between the tip material and the sample, thus allowing quantitative measurements of interaction force for the given materials. The details of the process are mentioned in Chapter 5.

2. Analysis of wetting by thermoplastics at high temperature

In insert moulding, the wetting of the insert by the molten thermoplastic can influence the adhesion at the interface. Generally contact angles are measured to estimate the wetting and they have been a cornerstone of the study of fundamental adhesion. Sessile drop and immersion-emersion are some of the most widely used techniques for measuring contact angles made by molten polymers on metal surfaces. The details of the experiments are mentioned in Chapter 6.

3. Analysis of mechanical strength at the interface

It must be noted that testing the actual component is the best way of assessing the mechanical strength at the interface. However, mechanical strength tests performed on the substrateless packaging samples would shed little light on the adhesion at the interface between the legs of the electronic components and the thermoplastic overmould as it is largely the macro level mechanical interlock between the electronic component and the overmould that would be tested. Hence tests on purpose designed test parts were performed. In this work, a pull test sample was selected as described later in Chapter 7. The aim was to provide information on system level adhesion.

4. Numerical simulations

The flow of thermoplastics during injection moulding and the effect of insert temperature on interactions at the metal-thermoplastic interface can be effectively understood by use of numerical simulations. Moldflow is a software package which simulates the flow of polymer into the mould cavity. In this work, numerical simulations performed using Moldflow are described in Chapter 8. The pull test

sample geometry was modelled and the effect of insert temperature, differential cooling etc. on the interface formation was investigated.

4 Materials and Properties

Contents

- *Introduction*
- *Background*
- *Use of Thermoplastic for Electronic Interconnection*
- *Choice of Materials for this Study*
- *Selected Thermoplastics and their Properties*
- *Selected Insert Material.*

4.1 Introduction

The selection of materials for any newly developed process depends upon the final application. Substrateless packaging involves the process of injection overmoulding of electronics by thermoplastics. There are two classes of materials that must be chosen for this study: the material of the overmould, and the material of the insert. One approach to choosing the overmould material is to consider the requirements of existing PCB materials. These requirements are described below and are used to justify the choice of overmould materials selected for this study. Also, there have been a few competing processes that have been developed for manufacturing electronics. The materials used for these processes were also given due consideration while selecting the thermoplastic overmould. The choice of the materials for the insert is based on the most common materials at the surface of the 'legs' of the electronic components. These are also described below and the choice of materials for the study is justified.

4.2 Background

The area of focus for this study of adhesion at the interface between materials in an insert injection moulding process is a subset of a project to create substrateless packaging of electronics. The selection of materials for this study therefore partly depends upon the class of materials used in electronics manufacture.

4.2.1 Electronic Assemblies

A typical electronic assembly consists of a PCB populated with electronic components. Surface Mount Assembly (SMA) technology accounted for more than 80% of electronics manufacture by the late 1990's [2]. The typical steps involved in electronics manufacture using SMA technology are:

1. Stencil printing solder paste on to a board
2. Placing the component on the board
3. Heating the entire assembly so that the solder melts and forms solder joints.

Details of this process can be found elsewhere [2]. It is clear that PCB's are central to the SMA technology as they carry all the electrical interconnections and mechanically support the assembly. The concept of 'substrateless packaging' of electronics, if successful, will be an alternative to PCBs. Hence the deliverables for substrateless packaging will be on similar lines to the deliverables for PCBs.

4.2.2 Material Properties expected from PCBs

The expected properties of PCBs vary according to the conditions of usage. Good mechanical strength may be a prime requirement in applications like computers, control panels etc., while in some other applications where high packaging density is required, (mobile phones etc) substrates may be flexible. Some of the important properties of PCBs are [37]:

1. *High dielectric strength*: This is the maximum field strength that the insulating material can withstand without the failure of the material. It depends on the thickness, material and the type of application.
2. *High dimensional stability*: It is important to minimise the differential shrinkage between copper and base material. Machining to exact dimensions is also facilitated.
3. *Low coefficient of thermal expansion*: In general the expansion in the Z direction is much higher than the X and Y direction, when the boards are exposed to heat. This may result in mismatch with copper traces and components.
4. *Good mechanical strength*: This is not a very critical requirement as most of the components are light in weight. It may however vary with the type of application.
5. *Resistance to water uptake*: It is preferred to be high for the reliability of the product (mechanical strength etc.).
6. *Low Flammability*: In general, most of the materials used are flame retardant. It is a general requirement for any materials used in electronics.

4.2.3 IPC standard 4101B

Although the properties of the materials selected for the current project may or may not be similar to the properties of the PCBs, they will have to deliver the same or higher performance in operation. *IPC – 4101B* specifies guidelines about the materials properties and requirements of PCBs [38]. These requirements are similar to the expected properties of PCBs discussed earlier. As the current process will not be a one-to-one replacement of PCBs, all the requirements mentioned in the standard are not considered.

4.3 Uses of Thermoplastics for Electronic Interconnection

While selecting thermoplastics for the process, due consideration was given to the previous attempts to use them in electronics. Some of them are described in this section.

a) *Moulded Interconnect devices (MID)*

MIDs and factors affecting their successful manufacture have been extensively studied for almost two decades now. Table 5 gives the list of some of the materials used to manufacture MIDs.

Table 5: Materials used in MIDs

Material	Reference
Polycarbonate (PC), Polybutylene terephthalate (PBT), Polyamide 66 (PA 66),Polyphenylenesulphide (PPS)	Glendenning *et. al.* [5]
Polyamide 6 (PA 6), PA 66, PBT	Paproth *et. al.* [6], Paproth *et. al.* [7]

b) *Encapsulation of printed circuit boards* by thermoplastics

Work is on going to use thermoplastics for electronic packaging or encapsulation of PCBs. Some of these are listed in Table 6 below.

Table 6: Thermoplastics used for encapsulation

Material	Reference
PA 66	Glendenning *et. al.* [5]
Liquid crystalline polymer (LCP), PPS, Polyphthalamide (PPA), Polyetheretherketone (PEEK)	Gilleo *et.al.* [8][36]
Nylon, Polyester	Teh *et al.* [34]

4.4 Choice of Materials for This Study

4.4.1 Overmould

From the discussion in the previous section, it is clear that the thermoplastics used were 'engineering' plastics rather than commercial polyolefins like high density polyethylene, low density polyethylene (HDPE, LDPE). It is not a surprise that polyolefins, which are the most widely used class of thermoplastics, were neglected as they are not fire retardant. Comparatively the fire retardant properties of engineering plastics are far superior. Thus, it was decided that the choice of materials for this study should be limited to 'engineering' thermoplastics. Also, as this study is a subset of the substrateless packaging process, thermoplastics that can be plated (post-processing operation) were also one of the selection criteria.

4.4.2 Electronic Component Materials

A typical silicon chip electronic component packaging consists of the chip (die) wire-bonded to the lead frame, encapsulated with epoxy moulding compound (EMC). Only the package terminals or pins ('legs') are seen and everything else is completely sealed. The legs of the electronic components are made up of copper and are often coated with tin as tin acts as a solderability preservation coating [39][40].

4.5 Selected Thermoplastics and Their Properties

The following section gives the list of thermoplastics selected for analysis. All the materials selected conform to the basic criterion mentioned in IPC-4101B. Detailed description and properties are covered elsewhere [41][42].:

1. *Polycarbonate (PC):* Good adhesion to most metals. Compatible with adhesives based on epoxies, polyurethanes, silicones and cyanoacrylates though preliminary tests are essential. They can be metallised after suitable processing. Calibre 301-10 injection moulding grade from Dow (Ashland) was used for this study.
2. *Polystyrene (PS):* Can be metallised using vacuum evaporation and galvanometry. Styron 634 sourced from Rapra was used for this study.
3. *Acrylonitrile butadiene styrene (ABS):* It shows good adhesion to metals. It can be electroplated. Polylac PA-747 from Chi Mei Corporation was used for this study.
4. *Polybutylene terephthalate (PBT):* It has been used as substrate for MID. Shows good adhesion with other thermoplastics. Celanex 2500 (unfilled) injection moulding grade from Ticona engineering polymers was used for this study
5. *Polymethylmethacrylate (PMMA):* Good adhesion to polymers and metals. Plexiglas 8N (glasklar) from Rohm was used for this study.
6. *Polyamide 6 (PA 6):* Has been extensively used in MIDs. It can be metallised. Ravamid R 200 S from Ravago was used for this study.

It should be noted that PC, PMMA, PS and ABS are amorphous in nature while PBT and PA 6 are semicrystalline thermoplastics.

Table 7 summarises the general properties of these thermoplastics. For more information refer to material data sheets in Appendix 2.

4.6 Selected Insert Material

This study focuses on the interconnections between the components that require no gaps between the pin and overmould and hence, the study of adhesion of the metal thermoplastic interface is the area of focus rather than the EMC-thermoplastic overmould interface. The legs of the electronic components are usually tinned copper. Hence tin was selected as the insert material for insert injection moulding experiments and tin foil and tin particles were used for the contact angle analysis and the AFM force-distance experiments respectively. In fact the surface of tin is always oxidised. It should therefore be borne in mind that although in this work adhesion between thermoplastic and tin is spoken about, it is actually adhesion between thermoplastics and tin oxide which is being measured. The details of the materials ordered are covered later in the respective experiment Chapters.

Table 7: Key properties of thermoplastics used

Sr. No.	Property	Unit	PC	PS	ABS	PBT	PMMA	PA 6
1	Glass transition temperature(T_g)	°C	152	89	110	47	117	48
2	Melting temperature(T_m)	°C	-	-	-	225	-	226
3	Mould shrinkage	e^{-4}mm/mm	50 – 70	40 - 70	30 – 70	180-200	10 - 80	70
4	Thermal conductivity	W/m.K	0.193 – 0.218	0.121 – 0.131	0.254 – 0.264	0.2741 – 0.2851	0.167 – 0.251	0.233 – 0.253
5	Flammability	UL 94	V2	V0	V0	HB	V0	V2
6	Coefficient of thermal expansion	µm/m-°C	68	70-80	111	1.1	80	-
7	Drying		120°C, 3-4 hrs	70-80°C, 2-3 hrs	85-90°C, 2-3 hrs	120-140°C, 2-4 hrs	98°C, 2-3 hrs	80°C, 4-16 hrs
8	Processing Temperature	°C	280	220	220	260	235	260

5 Atomic Force Microscopy

Contents

- *The Atomic Force Microscope*
- *Force-distance Curve*
- *Functionalising the AFM Tip*
- *Study of Adhesion Using the Force-distance Curves*
- *Methodology*
- *Results*
- *Discussion*
- *Conclusions*

The atomic force microscope (AFM) has the ability to measure the strength of inter-atomic interactions and so is one of the few instruments that can be used to characterise solid-solid surface forces directly. The examples of these solid-solid / inter-atomic forces are electrostatic, magnetic, double layer, Van der Waals and frictional forces. The quantitative measurement of these inter-atomic forces can in principle be used to calculate the work of adhesion between the material of the probe and the substrate.

In this chapter, an experimental methodology is described to obtain force-distance curves by attaching tin particles to the AFM cantilever. The adhesion force for each of the tin-thermoplastic pair were quantified and compared. Implications of the interaction forces at interface on adhesion between tin and thermoplastics used were discussed.

5.1 The Atomic Force Microscope

The AFM was invented in 1986 by Binning and Rohrer. It is a scanning probe microscope that can be used for imaging conducting as well as insulating surfaces. The AFM is also known as a scanning probe microscope. This name is derived from the fact that in an AFM the sample is scanned by a tip mounted on a spring cantilever (Fig.18). Typically the cantilevers and tips are made of silicon or silicon nitride with the radius of curvature of the tip of the order of a few nanometers. In the simplest mode of operation the tip moves vertically during scanning due to force interactions with the surface. This movement of the tip is monitored optically using a laser spot reflected off the top surface of the cantilever.

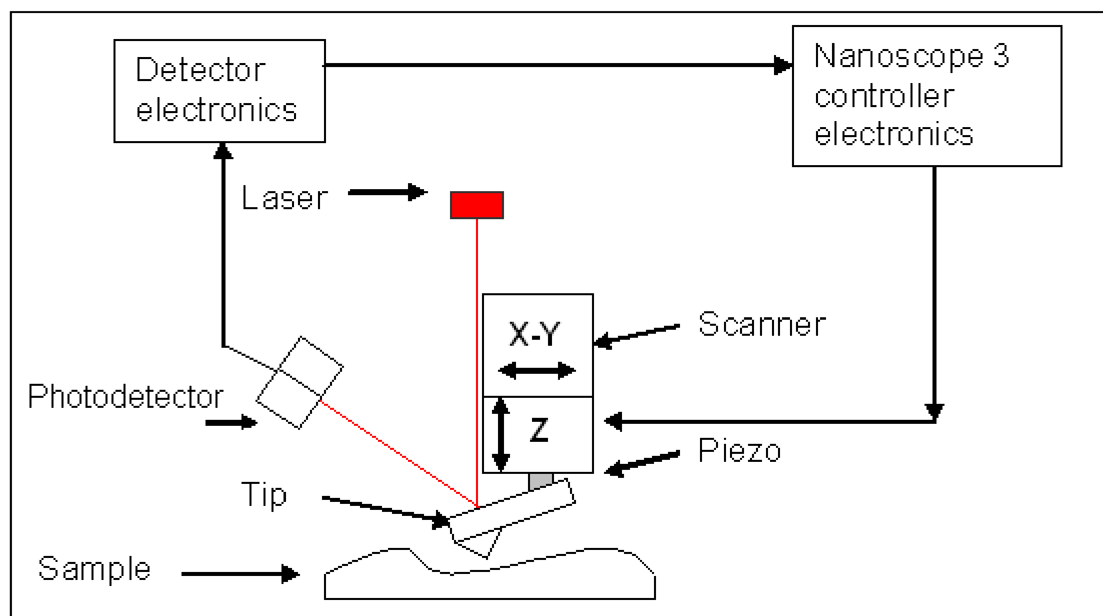

Figure 18: Set up of the AFM

Thus, for example, undulations in the surface can be mapped by moving the tip over the sample, generating a topographical image. A feedback mechanism is usually employed to move the cantilever mounting vertically to maintain a constant force between the tip and the surface as the tip scans across the surface and this mechanism avoids any collision thus avoiding damage to the tip.

5.1.1 Imaging Modes

The AFM is typically operated in the *static mode* or *dynamic mode*. In the static mode the AFM tip is moved across the surface and the undulations of the surface are mapped. This mode is also known as *contact mode*. In dynamic mode, the tip is oscillated at a resonance frequency with amplitude of a few nanometers near the surface. The interaction of the tip and the surface changes the resonance frequency of the cantilever which is monitored and the feedback loop maintains a constant frequency or amplitude by varying the tip-sample distance. The scanning software can create a topographical image by analysis of the tip-sample distance at each data point. This mode is therefore also known as *non-contact mode*. Along with these two modes of operation, the AFM can also be operated in *tapping mode*. This is a combination of the static and dynamic modes. The tip is oscillated close to the surface at resonant frequency, however the amplitude can be greater than the one used in non-contact mode. The principles of image generation are similar to the non-contact mode, with the exception that the tip makes intermittent contact with the surface.

5.2 Force-distance Curve

Along with the topography of the surface, the AFM can also be used to measure the interactions between the tip and the surface. An AFM force-distance curve is a plot of tip-sample interaction forces Vs tip-sample distance. The vertical height (Z) of the cantilever mounting is represented on the horizontal axis and the cantilever deflection (δ_c) is represented on the vertical axis. (Fig 19)

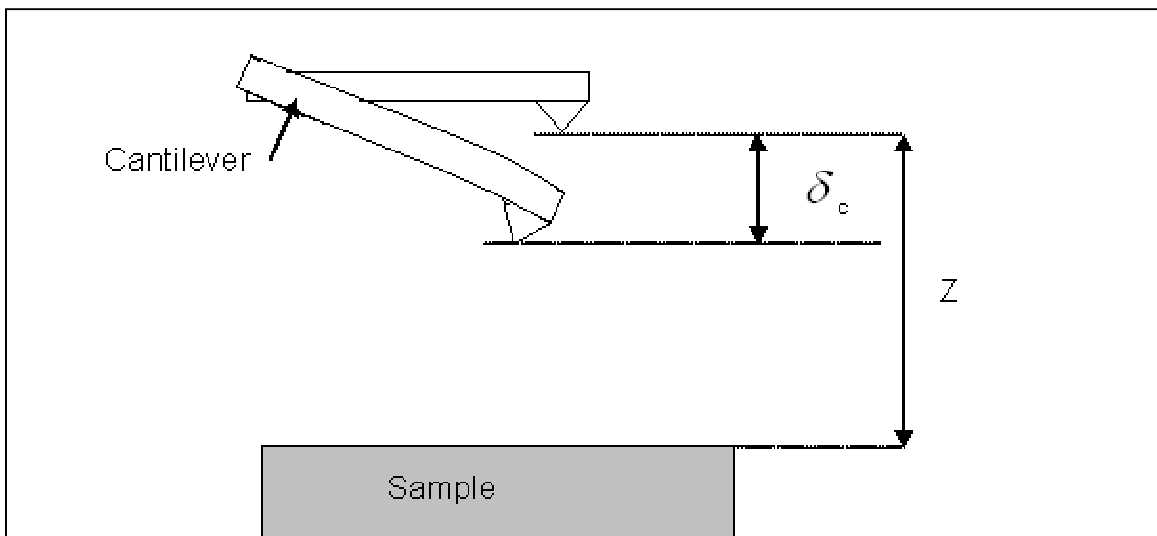

***Figure 19*: A typical tip-sample system**

Using the spring constant of the cantilever, the tip deflection can be converted into force using Eqn. 7 and thus, the magnitude of the forces of interaction between tip and sample can be mapped.

$$\boldsymbol{F = -k\delta_c} \qquad \text{.................... [7]}$$

Where,

F = Force,

k = Stiffness of cantilever,

δ_c = Distance the cantilever is bent/ cantilever deflection.

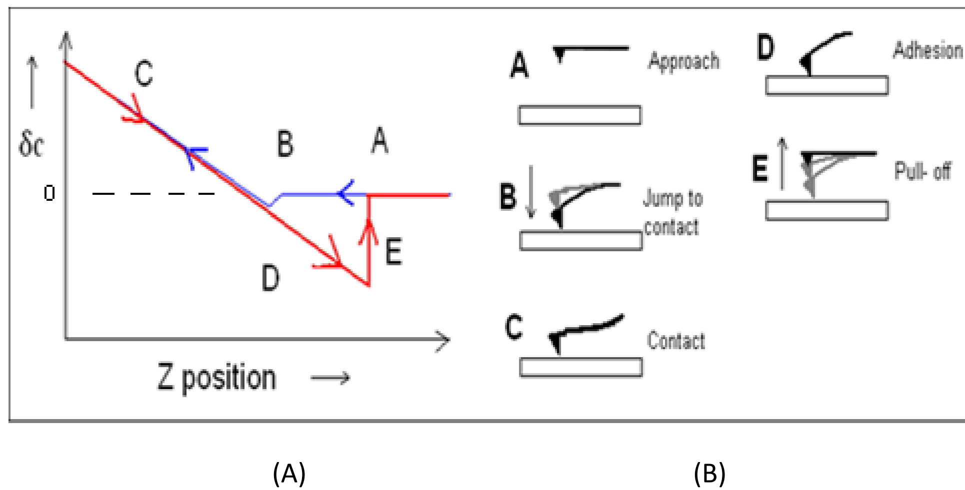

(A) (B)

Figure 20: Typical force curve with labelling corresponding to tip-sample interaction points

A typical force-distance plot (δ_c Vs Z position) is shown in Fig. 20. The various regimes of the plot (Fig. 20(A)) correspond to the positions of the cantilever (Fig. 20(B)). The blue line on the plot represents the extending plot, i.e. plot of measurements during the approach of the cantilever mounting to the surface, and the red line represents the retracting plot. At stage A the cantilever is approaching the surface and δ_c is 0 (non contact regime). At a critical distance i.e. at stage B, the cantilever jumps into contact with the surface due to the interactions between the tip and the surface and the following stage, C, is therefore referred to as the contact regime. It should be noted that the jump-to-contact feature is not always seen. In stage C the cantilever mounting continues to the surface and is stopped at a preset

height. The mounting is then retracted, stage D, during which the cantilever tip remains in contact with the surface due to the adhesive forces. At a certain point, E, the elastic force due to the flexure of the cantilever is sufficient to overcome the adhesive forces between the tip and the sample, and the tip separates from the sample surface. The movement distance of the tip when it separates represents the pull off force and can be related to the force of adhesion between the tip and surface.

According to Derjaguin for the case of a spherical tip interacting with a flat surface, the work of Adhesion (W_a) is directly proportional to the pull off force ($F_{pull\ off}$) between the AFM cantilever tip (radius R_{tip}) and sample surface (Eqn.8) [43].

$$W_a = -\frac{F_{pull\ off}}{2\pi R_{tip}} \qquad \text{......................................} \ [8]$$

Thus, if the radius of the tip is kept constant i.e. if the same tip is used to test various samples, the extent of adhesion can be estimated by the magnitude of the pull off force ($F_{pull\ off}$). The pull off measurements require that the material of the tip surface and the substrate are representative of the materials for which adhesion measurement is sought. It is easy to change the substrate used in the test. Changing the material on the tip side of the interacting pair is more difficult and is referred to as “functionalising” the tip. Good methods for the production and use of functionalised AFM tips are thus necessary for such studies to provide useful data.

5.3 Functionalising the AFM Tip

While tips can be functionalised with coatings, e.g. gold, in this section functionalisation by attachment of a particle is discussed. Gan has written a detailed critique about the various particle attachment techniques to AFM probes for surface force measurements [44] and a support note supplied by AFM manufacturer Veeco also covers the methods to attach particles to AFM cantilevers [45]. Some of the techniques in the literature to functionalize AFM probes are as follows

- Attaching of particles to the AFM cantilever with the help of an adhesive [46]. The attached particles act as ‘‘replacement’’ tips.
- High temperature sintering of borosilicate glass onto the AFM cantilever [47].
- ‘Inversed self assembly’: i.e. grafting of nanoparticles onto the tip to act as a coating [48].
- Use of wet chemistry surface assembly to attach gold nanoparticles to the tip of an AFM cantilever [49]. The advantage of this process is that it does not require any high temperature equipment.
- Direct deposition by use of focussed electron beam or similar equipment to ‘‘weld’’ the particle of interest to the AFM cantilever. [48].

The advantages and disadvantages of these techniques have been discussed elsewhere in detail [44] but briefly, the use of high temperature sintering is limited to

borosilicate glass particles while grafting and wet chemistry surface assembly techniques are suitable only if the particles or surface coating are nano size. Typically, gluing of particles and direct deposition techniques are used to functionalise the AFM tip when the particle size is in *μm*. Each of these techniques requires customised instrumentation and expertise and the selection of a technique depends upon the availability of resources and the nature of the functionalisation needed.

5.4 Study of Adhesion Using Force-distance Curves

Many studies have used AFM to identify and quantify the interatomic interactions between materials. Capella *et.al.* Butt *et.al.* and Ralston *et.al.* have written comprehensive guides on force measurements with the atomic force microscope, explaining technique, interpretation and applications [43][50][51]. Wiling *et.al* obtained maps of the adhesion between an individual lactose particle attached to a tip and gelatine capsules [52]. Schaefer *et.al.* also obtained maps of adhesion using the AFM force-distance technique. They have described ‘‘jump mode’’ as a way of mapping adhesion for a surface [53]. Eve *et.al.* brought a salbutamol functionalised AFM tip to various surfaces of interest and measured the force experienced by the cantilever as a function of tip–sample separation. This study was used to rank adhesion of salbutamol with glass, PTFE and other materials [46]. Lantz *et.al.* reported direct force measurements of the formation of a chemical bond between silicon AFM tips and silicon samples [54].

Use of an AFM to understand adhesion at the material level and linking it to the macroscopic level has been attempted before. Schirmeisen *et.al.* calculated the force of adhesion between aluminium and polycarbonate and tried to compare the theoretical work of adhesion results with stud pull out tests. They concluded that the adhesion strength suggested by the AFM force-distance measurement is much higher than that of the mechanical strength test [55]. Wong *et.al.* used AFM to characterise the nanoscale adhesion force in a Cu–SAM–EMC system and used it as a criterion for selection of the SAM. The results were shown to be consistent with the results of macroscopic shear tests [56]. Han *et.al.* used (AFM) pull-off measurements to predict adhesion at the solid–solid interface. The results were compared to microvalves that had been fabricated with different surfaces at the seat⁄membrane interface, and they found good correlation between the AFM results and the macroscopic measurements [57].

5.5 Methodology

The primary aim of the AFM force-distance work reported in this chapter was to establish an adhesion hierarchy between tin and the selected thermoplastic polymers. According to Eqn. 7 the adhesive force can be calculated using the product of the spring constant of the cantilever and its deflection (δ_c). However, if the same cantilever is used (with the same particle on its tip and under similar ambient conditions) for all the tin-thermoplastic pairs, then δ_c measured for each tin-thermoplastic pair can be compared to establish relative adhesive strengths. Hence for the purpose of this study and for the reasons discussed later, δ_c readings were

not converted into force readings using the cantilever spring constant. Plots of δ_c vs Z were gathered for each thermoplastic-tin pair and used to derive bar charts showing the relative adhesive strength.

In order to carry out the experiments, a number of key steps were required.

Functionalising the probe: A reliable method of attaching tin particles to the AFM cantilever tips was required. Two techniques were shortlisted for the attachment.

a) Adhesive attachment of the particle to the tip: This method was carried out first as it does not require the use of any specialised equipment. This technique involved the use of a micromanipulator to attach the particle to the cantilever with the help of an adhesive. However, this technique was found not to be suitable for reasons discussed in section 5.5.3.2.1

b) Metallurgical bonding of the particle to the tip: This method involved ‘‘welding’’ particles to the tip within a dual beam focussed ion beam (FIB) microscope. This was found to be more successful and was used for the majority of trials.

Cantilever deflection measurements: A design of experiment was established to ensure the reliability and reproducibility of the data obtained and is discussed in section 5.5.4.2.

5.5.1 Materials and Experimental Apparatus

5.5.1.1 AFM

A Dimension 3100 instrument from Veeco (Digital Instruments) was used for this experiment. The AFM can be operated in tapping and contact mode. Nanoscope 6.12rl was the software interface (also provided by Veeco) that was used to record the data.

5.5.1.2 Tin Powder

Tin particles from Goodfellow (average size 45 micron 99.9 % pure) were used to functionalise the AFM cantilevers. When observed under a scanning electron microscope, the size of the tin particles was observed to vary from about 15 µm upwards. Not all the particles were spherical. Based on usage in the articles in the literature review of force- distance measurements reported earlier, spherical tin particles of size 15 +/- 2 µm were chosen for this experiment.

5.5.1.3 Polymer Samples

The polymer samples used for this experiment were injection moulding granules as received from the manufacturers. There was no particular reason to pre-process the granules and doing so would risk contamination e.g.: mould release agent coming in contact with the sample surface. The granules were however dried before the experiments in a fan oven. The time of drying was as recommended by the manufacturers for injection moulding processing.

5.5.1.4 AFM Probes

DNP 10 probes from Veeco were used first for this experiment. A DNP 10 probe has 4 cantilevers of varying nominal stiffness. The stiffest of the 4 cantilevers (highest spring constant) was functionalised. Table 8 gives the nominal properties of the DNP 10 probe cantilever that was functionalised. TESP probes from Veeco were also used for this experiment. Table 9 gives the nominal properties of the TESP probe cantilever that was functionalised.

5.5.1.5 Dual Beam Focussed Ion Beam Microscope

The Dual beam focussed ion beam (FIB) Microscope consists of a high resolution field emission gun electron column and gallium source focused ion beam column combined within the same instrument. An FEI Nova 600 Nanolab dual beam FIB FEG-SEM was used for this experiment.

Table 8: Properties of the DNP 10 cantilevers used

Thickness	0.6 µm
Length range	115-125 µm
Width range	20-30 µm
f_0 (frequency) range	50-80 kHz
k (spring constant) range	0.175-0.7 N/m
Backside coating	45 +/-5nm Ti/Au
Material	Silicon nitride

Table 9: Properties of the TESP cantilever used

Thickness-range	3.25-4.75 µm
Length-range	110-140 µm
Width-range	30-50 µm
f_0(frequency) -range	230-410 kHz
k (spring constant)-range	20-80 N/m
Coating	None
Material	0.01-0.025 Ώcm Antimony (n)doped Si

There was a micromanipulator attachment that can be used to move particles and samples inside the chamber.

5.5.2 Cantilever Deflection Measurements

The procedure for obtaining cantilever deflection (δc) for tips functionalised using both the methods is same. The details are as follows:

The sensitivity of the instrument along with the tip has to be calibrated before starting any set of experiment. This is done in order to allow the software to convert the signal in volts into deflection readings in spatial units i.e. nanometers. The procedure was:

1. The cantilever with the particle on its tip was mounted in the probe holder and attached to the AFM.

2. The AFM software was switched on.

3. The laser was directed at the back of the tip. It reflects to the light detection sensor. This signal in the relaxed state corresponds to 0 volts. Any subsequent movements of the cantilever cause fluctuations in the signal from the laser.

4. For the purpose of the force-distance experiment, contact mode was selected from the software control menu.

5. The engage command was given to the software. This brings the tip down steadily, towards the surface.

6. When the software indicated the contact of the tip with the surface, the force mode command was given to the software. This mode gives the force-distance curve as an output.

7. Sensitivity was calibrated by taking the slope of the contact part of the retracting curve.

8. The above procedure was repeated to obtain the cantilever deflection.

The sensitivity depends on the precise positioning of the laser on the probe. Hence, sensitivity was calibrated after placing the probe in the holder and the position of the probe was not changed for the entire experiment. The sensitivity calibration has to be redone if the position of the laser or the probe is disturbed.

5.5.3 Adhesive Attachment of the Particle to the Tip

5.5.3.1 Method

A modified sample stage with manual control over the X, Y and Z axis motion and an objective lens attached vertically, normal to the stage was used for this purpose (Fig. 21). The objective lens was connected to a monitor. A selection of tin particles were placed on a clean glass slide and placed under the stage such that they could be viewed on the monitor. The AFM probe was then placed in a holder (Fig. 22) that fits into a slot in the stage, over the glass slide. UV curing adhesive

from Loctite was used for this experiment. The adhesive was placed on the glass slide with the help of a dropper, in an area away from the particles. The AFM probe was then moved to a position over the adhesive using the X and Y axis controls of the stage, such that when the tip was lowered it would come into contact with the edge of the adhesive drop. This was done in order to avoid excess adhesive getting attached to the tip.

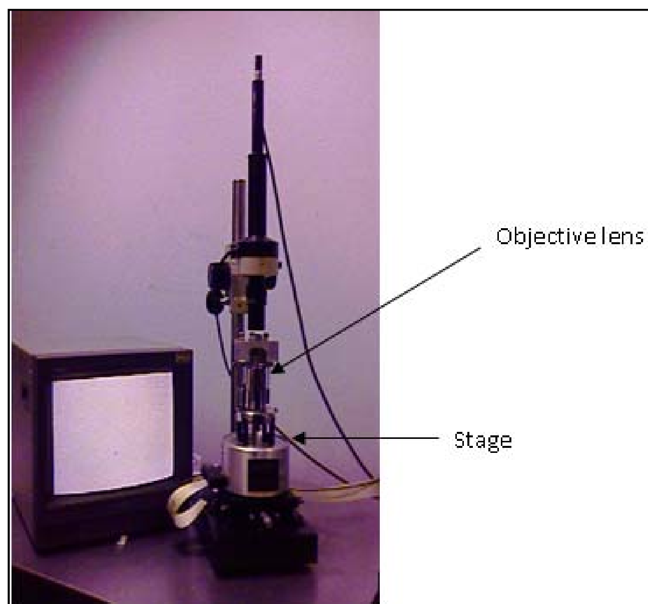

Figure 21: AFM with manual Z axis control used for gluing particles to the probe

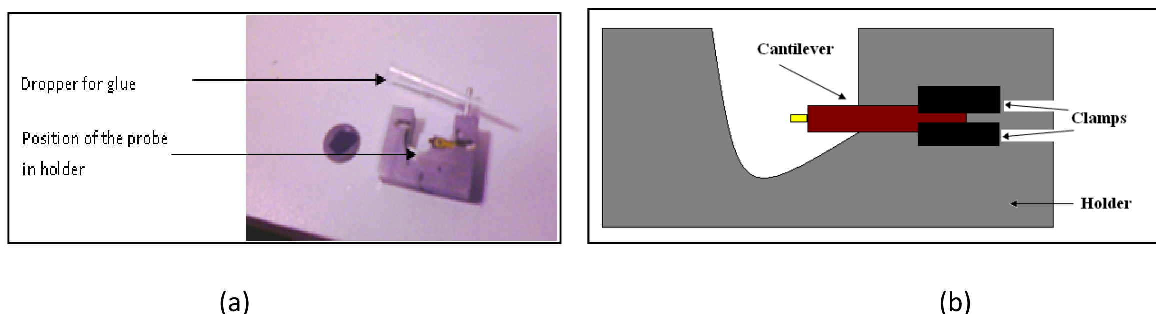

(a) (b)

Figure 22: (a) The holder for the probe (b) Schematic

Also, care had to be taken to avoid contact for a long duration, as the capillary action of the adhesive would result in excess glue on the probe. Once the adhesive was on the tip, it was moved to a position over a suitable tin particle selected to be near spherical and with a diameter of 15 ± 2 μm. The tip of the probe was aligned to the centre of the particle in such a way that when the tip was lowered using the Z axis movement, it exactly touched the intended particle (Fig. 23). Care was taken, as multiple contacts or rolling of the particle would most certainly result in adhesive being deposited on the side of the particle which was going to be used for analysis.

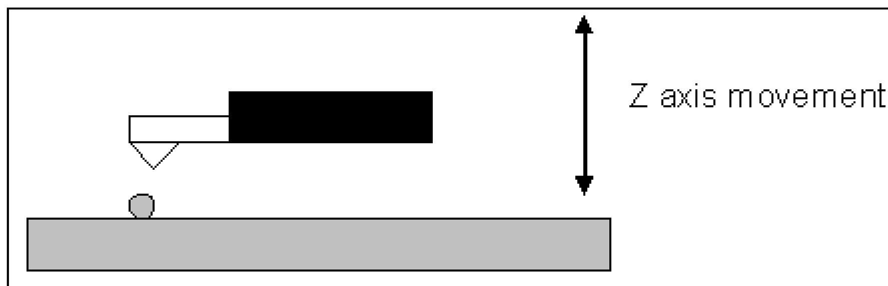

Figure 23: The relative position of the cantilever with respect to the particle for attachment by glue

The probe with the attached particle was then removed from the holder and placed under UV light for 30 min (Fig. 24). When the adhesive was cured, the particle was strongly attached to the probe and could be used for further testing.

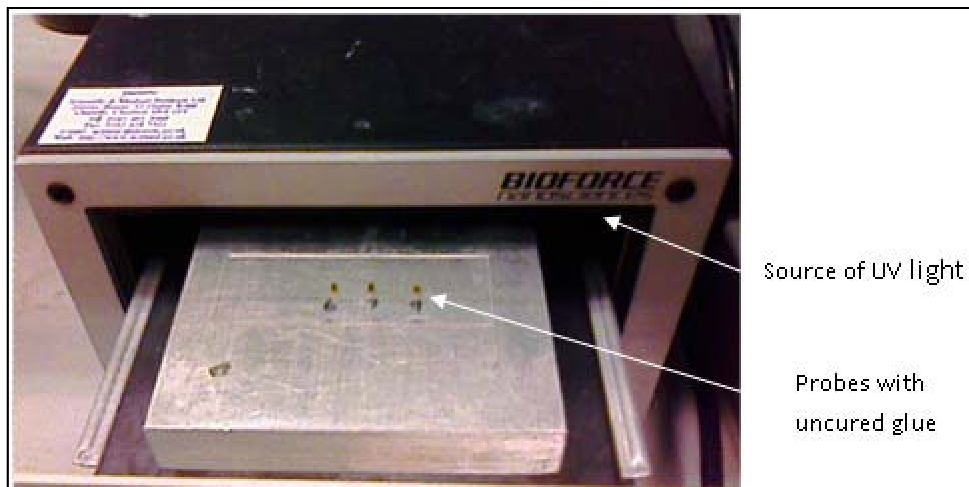

Figure 24: The UV light chamber

5.5.3.2 Results

5.5.3.2.1 Initial Measurements with Glue Method Functionalised Probes

Initially DNP-10 probes functionalised by the glue method were used in the AFM to obtain cantilever deflection curves as described above. It was found that the experiment did not give meaningful readings as the data was either out of scale or the plot was dissimilar to that expected. Fig. 25 shows an example of the results obtained with a PMMA substrate. As the probe approached the sample (the curve labelled as ‘‘extend’’ in the figure), the cantilever deflection (δ_c) did not remain constant leading to a curved trace in contrast to that normally expected (see region A in Fig. 20). This was thought to be due to insufficient stiffness in the cantilever. When the critical point was reached however a snap to contact feature was observed. Further downward motion of the cantilever led to deflection similar to that shown in region C of Fig. 20. However, during the return trace the deflection did not follow the

original line and instead showed a flat line response that was interpreted as the cantilever having bent beyond the measurable range. It appears that as the pull-off force is a product of cantilever stiffness and (δ_c), the lower stiffness of DNP-10 probe resulted in high δ_c values. After withdrawing the probe for some distance it did appear to separate from the surface, but it was not possible to measure the pull off force from the curve produced as the maximum deflection of the cantilever was not recorded.

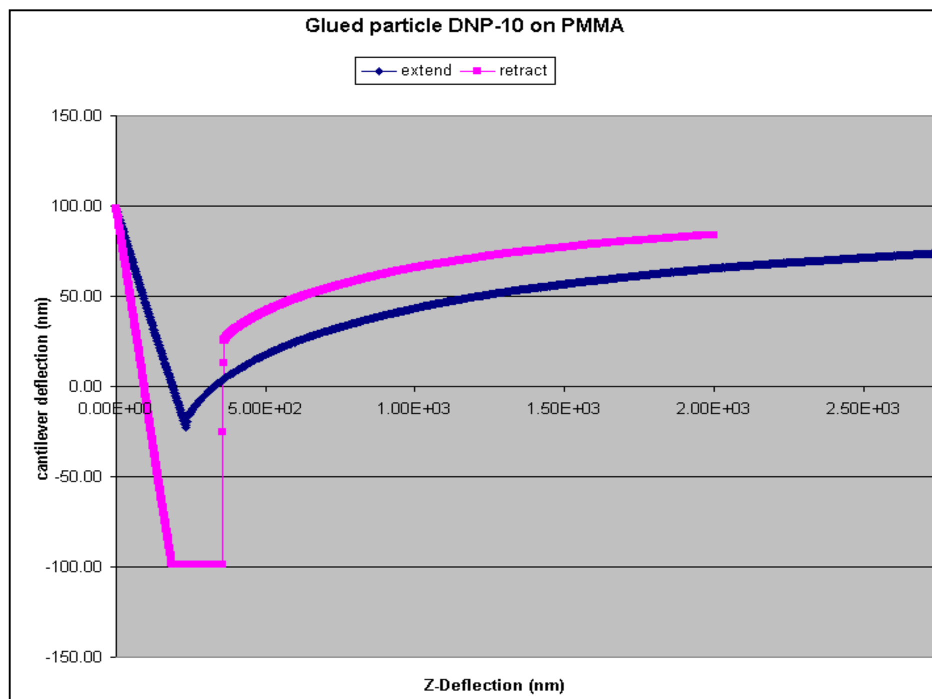

Figure 25: Out of scale results for the DNP-10 tips

The conclusions from the initial experiments were therefore that cantilevers with higher spring constants should be used so that the data would be within the measurable deflection range. The alternative considered was to reduce the particle size which may result in reduced adhesion force, also reducing the degree of

maximum deflection [43]. However, it would be very hard to reduce the particle size below 15 +/- 2 μm, as the area of contact of the particle (the test surface) would be far more likely to become contaminated with adhesive due to capillary action. Hence, the use of a stiffer tip was accepted as the way forward and a Veeco TESP cantilever was trialled for the next experiment.

Attempts to attach a tin particle to the TESP cantilever were unsuccessful due to the tip geometry. With the glue method the particle attaches to the cantilever close to the tip rather than to the tip itself, as shown in Fig. 26. Unlike the DNP 10 tip which has a height of 5μm max., the TESP tip has a height of 15 μm (25 μm max.). It was attempted to place the particle at the end of the tip but it always rolled off. Thus the particle would not come in to contact with the surface and if it did it would be contaminated with adhesive. As a result, the use of adhesive to attach the particles was discounted and a new method of attachment was investigated.

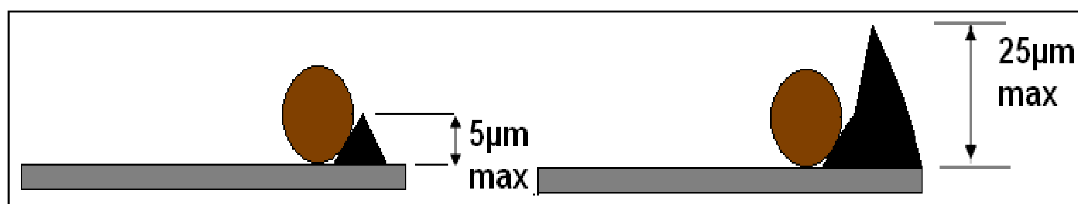

Figure 26: Illustration of the glued particles on DNP 10 tip and TESP tip

5.5.4 Metallurgical Bonding of the Particle to the Tip

5.5.4.1 Method

This technique used the dual beam SEM/FIB system with a micromanipulator attachment. This method of particle attachment was adapted from work done by Sqalli *et.al.* [48]. The stages in the attachment of the particles were as follows:

1. The AFM cantilever to be functionalised and a selection of tin particles were spread on a gold plated glass slide and placed in the vacuum chamber of the dual beam microscope. (Fig. 27)

2. The tip of the micromanipulator was sharpened so that the point of contact between the micromanipulator and particle was minimised. It also helped in detaching the particle from the micromanipulator (Fig. 28).

3. After scanning the slide a particle was selected for use (Fig. 29). The size of the particle was generally limited to 15-20μm.

4. The micro-manipulator was manoeuvred towards the particle and the particle was attached to the micromanipulator by platinum deposition. Platinum was locally melted (in the vacuum chamber) with the help of the electron beam (Fig. 30)

5. The micro-manipulator with the particle attached was then manoeuvred towards the AFM cantilever, touching the tip.(Fig. 31)

6. Platinum was deposited on the back of the cantilever through to the particle. The process effectively ‘‘welded’’ the particle to the tip position.

7. Finally, the gallium ion beam was used to cut the micromanipulator away from the particle to release the functionalized tip (Fig. 32).

5.5.4.2 Design of Experiment

Having established a method for functionalising a probe, a design of experiment was conducted before carrying out measurements. The spring constant of the cantilevers, surface roughness, humidity, temperature, size of particle, contamination etc. can all affect the results obtained from a force-distance calculation. Thus, the magnitude of adhesion obtained for a particular tin-thermoplastic pair depends upon the variables involved during that particular experiment in addition to the inter-atomic forces. In order to be able to compare and rank the tin-thermoplastic pairs, these variables had to be accounted for through the design of experiment. The basic principles were to generate a set of measurements, consisting of readings from all the 6 thermoplastics, with the same tip in a single sitting; to generate multiple sets of measurements taken on different days and at different times of day; and to vary the order of materials within each set. The design of experiment should therefore have guarded against systematic errors due to the variables listed above distorting the results.

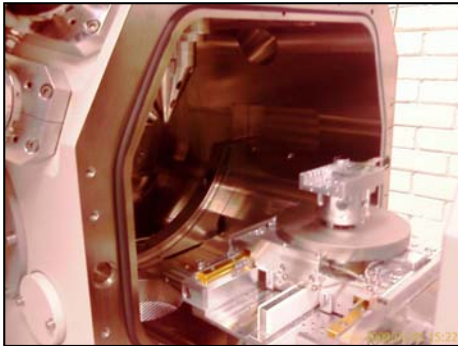

Figure 27: Vacuum chamber of the dual beam microscope

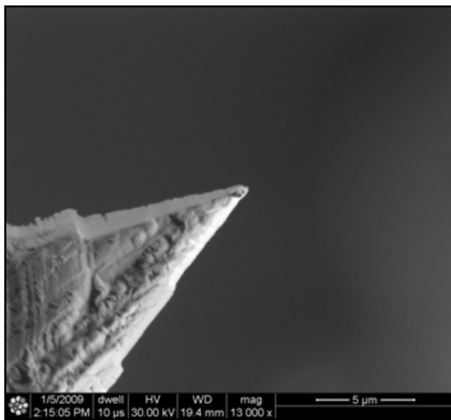

Figure 28: Sharpened tip of the micromanipulator

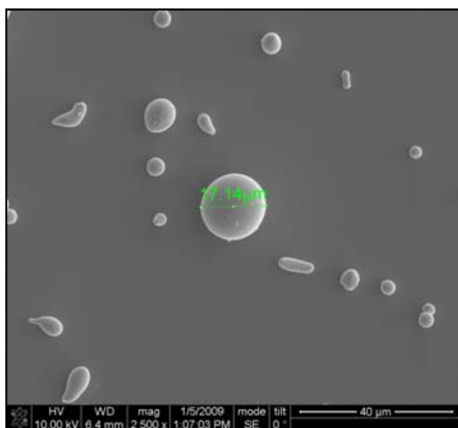

Figure 29: Size of the selected particle

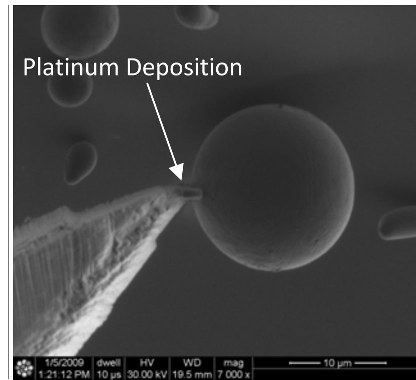

Figure 30: Platinum deposition to join micromanipulator to the particle

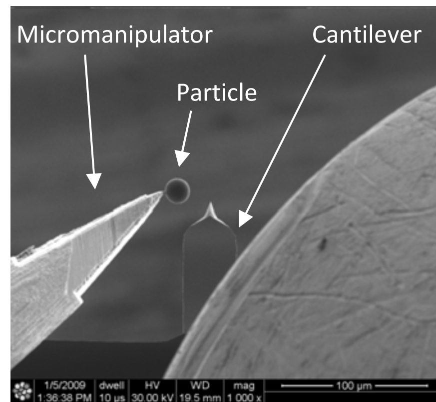

Figure 31: Micromanipulator with particle attached moving towards the tip of the probe

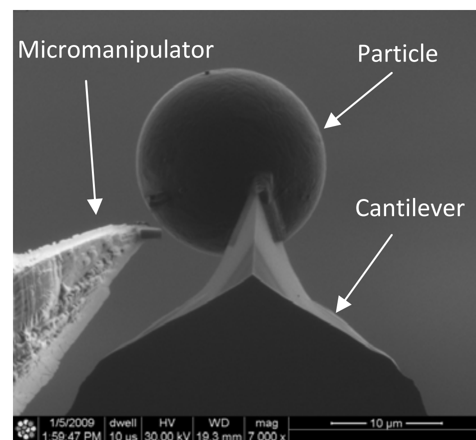

Figure 32: Micromanipulator detachment

- **Spring Constant of Cantilevers:** In all three tips were functionalised. Although all the cantilevers had the same nominal specifications, their actual spring constants can vary. According to the specifications they can be anywhere between 20-80 N/m. The exact value of spring constant is necessary if an absolute force reading is to be obtained from the cantilever deflection (δc). As the purpose of this study was only to obtain the relative adhesion strengths of the tin-thermoplastic pairs, taking care to use a single cantilever over a full reading set allowed direct comparison between materials and eliminated the need to measure spring constants.

- **Surface roughness:** Surface roughness may affect the results as the area of contact between the particle and the surface changes with the change in surface roughness. To mitigate against this, readings were taken from multiple areas on each sample surface and an average was calculated.

- **Humidity and temperature effects:** All the samples were dried before the experiments. However, on subsequent exposure to normal atmospheric conditions the polymers would begin to re-absorb moisture and develop a surface film of moisture. In order to reduce variation in results due to variation in atmospheric humidity, measurement runs were conducted in one sitting. A measurement run consisted of a set of readings on all six tin-thermoplastic pairs, ensuring that the humidity and temperature conditions remained more or less constant across all the samples. Also, in order to confirm that the variation in humidity and temperature did not affect the relative adhesive strengths,

each run of readings was produced at a different time of day and on different days. The order in which the polymers were tested was also varied so that a systematic absorption of moisture during the course of the experiment would not affect the results.

- **Size of particle:** The magnitude of the cantilever deflection can vary to a large extent due to the difference in contact area on account of the difference in particle size. Hence, the results from one functionalised tip could not be compared (in absolute terms) to the other functionalised tips. However, the ratios among the materials could be compared.

- **Wear of particles causing change in contact area:** Repeated use of the functionalised probes could result in systematic variation in the data on account of wear of the particles. In order to mitigate against this, the same cantilever was used for three different measurement sets, and an average of all the 3 sets was taken to be the adhesion strength. Also the order of materials tested was changed for every set. To further validate the data, the experiment was repeated with two other functionalised cantilevers.

- **Contamination:** Contamination of samples produced by the injection moulding process is unavoidable. Processing generally involves the polymers coming in contact with the mould surface. The moulds are sprayed with mould release agents and may have other impurities. Also the polymer melt can pick up impurities in the hopper, barrel etc. on its way to the mould. Hence to avoid all these impurities on the surface and to avoid batch to batch variations,

polymer granules from manufacturers were used for this test without any further processing.

In order to compare adhesion strength measurements among the results from the three different cantilevers, cantilever deflection values were normalised with respect to PA 6. Thus, although the average magnitude of the cantilever deflection for each material was dependent on the cantilever used, the normalised values should be comparable.

5.6 Results

As described above, tin particles were FIB welded to the TESP probes and used. Sensitivity calculations were done and cantilever deflection (δc) Vs Z plots were obtained. Fig. 33 shows a representative plot obtained using cantilever 1 with PA 6. The plot represents two traces, the approach (extend- blue line) and the pull off (retract- red line). The extend phase starts from the right (high Z value) and moves left towards zero while the retract phase starts at the left of the plot and moves to the right. During the extend phase of the plot the cantilever moved towards the sample. At a critical distance, due to the forces of attraction between the tin and the sample, it was expected to jump to contact. However in this case this was not clearly observed as the magnitude of the cantilever deflection may vary depending on the tip-sample interactions. As the cantilever moved further towards the sample, the cantilever deflection started to increase. This region, marked “X” in the plot, corresponds to when the tip was in contact with the surface, i.e.; the contact regime. At the end of

the extend phase, the cantilever started moving away from the sample - this marks the start of the retract phase. On account of adhesion forces acting between the materials attached to the tip of the cantilever and the polymer sample, more elastic force is required for the cantilever to jump out of contact. This force is normally referred to as ‘pull off force’. Normally after the cantilever jumps out of contact, the retract plot re-traces the extend plot as seen here.

Overall, the traces showed behaviour that was consistent with the expected curve shown earlier in Fig. 20. At the start of each run, should the cantilever experience a long range attractive (repulsive) force in the non-contact region i.e. before the jump to contact, it will deflect downwards (upwards) before making contact with the surface giving rise to a curved rather than a straight line. This was the case for the glued particle on the DNP-10 probe shown earlier that showed a curved approach / retract plot as a result of larger particles and lower spring constant. In the results for the FIB welded particle on TESP cantilever, a straight line was obtained instead and demonstrated that, this effect can be avoided by using a cantilever with a high spring constant.

Fig. 33 to 38 represent one set (set 1) of readings for all six polymers recorded using cantilever 1. It is clear from the figures that each polymer has a unique cantilever deflection plot. The form of the curves is very similar except that the degree of cantilever deflection varies. In particular, in the contact regime the loading and unloading curves seldom overlap; it can be seen that the loading curve does not exactly retrace the unloading curve. In fact in the case of ABS the difference is very

apparent. This may be because of the viscoelastic nature of the materials [43] [50]. The curves would be expected to have overlapped exactly in the case of perfectly elastic materials. However, in the case of viscoelastic materials the sample undergoes some plastic deformation during loading and it does not regain its shape during unloading. Most samples have mixed behaviour and hence the curves seldom overlap. In general the nature of the curves is still very similar to the ones reported in literature.

The jump to contact feature during the extend phase of the plot varies from polymer to polymer as it occurs when the gradient of attractive forces exceeding the spring constant. The majority of the samples showed very little jump to contact, except ABS that showed a clear interaction. The difference in δc between the point at which the cantilever came free from the surface and the non contact level (straight line) was used to define the pull off force for all plots as described in Section 5.2.

Table 10 summarise the results from all of the experiments. It can be seen that the results were very consistent for the same cantilever such that the results obtained from each sample were within a range of the average of the three readings obtained from each sample. In order to be able to compare the results, the cantilever deflections were normalised to the value for PA 6. Fig. 39, 40 and 41show bar graphs of these normalised values for the three cantilevers used. For all three cantilevers the observed trend was almost the same except for cantilever 2 where ABS and PBT exchanged places. However the value obtained for these polymers with all three cantilevers were very close. It is clear that the cantilever deflections can be robustly

ranked in order to understand which polymers show better surface-surface adhesion to tin. In general the order is (strongest to weakest adhesion)

PC > PMMA > PBT > ABS > PS > PA 6

PC and PMMA were noticeably stronger than the other polymers.

Table 10: Cantilever deflection experiments

Cantilever 1						
	PS	PBT	PC	ABS	PMMA	PA6
Cantilever deflection (nm)	9.30	11.20	19.90	10.40	18.10	7.90
	9.60	11.40	19.80	10.10	18.30	7.80
	9.20	11.10	20.70	10.10	17.90	8.10
Avg. Cantilever Deflection	***9.37***	***11.23***	***20.13***	***10.20***	***18.10***	***7.93***
Ratio	1.18	1.42	2.54	1.29	2.28	1.00
Cantilever 2						
	PS	PBT	PC	ABS	PMMA	PA6
Cantilever deflection (nm)	13.40	14.20	25.10	14.30	23.70	10.10
	12.00	14.60	25.60	14.40	23.60	11.50
	13.10	14.20	25.30	14.80	23.10	11.10
Avg. Cantilever Deflection	***12.83***	***14.33***	***25.33***	***14.50***	***23.47***	***10.90***
Ratio	1.18	1.31	2.32	1.33	2.15	1.00
Cantilever 3						
	PS	PBT	PC	ABS	PMMA	PA6
Cantilever deflection (nm)	13.40	18.20	28.50	16.30	26.20	11.10
	12.30	18.60	28.10	16.10	26.90	11.50
	11.70	19.20	28.30	15.80	26.50	11.10
Avg. Cantilever Deflection	***12.47***	***18.67***	***28.30***	***16.07***	***26.53***	***11.23***
Ratio	1.11	1.66	2.52	1.43	2.36	1.00

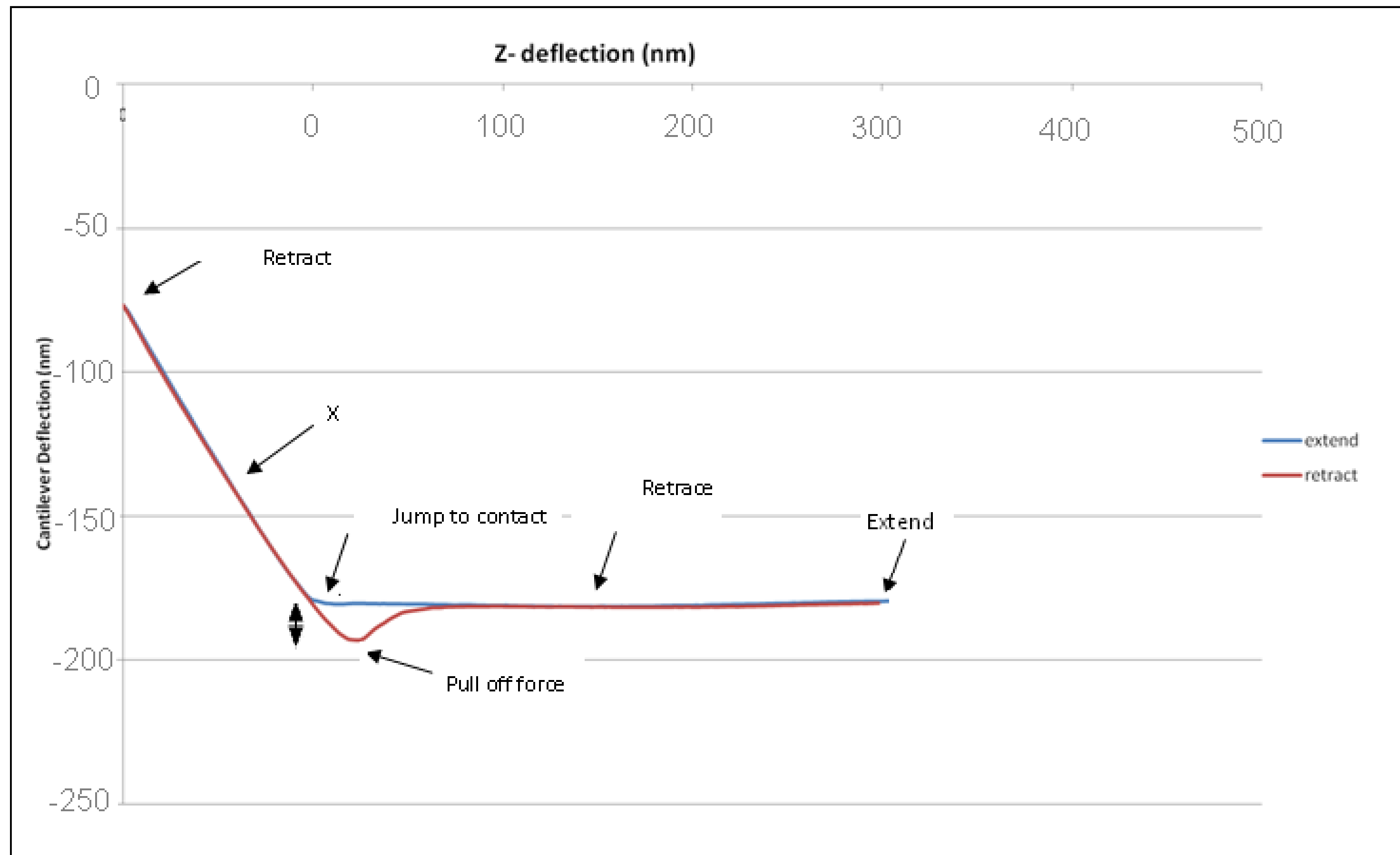

Figure 33: Cantilever deflection Vs Z deflection for tin functionalised TESP probe and PA 6

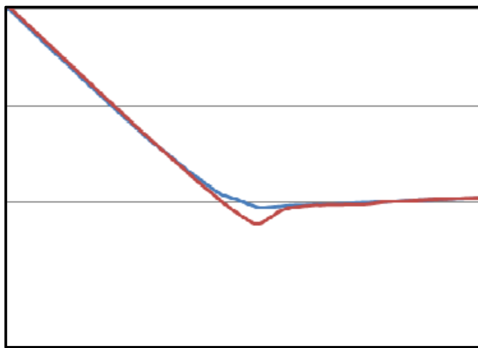

Figure 34: Cantilever deflection Vs Z deflection Sn functionalised TESP and PS. Axis scales as for Fig. 33

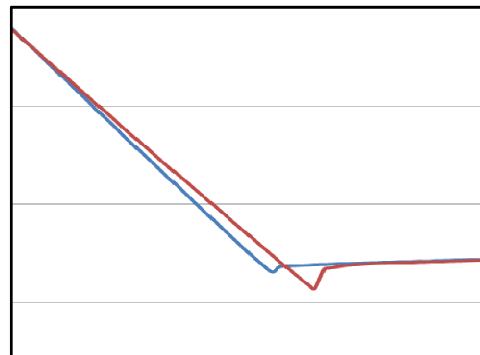

Figure 37: Cantilever deflection Vs Z deflection Sn functionalised TESP probe and ABS. Axis scales as for Fig. 33

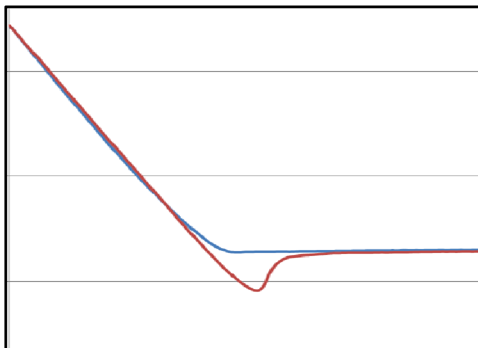

Figure 35: Cantilever deflection Vs Z deflection Sn functionalised TESP probe and PC. Axis scales as for Fig. 33

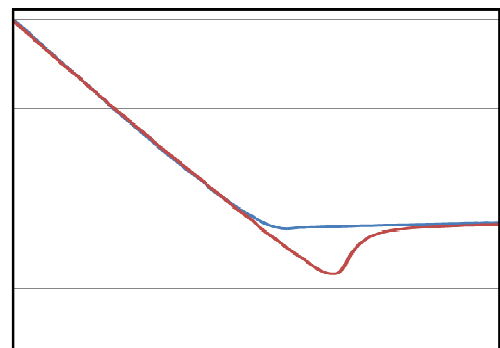

Figure 38: Cantilever deflection Vs Z deflection Sn functionalised TESP probe and PMMA. Axis scales as for Fig. 33

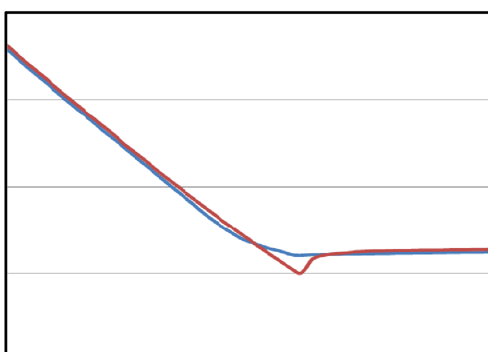

Figure 36: Cantilever deflection Vs Z deflection Sn functionalised TESP probe and PBT. Axis scales as for Fig. 33

Experiment 1

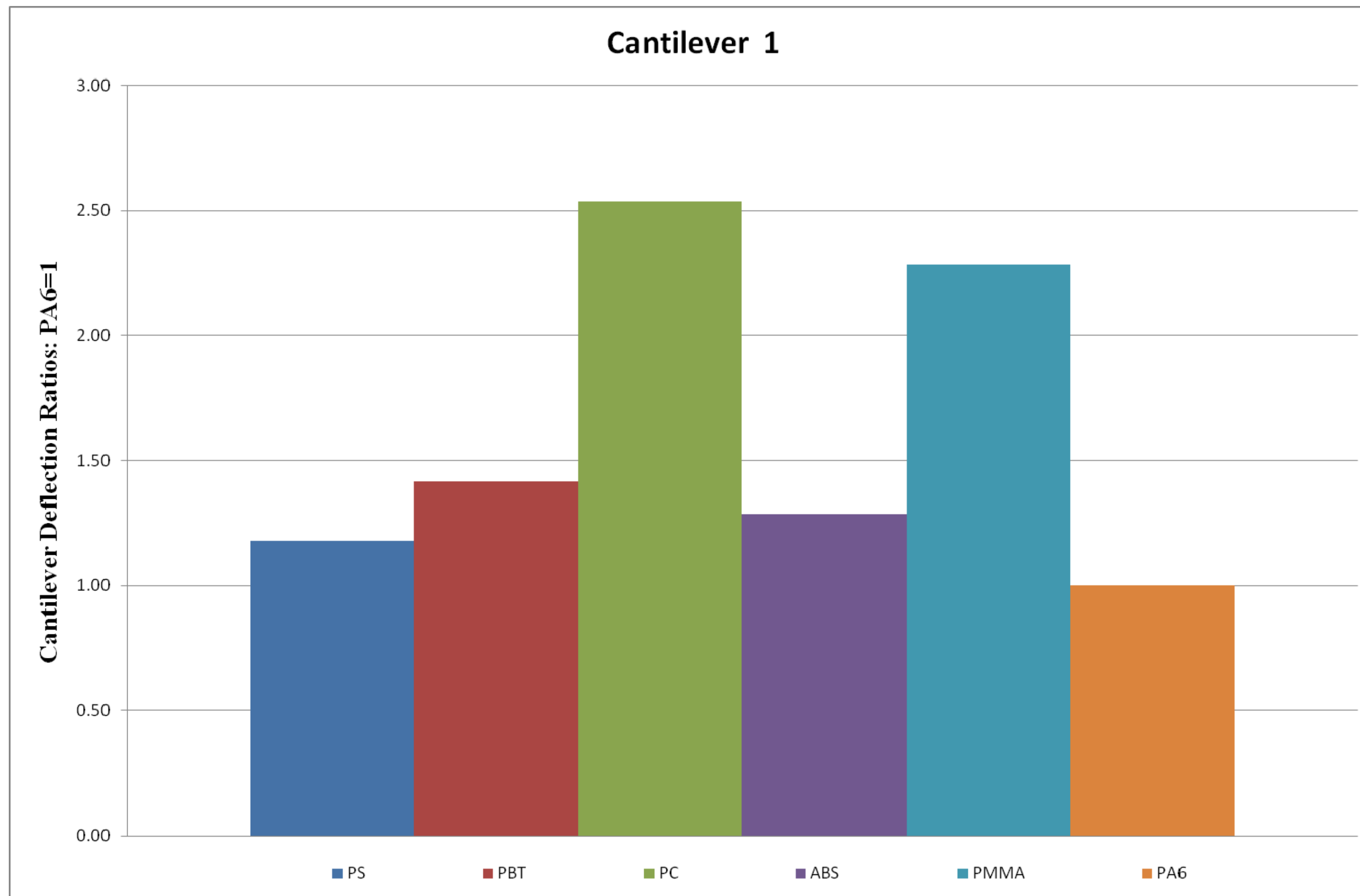

Figure 39: Cantilever deflection ratio obtained from AFM for Cantilever 1

Experiment 2

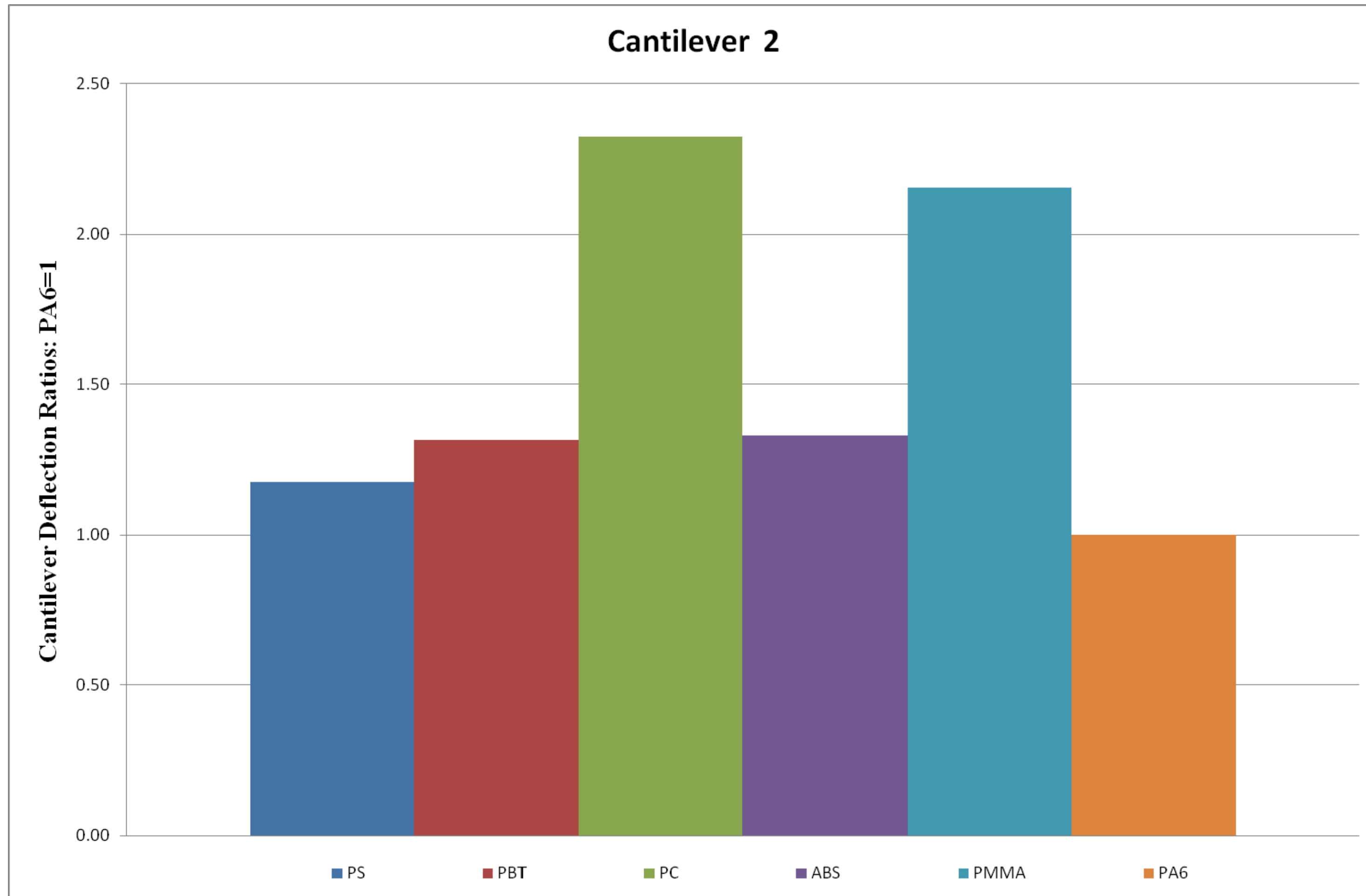

Figure 40: Cantilever Deflection Ratio obtained from AFM for cantilever 2

Experiment 3

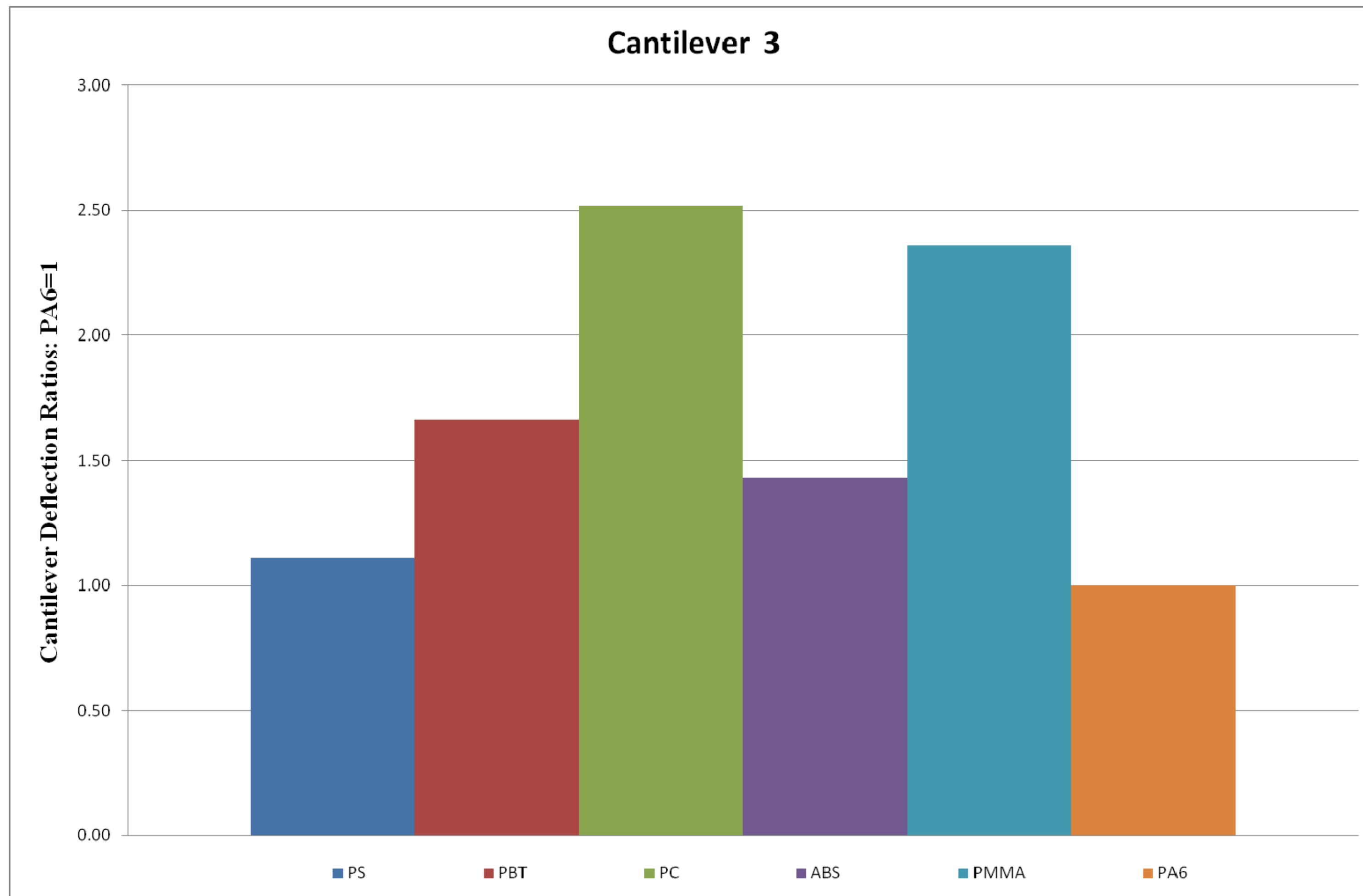

Figure 41: Cantilever Deflection Ratio obtained from AFM for cantilever 3

5.7 Discussion

Work of adhesion depends on the surface energies of the interacting surfaces. According to Eqn. 8 work of adhesion is directly proportional to the pull off force when the radius of the tip is kept constant. Also for a given cantilever (tip radius) the pull off force is directly proportional to the cantilever deflection (Eqn. 7). Therefore, the work of adhesion hierarchy will be the same as the cantilever deflection hierarchy presented earlier in the results section.

As this experiment was designed to investigate the relative interactions between thermoplastics and tin metal, the use of absolute force values was deemed unnecessary. A simple comparison of the cantilever deflection values is sufficient. Hence, the need to measure the spring constant of a cantilever was eliminated. It is clear that the experiment shows consistent readings (Table 10) independent of measurement set and cantilever. The data can thus be used to roughly determine the relative spring constants of the three cantilevers. Using the ratios of the average cantilever deflections for PA 6 shows that the spring constants of cantilevers 2 & 3 were approximately 1.5 times that of cantilever 1. However, such a direct comparison of data can be a good approximation at best, as it assumes that the particle size of the functionalised tip (and therefore the area of contact) is the same.

The interaction between the particle and the surface depends on electrostatic forces, capillary forces, and other forces as well as Van der Waal's forces [13][43][50]. The capillary forces arise due to a thin layer of water that normally covers most surfaces under ambient air conditions. The thickness of this layer depends upon the hydrophilicity / hydrophobicity of the surface as well as humidity. In

the case of capillary forces being high the approaching tip 'jumps to contact' as the tip approaches the thin water layer and a large cantilever deflection value is observed during retraction. For the six thermoplastics tested, the jump to contact was not observed except in the case of ABS. This is counterintuitive as nylons in general are more hygroscopic than ABS [58], but no such jump to contact was seen in case of PA 6.

Electrostatic forces arise from the difference in charge between tip and substrate. Certain materials become electrically charged when they come in contact with another different material and are then separated. The polarity and strength of the charges produced depends on the materials, temperature and other factors. Hearn *et.al.* used this property of polymers to segregate PP, PET, PS, PVC, and HDPE from one another for recycling [59]. Diaz *et.al.* compiled a triboelectric series for the polymers when tested with gold [60]. They reported that the magnitudes of the charges developed by the polymers are all of the same order apart from nylons which are larger. They found that polymers with nitrogen functional groups (e.g. ABS and PA 6) develop a positive charge. Polymers with oxygen functional groups (PMMA and PC) also develop a small positive charge, but less than the nitrogen functional group polymers. Polymers with hydrocarbons as functional groups show little charging and generally are close to 0 (PS and PBT). Thus for the experiment discussed here the electrostatic force should be largest for the PA 6 and of comparable magnitude among all the other polymers. In fact PC and PMMA showed much the highest pull off force as compared to other thermoplastics, the pull off force for PA 6 was the least, and the pull off forces of PS PBT and ABS were comparable.

Thus, it was concluded that although electrostatic forces may contribute to the pull off forces, they were not dominant in deciding the measured values.

5.8 Conclusions

In this chapter, the use of AFM-force distance curves for study of interatomic interactions between materials was reviewed. A methodology was devised to test interatomic interactions between tin and the thermoplastics selected for this study. A detailed description of the process of functionalising the AFM cantilever with tin particles was done. The technique of attaching particles on the probe using adhesive was attempted. FIB/SEM based particle ‘welding’ technique was adopted in order to overcome the particle contamination issues faced in adhesive based method. Force-distance (cantilever deflection) curves were obtained for each thermoplastic tin pair. Highly consistent results (maximum error less than 8%) were obtained. Cantilever deflections were ranked in the of the interatomic interactions between the thermoplastic and tin (strongest to weakest adhesion)

PC > PMMA > PBT > ABS > PS > PA 6

PA and PMMA interatomic interactions with tin were found to be noticeably stronger than the other polymers. The results were discussed on the basis of the various interatomic interactions viz. electrostatic forces, capillary forces. It was concluded that the trend of interatomic interactions obtained is a combination of electrostatic forces, capillary forces and dispersion forces acting between the materials tested. It will be interesting to see if the trend of adhesion force and consequently work of adhesion obtained between tin and various thermoplastics is

repeated on a macroscopic level (mechanical strength tests). If the trend is repeated, then a simple comparison of the interatomic forces can be used to filter pairs of suitable metals and thermoplastics to obtain optimum adhesion strength in an insert moulded component.

6 Contact Angle Analysis

Contents

- *Introduction*
- *Theory*
- *Review of the Literature*
- *Methodology*
- *Results*
- *Discussion*
- *Conclusions*

6.1 Introduction

It is widely accepted that good wetting of an adherend by an adhesive improves adhesion strength at the joint interface formed [12-14]. Therefore, for insert moulding, quantifying wetting of the insert by thermoplastic melts assumes importance because the thermoplastic melt comes in contact with the insert at temperatures close to the processing temperature of the thermoplastics. Generally, the contact angle (θ) at thermodynamic equilibrium is used as a comparative indicator to assess wetting of a substrate by an adhesive.

In this chapter a brief review of the theory of contact angles and high temperature contact angle measurement techniques is presented. Contact angle analysis of thermoplastic melts was difficult because of their high viscosity and low thermal conductivity. Failed attempts at using the immersion-emersion technique to measure contact angle are reported. The development of a high temperature sessile drop (sample processing and testing procedure) is described in detail. Results of measurements using the procedure are presented with a detailed discussion of the

usefulness of the results in understanding the importance of processing conditions on the joint strength of the insert moulded composite.

6.2 Theory

The theory of wetting was presented in Chapter 2, but is re-presented here for convenience. Wetting is a surface phenomenon and is usually attributed to the surface energy differences of the interacting liquid and solid surface. For a solid-liquid-vapour system Young's contact angle θ is generally used to quantify wetting of a surface by a liquid. Fig. 42 shows a typical sessile drop solid-liquid-vapour system with liquid making contact angle θ with the adherend. γ_{lv}, γ_{sv} and γ_{sl} represent surface tension components of liquid, adherend and the interface respectively.

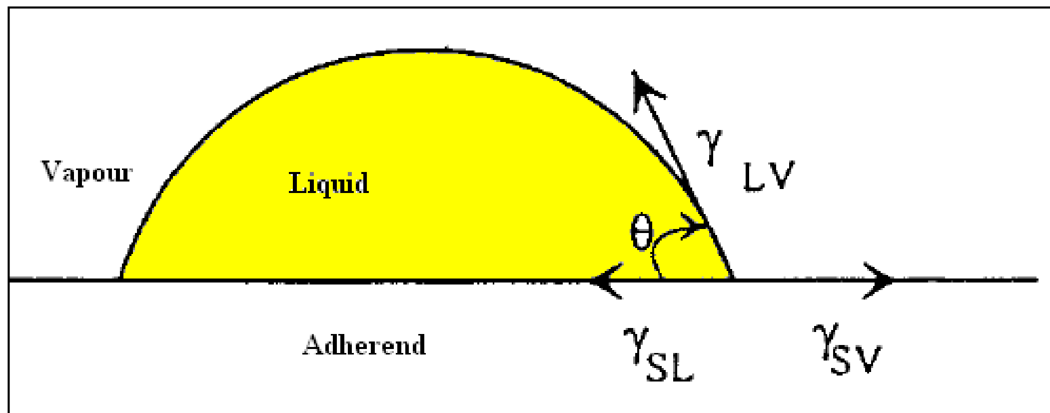

Figure 42: Typical solid-liquid-vapour system. θ is the contact angle.

Eqn. 1 from Chapter 2 is reproduced for convenience,

$$\gamma_{sv} = \gamma_{sl} + \gamma_{lv}(cos\theta) \quad \text{.................................} \ \mathbf{[1]}$$

Measurements of θ and the liquid surface tension γ_{lv} make it possible to evaluate the work of adhesion from Young-Dupre's equation (Eqn. 3 Chapter 2)

The work of adhesion characterises the thermodynamic stability of interfaces between dissimilar materials and is widely used in practice for predicting their potential bonding properties. It is clear from Eqn. 3 that quantitative assessment of work of adhesion to a given surface can be done, if the liquid surface tension is known, by measuring the contact angle θ of the liquid on the surface.

6.3 Review of the Literature

Wetting of the insert with the thermoplastic melt at high temperature is central to the process of insert injection moulding and hence knowing the wet-ability of the insert material by the 'adhesive' at the processing temperature becomes necessary. This requires measuring contact angles at high temperatures. Despite the apparent simplicity of the sessile drop experiment to measure contact angles, the experimental evaluation of reliable values of θ at high temperatures remain a major problem and an obstacle to the development of scientific approaches to wetting phenomenon. Eustathopoulos *et.al.* in a review of measurement of contact angle at high temperature and Duncan *et.al.* in a report on hot melt adhesives report high levels of inter-laboratory scatter in the values of θ [61-62]. The possible causes of this were substrate preparation, experimental procedure and other factors.

There have been a few attempts to characterise wetting by polymers at high temperature. Wouters *et.al.* used a drop of the polymer melt formed at elevated temperature on a sample holder in a measurement chamber equipped with a heating element. Surface tension calculations were done by measuring the contact angles. It was concluded that surface tension of the polyester decreased with increase in temperature and resulted in better wetting [63]. The wetting balance technique is often used to study wetting of copper by hot Sn-Pb solder [64-65] Grundke *et.al.*

used the Wilhelmy balance technique (similar to the wetting balance technique) to test the wetting kinetics of polypropylene melts and a thin quartz fibre. They found good correspondence in the surface tension values between the Wilhelmy balance test and the pendant drop test [66]. Yang *et.al.* measured the contact angles at thermal equilibrium between PS and PMMA on substrates of nickel and silicon and reported that with increase in temperature the contact angle decreases for both the materials on both the substrates [67]. Sauer *et.al.* used a modified Wilhelmy apparatus (with a baffle and a glass probe) to measure the surface tension and dynamic wetting of PP, PTFE, PEKK and LCP polymers and found good correlation between the surface free energies of the polymers in solid state and the extrapolated surface tension data in molten state [68]. Lee *et.al.* performed contact angle measurements between PMMA and a stamper (nickel coated) used in nano-moulding process and concluded that with higher temperatures (around the melting point of PMMA) wetting of the stamper by PMMA increases [69]. Duncan *et.al.* performed contact angle measurements for hot melt adhesives on various substrates and reported that contact angle may depend on the complex dynamic modulus (G*) if it is measured at temperatures significantly below the adhesive processing temperatures [62]. Eustathopoulos *et.al.* in a critical review of the various techniques used for measurements of contact angle and work of adhesion at high temperature have listed the immersion-emersion technique and its variant the wetting balance technique along with the sessile drop technique and its variant the transferred drop technique for measuring contact angle at high temperatures [61].

Based on the works reviewed above, wetting of metals by polymers might be expected to improve with the rise in the temperature of the interface. However, Imachi studied the relationship between bond strength and wettability of the

polyethylene / metal system at temperatures close to the melting point of the metal. The metal used was a Sn-Pb alloy with a melting point of about 183°C [70]. He concluded that the bond strength of the joint increases when the temperature is around the melting point of the adherend. It is also interesting to note that the contact angles reported show a drop at around this temperature. This appears to contradict the generally accepted principle that adhesion increases with increased wettability. Chen *et.al.* have even questioned the importance of wetting in the process of insert injection moulding, stating that the injection pressure during the moulding process forces the molten thermoplastic in contact with the insert surface, although they cite no data to support the assertion [71].

The melting point of tin is 232°C. To see if there is any effect similar to that reported by Imachi, the range of temperatures used in the wetting experiments reported below was extended to cover this temperature.

6.3.1 Techniques for Contact Angle Measurement at High Temperature

In the literature reviewed, the sessile drop, the immersion-emersion technique and the wetting balance test were reported as being used extensively to measure contact angle at elevated temperatures and so were selected for trial in the present study. The sessile drop technique was described earlier in this chapter (Fig. 42). A brief overview of the other two techniques is as follows

6.3.1.1 Immersion - Emersion

Fig. 43 explains the basic principle of the immersion-emersion technique. The solid to be wetted is immersed and then withdrawn from the liquid and the *advancing*

and receding contact angles are measured, using a camera and software. Advancing contact angles (θ_a) are those made by the liquid in contact with the substrate/plate when it was immersed in the liquid and receding contact angles were made by the liquid in contact with the substrate/plate while it is moving into the liquid.

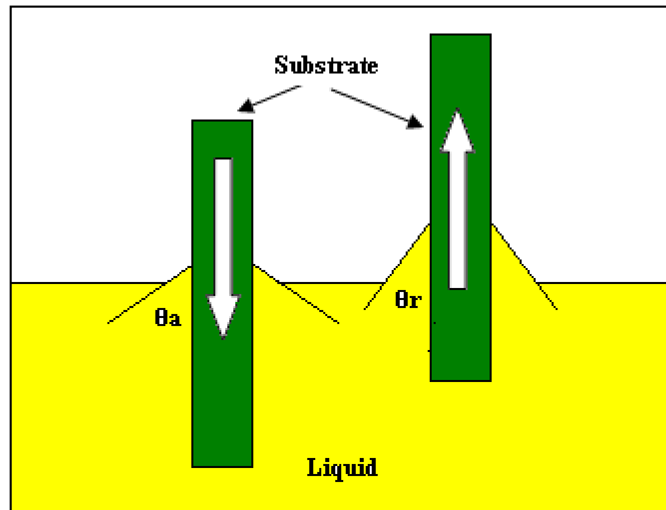

Figure 43: Typical Immersion Emersion set-up.

6.3.1.2 Wetting Balance Test

Like the immersion-emersion technique, the wetting balance involves dipping a foil or substrate into molten thermoplastic. The measured quantity however is the wetting tension at the solid polymer melt interface. This tension is equal to the force F of the unit length of perimeter p of a solid sample recorded by an electrobalance.

$$\frac{F}{p} = \frac{g\Delta m}{p} \qquad \text{................................[9]}$$

Where,

g = gravitational constant

Δm= change in apparent mass before and after the foil is immersed

6.4 Methodology

The wettability of a surface is often characterised through use of one or more probe liquids (e.g. water) to infer suitability of the surface for bonding. However, the interfacial properties of the probe liquid may differ considerably from the liquid that wets the substrate in an application. E.g.: at room temperature the surface tension of water is approximately 72 mN/m while the surface tension of polymer melts (at high temperatures) vary from 20-50 mN/m. Hence, probe liquids were not used for contact angle measurements.

The three techniques mentioned above viz. sessile drop analysis, immersion-emersion technique and modified wetting balance test were all trialled.

6.4.1 Materials and Experiment apparatus

6.4.1.1 Tin Foil

Tin foil was used as the substrate to be wetted and was obtained from Goodfellow. The thickness of the foil was 0.1mm while its purity was 99.95%.

6.4.1.2 Thermoplastics

The polymer samples used for this experiment were granules as received from the manufacturers. Unprocessed granules were used in order to prevent any contamination that may occur during processing of the samples, e.g.: mould release agent from a mould coming in contact with the sample surface. The granules were dried before the experiments in a fan oven. The time of drying was as recommended by the manufacturers.

6.4.1.3 Contact angle measurement

A DataPhysics OCA 20 was used for contact angle analysis. Contact angles were recorded with the help of the SCA 20 imaging system and semi-automatic image analysis software. The software can be operated in pendant drop mode, sessile drop mode, and lamella mode. The lamella mode of image analysis was used for the immersion-emersion technique while the sessile drop mode was used for sessile drop analysis. The apparatus came with a heated chamber attachment that was used for both immersion-emersion and sessile drop experiments.

6.4.1.4 Wetting Balance tester

A commercial wetting balance tester from Robotic Process Systems (R.P.S.) 6-Sigma was used for the experiment. This equipment is typically used for testing the wetting of copper by solder. The equipment was modified for the use with thermoplastic melts as described in Section 6.4.3.

6.4.2 Immersion-Emersion

The DataPhysics OCA 20 with the heated chamber attachment was used for this experiment. The contact angle software was used in lamella mode. Granules of PMMA were placed in a metal container which was located in the heated chamber. The container was heated to and maintained at the processing temperature of PMMA of 235°C. The movement of the foil towards the container was done manually with the help of a mechanism that ensured a perfectly vertical descent. The foil was introduced manually from the top of the container and the images were obtained.

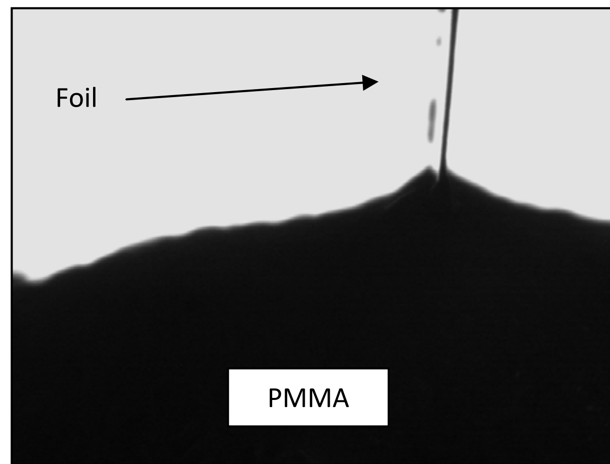

Figure 44: The immersion-emersion technique for PMMA.

Several experimental difficulties made it difficult to measure a contact angle from the images obtained. Firstly the molten thermoplastic continuously bubbled. Although the mechanism used for the movement of the foil towards the container maintained a perfectly vertical descent, as a result of the bubbling, the foil would deflect from vertical once it came into contact with the thermoplastic (Fig. 44). Secondly, the entire surface of the thermoplastic was disturbed by the motion of the plate and did not subsequently relax due to local cooling, so that a horizontal baseline could not be defined. Thus, neither a vertical nor a horizontal baseline could be established which is vital for contact angle measurement using lamella mode. This behaviour was observed across the board for all the thermoplastics tested and hence no contact angle data was generated from this experiment.

6.4.3 Wetting Balance Technique

Like the immersion-emersion technique, the wetting balance involves dipping a foil into a liquid. A Robotic Process Systems (R.P.S.) 6-Sigma wetting balance tester used for copper-solder paste wetting analysis was modified in order to use it for the tin-thermoplastic system.

6.4.3.1 Description of the Set-up

. Fig. 45 is a schematic diagram of the modified apparatus. A ceramic crucible containing the thermoplastic was located in a plate with a hole punched in the centre. The plate was placed over a heated bath that contained a molten tin-copper-silver solder, so that the crucible was immersed in the solder and the polymer contents melted. The temperature of the thermoplastic melt was tracked using a thermocouple. Tin foil was attached to the micro balance of the wetting balance tester and introduced in the ceramic crucible when the desired temperature of the thermoplastic melt was reached.

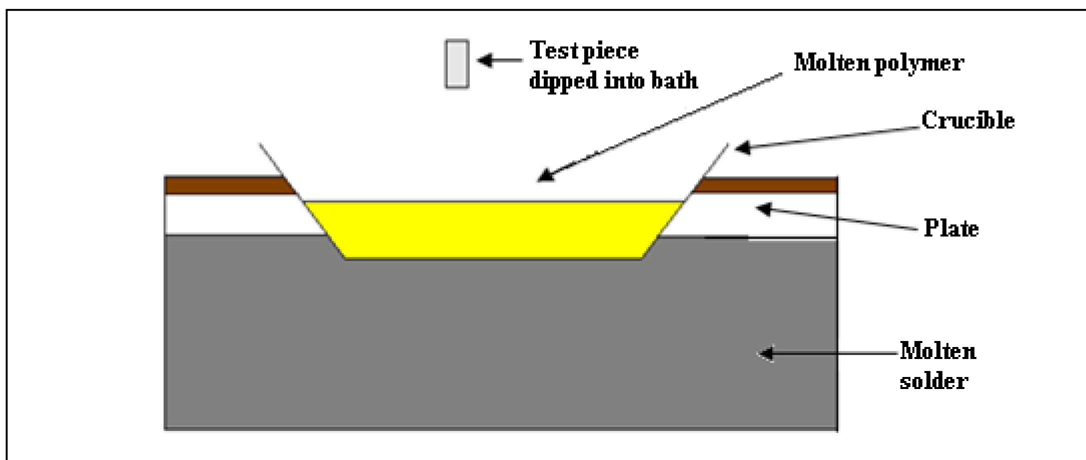

Figure 45: Schematic of the modified wetting balance tester.

6.4.3.2 Experimental procedure

PBT was introduced in the ceramic crucible for testing and was heated to its processing temperature. Tin foil attached to the micro balance was lowered in the ceramic crucible. It was observed that the foil did not penetrate the viscous surface of the molten thermoplastic. This was attributed to the surface of the thermoplastic losing heat rapidly and becoming viscous as compared to the hot interior. Even

prolonged (1hr after steady state was achieved) heating of the crucible did not change this situation.

After the above experiment, it was felt that the ceramic crucible due to its low heat conductivity was not a suitable option for this type of experiment. Also, the non-uniform diameter of the crucible meant a relatively high surface area of the thermoplastic was exposed to atmosphere compared to the bulk. To address these problems, a cylindrical aluminium crucible was made with thick walls. The depth of the cylinder in the bath was increased. A 'U' shaped design was adopted for the plate. This was done to increase the rate of heat transfer from the bath to the crucible. (Fig. 46)

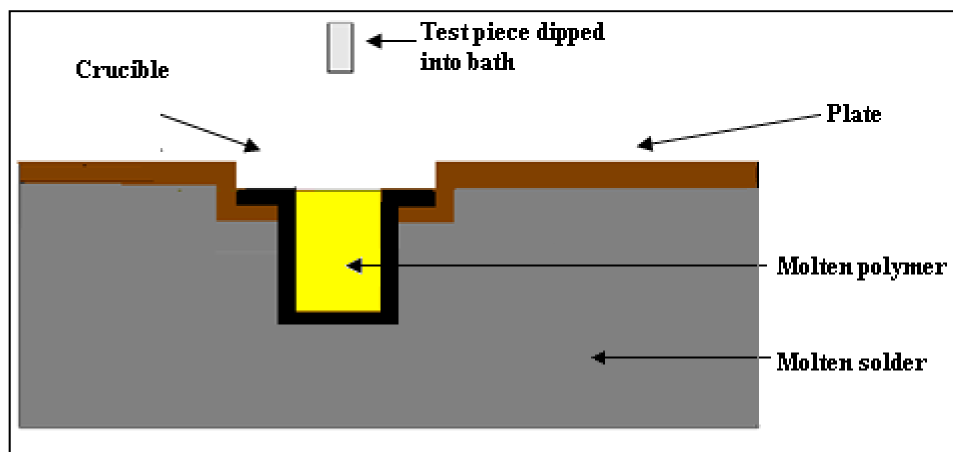

Figure 46: Schematic of the re-modified wetting balance tester

Conceptually, the second stage modified apparatus was an improvement over the ceramic crucible. To maintain high temperature in the airspace immediately above the polymer surface and avoid the formation of the highly viscous layer a cover was placed on top of the crucible (not shown in Fig. 46). However the problem of a semi-solid, viscous surface still persisted and the tin foil did not penetrate the thermoplastic surface. This problem was observed for all the thermoplastics tested and hence no readings were recorded.

6.4.4 Sessile Drop Analysis on Heated Substrate

Sessile drop is one of the most widely used techniques for wetting and contact angle analysis. It was attempted to use this method to characterise the wetting of tin by the list of thermoplastics chosen for the study, using tin foil as the substrate.

6.4.4.1 Description of the Set-up

The DataPhysics OCA 20 and SCA 20 software were used to record the development of sessile drop contact angles at a frame rate of 0.05 frames per second. The imaging software either detected the difference between the sessile drop and the substrate automatically and marked the baseline at the interface or a baseline was drawn manually connecting the two extremities of the sessile drop in contact with the substrate. Similarly identification of the boundary of the sessile drop was either automatic or a boundary marking the sessile drop (cap) was drawn manually. Contact angle was then measured automatically by the software as the angle of a tangent to the edge of the drop at the baseline.

6.4.4.2 Experimental Procedure

In initial trials the thermoplastics were maintained close to their processing temperatures in the heated syringe. A drop of the thermoplastic was squeezed out so that it fell and rested on the tin foil. It was observed that, for all the six thermoplastics, as the thermoplastic melt drop was squeezed out of the syringe, it started cooling down and became very viscous by the time it came in contact with the tin foil. Due to this a molten sessile drop in equilibrium did not form on the substrate. Thus, the contact angle, even where it could be measured, was considered invalid.

The problems encountered in this and previous attempts with other methods were attributed to the very low thermal diffusivity and high viscosity of the thermoplastics. It was therefore considered that the complete liquid/solid system must be in thermodynamic equilibrium before the contact angle can be measured. A heated chamber add-on to the DataPhysics OCA 20 became available which potentially offered better control over the thermal conditions of the measurements. It formed the basis of the experimental technique adopted as described in the next section.

6.4.5 Experimental Technique Adopted

6.4.5.1 Description of the Set-up

The experimental technique eventually adopted was sessile drop contact angle analysis, using a commercial heated chamber add-on to the contact angle measurement apparatus designed to maintain the air around the sample at a controlled temperature. The set up is illustrated in Fig. 47. The heated syringe was located above the hole at the top of the heated chamber such that it could be lowered towards the chamber. The chamber was maintained at high temperature (190-240°C), hence the thermoplastic drop squeezed out of the syringe did not become viscous before it came in contact with the tin foil.

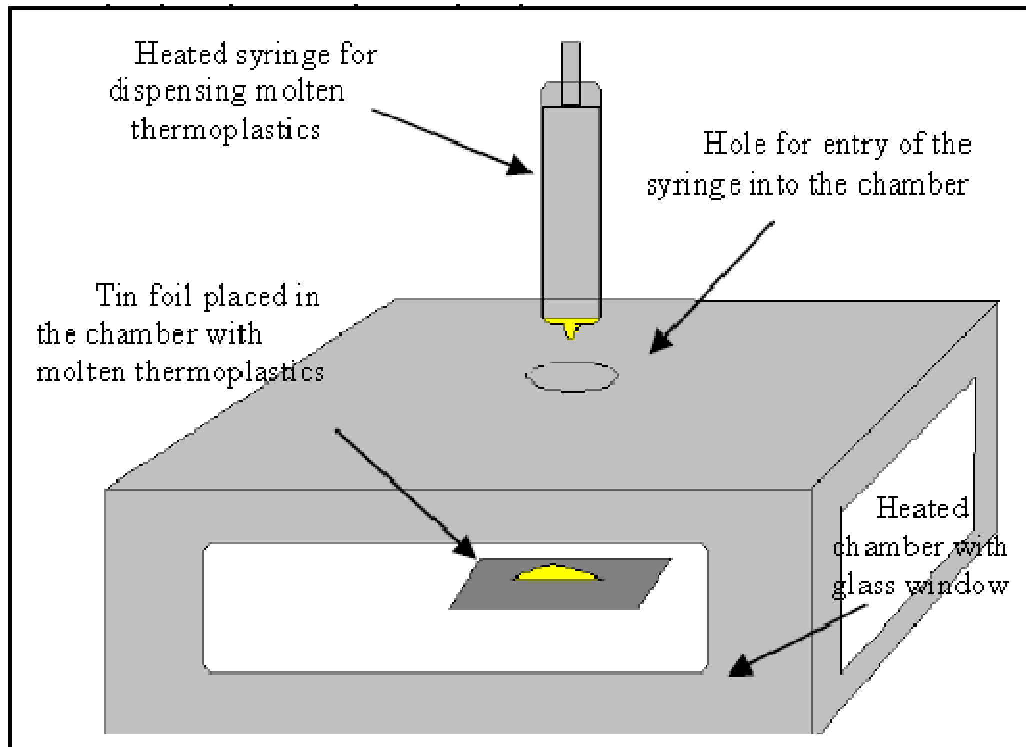

Figure 47: Heated chamber and heated syringe set-up for sessile drop experiment.

6.4.5.2 Experimental details

The heating chamber was heated with a heating coil at the top and base. The tin foil substrate to be wetted was placed on glass slides in the base of the chamber, to avoid localised heating of the foil assembled as shown in Fig. 48.

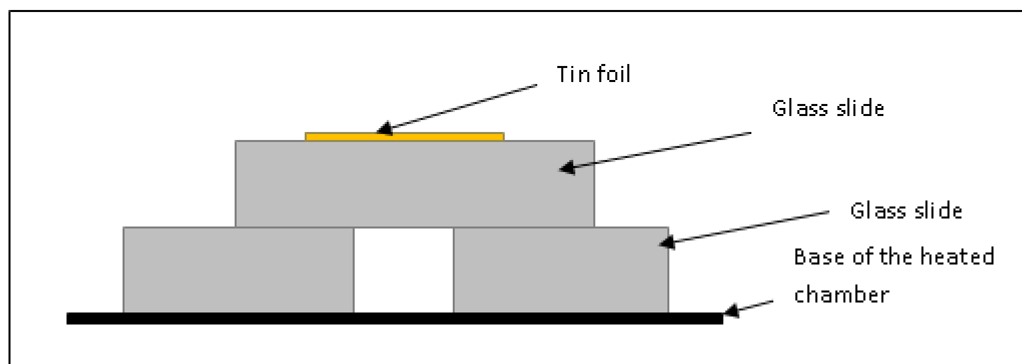

Figure 48: Heated chamber set-up for sessile drop experiment

The temperature of the heated chamber was maintained at varying temperatures in the range 190-240°C, as it covers both the processing temperatures

of the thermoplastics and the melting temperature of the tin (232°C). It was observed that none of the materials achieved equilibrium when the chamber temperature was maintained below 190°C. This lower limit temperature was higher for some thermoplastics. The upper limit was chosen because when temperatures beyond 240°C were maintained in the heated chamber, the tin foil melted. The thermoplastic under test was maintained at its processing temperatures in the heated syringe before dispensing. The foil was placed in the chamber and allowed to heat for 20 minutes. A drop of the thermoplastic was then squeezed out so that it fell and rested on the foil. The contact angle for the drop was taken to be that when the contact angle was stable with respect to time. Three experiments were done at each temperature for each material with fresh foils every time.

6.5 Results

Fig. 49 - 52 show typical plots of relaxation in contact angle after dispensing, for drops of PA 6 on tin foil at various heated chamber temperatures. In all plots the rate of decline in contact angle decreases with time and eventually reaches steady state. The relatively long equilibration time is due to the relatively high viscosity of the polymer melts as compared to typical liquids used in contact angle measurements like water. The contact angle measured for PA 6 decreased from the 70-85° range to the 50-55° range within the first 10-20 readings corresponding to 200s to 400s. A similar trend was observed for the rest of the thermoplastics apart from ABS i.e. the largest change in contact angle occurred within the first 400s after the melt was introduced onto the tin foil. ABS did not form a spherical cap (sessile drop), probably due to degradation. It was observed that prolonged exposure to high temperatures close to its processing temperature (220°C) caused it turn dark orange and char.

Even at lower temperatures, although no colour change was seen it did not adopt a spherical cap shape. ABS is therefore not included in the report of results and discussion below.

The time behaviour observed was in agreement with the literature. Duncan *et.al.* performed steady state contact angles experiments on hot melt adhesives in a heated chamber at 100°C and found that the contact angle drops rapidly when the melt is introduced on the substrate [62]. Similar results were observed by Yang *et.al.* and Lee *et.al.* when they tested various thermoplastics including PMMA and PS on silicon and nickel substrates [67] and PMMA on a metal stamper [69] respectively. The equilibrium contact angles obtained from the experiments are summarised in Fig. 53. Each contact angle reading in Fig. 53 is an average of three steady state contact angle measurements at the given chamber temperatures. The range in the three readings was always less than 1% of the mean. It was observed that the steady state contact angles for all the thermoplastics on tin foil decreased monotonically with increase in temperature.

A direct identification of wetting, and hence adhesion strength, with contact angle would lead to the conclusion that wetting of tin by the thermoplastic melts also improves monotonically with increasing temperature. However this does not take account of the surface tension of thermoplastic melts, as discussed in the following section. The order of the thermoplastics by contact angle (greatest to smallest) at 220°C in Fig. 53 is

PC > PBT > PA 6 > PMMA > PS

However, the values for PMMA and PA 6 are very close to each other. This order is maintained at all other temperature where there is some overlap among the temperature ranges of the curves.

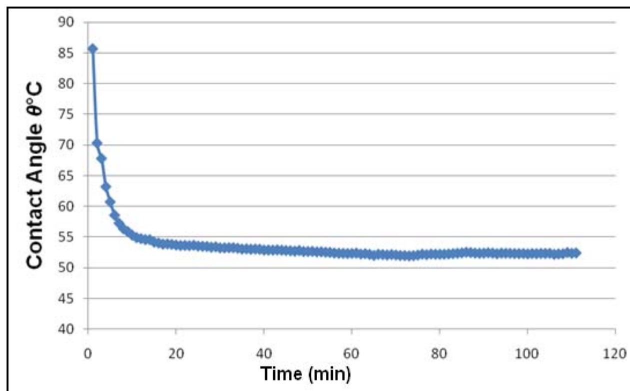

Figure 49: Contact angle of PA 6 on tin foil with heated chamber at 210°C

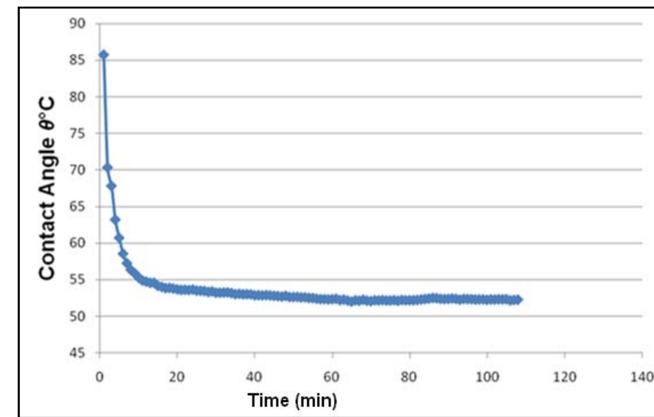

Figure 51: Contact angle of PA 6 on tin foil with heated chamber at 230°C

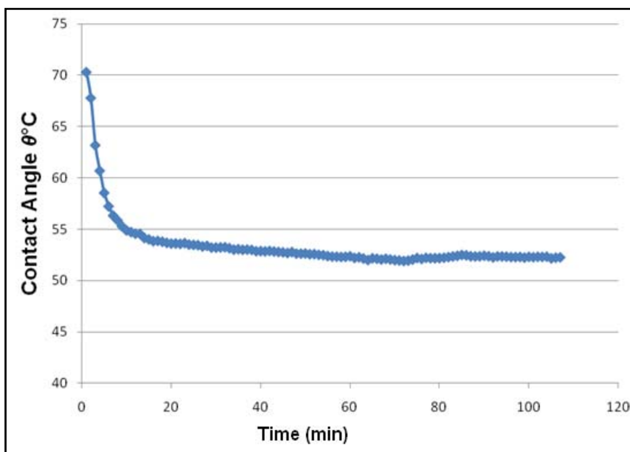

Figure 50: Contact angle of PA 6 on tin foil with heated chamber at 220°C

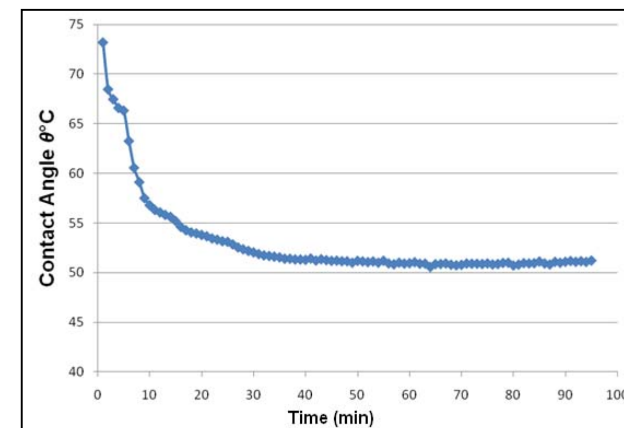

Figure 52: Contact angle of PA 6 on tin foil with heated chamber at 240°C

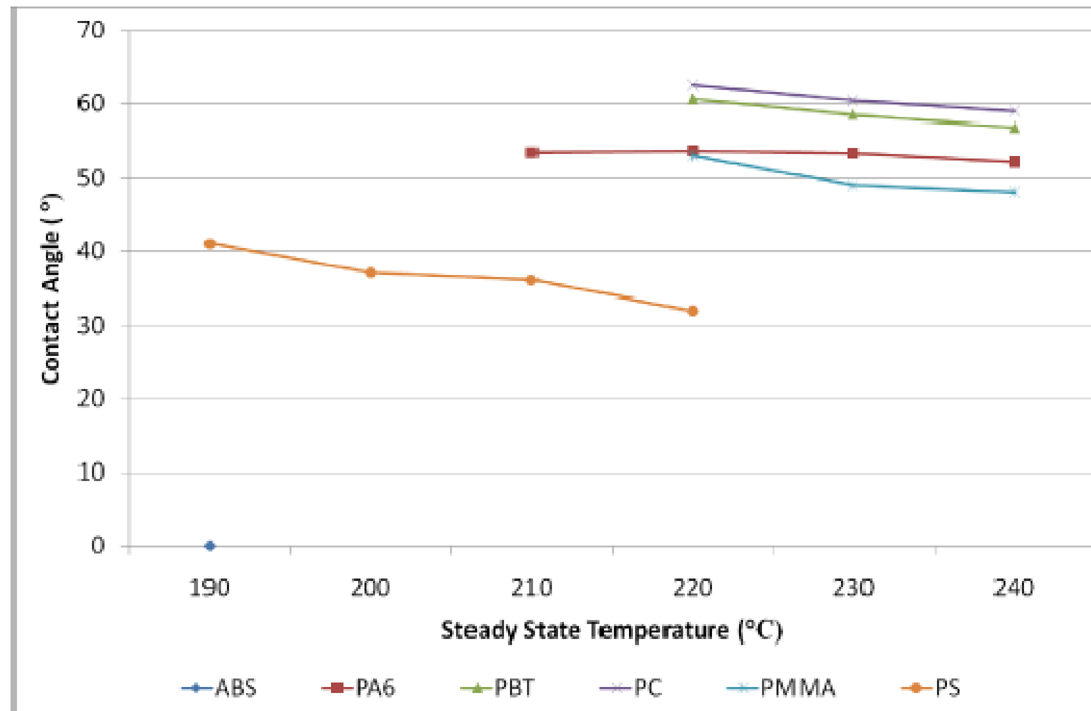

Figure 53: Contact angle vs. temperature for molten thermoplastic on tin foil

6.6 Discussion

In the literature contact angle is sometimes treated as a surrogate for degree of wetting. This is acceptable when comparing different surfaces with a particular test liquid as is typically done. In the current work however the surface was kept the same and the liquid was varied. Account must therefore be taken of the surface tension of the wetting liquid. The need for this can be seen by inspection of the Young-Dupre equation (Eqn. 3), for calculating work of adhesion from contact angle, where the surface tension appears as a term.

Surface tension in a liquid arises from unbalanced molecule-molecule attraction forces exerted on molecules at the surface of a fluid. Raising the temperature of the fluid increases the kinetic agitation of the molecules, hence reducing the magnitude of the intermolecular interactions and the surface tension [72]. This drop in surface tension of a liquid or adhesive leads to increased wetting at a solid-liquid interface. Data on measurements of the surface tensions of thermoplastic melts can be obtained from the literature. Table 11 summarises the surface tension for thermoplastics at various temperatures. If it were to be assumed that the interfacial forces between polymer and tin did not vary much with temperature among the materials, then the observed decrease in contact angle with temperature of the polymers studied is consistent with a decrease in surface tension.

Table 11: Surface tension of thermoplastics

Thermoplastic	Surface Tension (mN/m)	Temperature
PMMA	28.9	180 [73]
	25.97	220 [67]
	24.33	240 [67]
PS	26.09	190 [67]
	23.92	220 [67]
PBT	30.2	240 [74]
PC	46	250 [75]
PA 6	37.7	240 [76]

The relative bonding strengths at interfaces can also be studied by using the work of adhesion approach based on Dupre's equation. For the given tin-thermoplastic pairs, bond strength across the interface should improve with higher work of adhesion. The contact angle values from the experiments and surface tension values from literature were used to calculate the work of adhesion at 240°C and these are listed in Table 12. From the values, it was inferred that tin-PC adhesion strength will be the highest while tin-PMMA will be the lowest. The general order should be

PC>PA 6>PBT>PS>PMMA

Table 12: Work of adhesion at 240°C

Tin-thermoplastic pair	***Surface tension at 240°C (mN/m)***	***Contact angle (θ°)***	**Work of adhesion (mJ/m^2)**
PMMA	24.33	48	40.61
PS	≈ 23	≈ 25[1]	43.84
PBT	30.2	56	47.08
PA 6	37.7	52	60.91
PC	≈ 47	59	71

Table 13 shows the variation in work of adhesion with temperature calculated for tin-PMMA[2]. It is interesting to note that the work of adhesion decreases on either side of 230°C. Table 14 shows the work of adhesion similarly calculated for tin-PS[3]. The work of adhesion decreases as the contact angle decreases. This data suggests that there is a possibility of an optimum temperature to get the best adhesion at the interface for a given tin-thermoplastic pair.

Table 13: Work of adhesion for PMMA

Temperature (°C)	***Surface tension (mN/m)***	***Contact angle (θ°)***	**Work of adhesion (mJ/m^2)**
220	25.97	53	41.55
230	25.28	49	41.97
240	24.33	48	40.63

[1] The contact angle data for PS at 240°C was extrapolated from values given in fig.54.
[2] Surface tension for PMMA as reported by Yang *et.al.* [67]
[3] Surface tension for PS as reported by Yang *et.al.* [67]

Table 14: Work of adhesion for PS

Temperature (°C)	***Surface tension (mN/m)***	***Contact angle (θ°)***	***Work of adhesion* (mJ/m^2)**
190	26.09	41.5	45.66
200	25.31	37	45.55
210	24.61	36	44.54
220	23.92	32.5	44.01

An alternative to surface tension as a mechanism for reduction in contact angle with increase of temperature was suggested by Duncan *et.al.* in their work on steady state contact angle of hot melt adhesives [62]. They suggested that if the temperature of the melt drops considerably below the processing temperature of the adhesive, then the adhesives become viscous resulting in higher complex dynamic modulus values (G*). This effect then tends to dominate wetting rather than surface tension and consequently results in much higher contact angles at interface. In the present work, although a rise in contact angles at lower steady state temperature was observed, the rise was very gradual and not similar to the high spike suggested. It therefore seems likely that the viscosity of the thermoplastic melts was not very high in the temperature range used in the experiments and that the contact angles recorded were at thermal equilibrium.

There is some debate in the literature on the effect of insert temperature on adhesion in the insert moulded metal – polymer system. The injection moulded polycarbonate-aluminium system was reported to exhibit higher adhesion at the interface with heated inserts compared to unheated inserts by Ramani *et al* [25]. This rise in joint strength was attributed to the increased wetting at the interface due to the rise in temperature of the insert and consequently temperature at the interface of the metal - polymer system. On the other hand the role of adhesion was considered to play no role in *in-situ* injection moulded thermoplastic-metal blanks by Chen *et.al.* [71]. Instead they cited injection pressure as being sufficient to promote perfect contact at the metal-thermoplastic interface, negating any influence of wetting on joint strength. Imachi studied the relationship between bond strength and wettability of the polyethylene-metal system at temperatures close to the melting point of the metal (Sn-Pb system, melting point 183°C) and reported that wetting decreases as the temperature at interface rises reaching the melting point of the metal, a result which is contrary to the popular belief that wetting and consequently adhesion increases with increased wet-ability [70]. Imachis experiments suggested that in the case of substrates that have a melting point in the processing range of the adhesive, an inverse relationship exists between wetting and joint strength i.e. although wetting decreases, the adhesion at interface increased, leading to higher joint strengths [70]. Imachis results assume importance as tin has a melting point of 232°C which lies in the processing temperature range of the thermoplastics. However, from the contact angle data recorded in this study, there was no evidence of rise in contact angle with the rise in temperature of the interface.

6.7 Conclusions

On account of all the contradictory results in the literature, it was necessary to perform the contact angle analysis to establish the wetting characteristics of the thermoplastics on the surface of tin at or around their processing temperatures and the melting point of tin. In this chapter, the use of contact angle analysis to study interactions between thermoplastic melt and substrates was reviewed. A methodology was devised to test contact angles between tin and the thermoplastic melts selected for this study. High viscosity and low thermal conductivity of thermoplastic melts made it difficult to measure contact angles. Immersion-emersion and wetting balance techniques were attempted and contact angle measurement by sessile drop analysis was selected. A temperature controlled thermal chamber was used to achieve thermal equilibrium and except ABS, contact angles were recorded for all the materials used in this study. ABS degraded on prolonged exposure to high temperature and didn’t form a sessile drop. The readings were highly consistent with less contact angle range of less than 1% of the mean. It was observed that for contact angles go down monotonically with rise in temperature at interface. The order of the thermoplastics by contact angle (greatest to smallest) at 220°C was

PC > PBT > PA 6 > PMMA > PS

This order is maintained at all other temperature where there is some overlap among the temperature ranges of the contact angles recorded. An attempt was made

to interpret the adhesion at interface in terms of work of adhesion as described by Young-Dupre equation. Based on this approach the expected work of adhesion at interface was calculated (at 240°C) and the materials were ranked as follows: (highest to lowest)

PC > PA 6 > PBT > PS > PMMA

Also, the work of adhesion calculated for PMMA at various temperatures showed that the work of adhesion does not decrease monotonically with rise in temperature as was observed in case of contact angles. The trends observed from the contact angle analysis experiments can be compared with the mechanical strength tests to understand the relative importance of the wetting at interface in an insert moulded component.

7 Mechanical Strength Test: Pull Out Test

Contents

- *Introduction*
- *Mechanical Strength Tests for Adhesion*
- *Mechanical Strength Testing of Adhesion in Insert Moulding*
- *Methodology*
- *Results*
- *Discussion*
- *Conclusions*

7.1 Introduction

Mechanical strength tests are often used to quantify the adhesive strength at the interface in order to assess the joint strength of a material system. Unlike typical mechanical tests which are done to determine the physical properties of the materials viz. tensile strength, Young's modulus etc. adhesion strength tests are done in order to ascertain the performance of the products in field applications. Components can be tested in tension, compression, flexure and other modes. However, it is not always feasible to test actual components because of their cost, size etc. Hence representative laboratory samples are often used to test the joint strength of the material systems to give comparable results. Such samples are produced by mimicking the manufacturing process for the components. This chapter reports the development of a mechanical strength test procedure appropriate for the substrateless packaging process. Initial attempts at manufacturing samples for lap shear test and block shear test are discussed. The development of the eventually chosen pull out test method (sample manufacturing and testing procedure) is described in detail along with the reasons for the choice. Results of pull out tests

conducted with all six of the chosen polymers and tin coated copper wire, at different insert temperatures are presented along with a detailed discussion about the usefulness of the results in understanding the influence of processing conditions on the joint strength developed in the insert moulded composite.

7.2 Mechanical Strength Tests for Adhesion

Many laboratory strength tests e.g. the lap shear test, the pull out test and the peel test have been developed to test adhesion. Selection of an appropriate mechanical strength test to judge adhesion at the interface of a joint often depends on how closely the test mimics the actual component in production and field applications. Typically, an adhesive test is used to characterise the mode of failure e.g.: adhesive failure at the interface or cohesive failure in the adhesive. A brief review of some of the main mechanical strength tests used to characterise the joint strength of adhesive bonds is given below.

7.2.1 Shear Tests

Shear tests are done to gauge the forces acting in the plane of the adhesive. Although, pure shear is seldom encountered in adhesive assemblies, shear tests are some of the most commonly reported tests in study of adhesion.

A) *Lap shear test / thin adherend shear test*: The test set up is as shown in Fig. 54. It is one of the most common tests used for testing the adhesion strength of a joint as the test configuration is very easy to set up. The main disadvantage of this test is that the rotation of the overlap under the applied force causes adhesive stresses that are complex, including shear and direct (peel) stresses, both of which can be

non-uniform. The result of this is that the test does not measure any true shear material properties.

B) *Thick adherend shear test*: The test set up is as shown in Fig. 55. This is an attempt to obtain true shear adhesive material data by removing the non-uniformity in the adhesive stresses by significantly increasing the thickness of the substrates in a single-lap joint. The test is used to obtain modulus data for numerical analysis of structural bonded joints. However, there are a number of limitations, which include difficulties in measuring the adhesive shear displacement accurately and also the continued presence of direct stresses in the adhesive.

C) *Double Lap shear:* The test set up is as shown in the Fig. 56. It is essentially two single lap joints back to back. This test is designed to try to eliminate the bending stress experienced by the single lap shear joint. However, the adhesive stresses still include non-uniform direct and shear components and thus this suffers the same limitations as the single-lap joint.

7.2.2 Peel Tests

Peel tests are generally used for elastomeric or rubbery adhesives. In a peel test the force required to peel a flexible member is recorded and it gives a measure of adhesion.

A) *T-peel:* This configuration is normally used to assess the resistance of an adhesive joint to normal force peel loading. It is often used when both the bonding materials are flexible, such as a laminated plastic film.

B) *Flexible to rigid peel:* Fig. 57a is one of the set ups used for testing flexible to rigid adherend bonded systems, for example measuring the strength of adhesive tapes.

The angle of the test can vary between 90°C to 180°C (Fig. 57 a and b respectively)

7.2.3 Tensile Pull Tests

A) *Pull off and butt joint test:* Fig. 58 a and b show the set-up for the tests. The butt joint test and the pull off test are similar in how the force is applied. In the butt joint test two cylindrical columns of similar cross sections are bonded together end to end, while in a pull off test a cylindrical dolly is bonded generally to a flat adherend. The joints are pulled apart to obtain the tensile strength.

B) *Pull out test:* Pull out test specimens tend to be cylindrical rods or fibres contained within a block or cylinder of adhesive (Fig. 58c). In this test the locus of maximum stress is at the interface, hence the test provides information on the adhesion strength of the system at the interface [77].

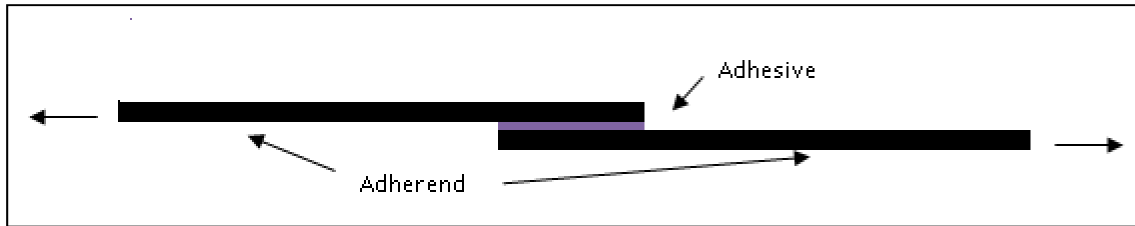

Figure 54: Lap shear test

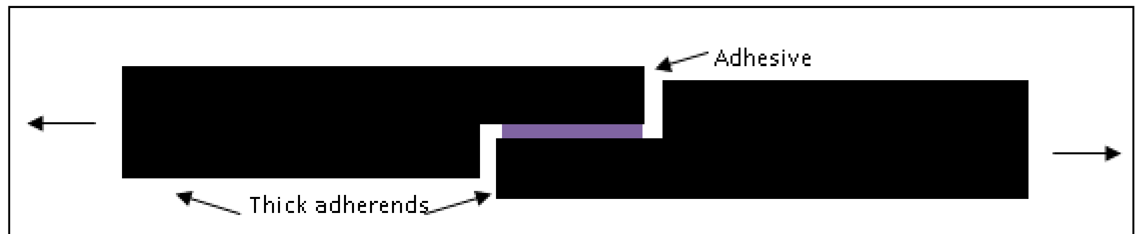

Figure 55: Thick adherend lap shear test

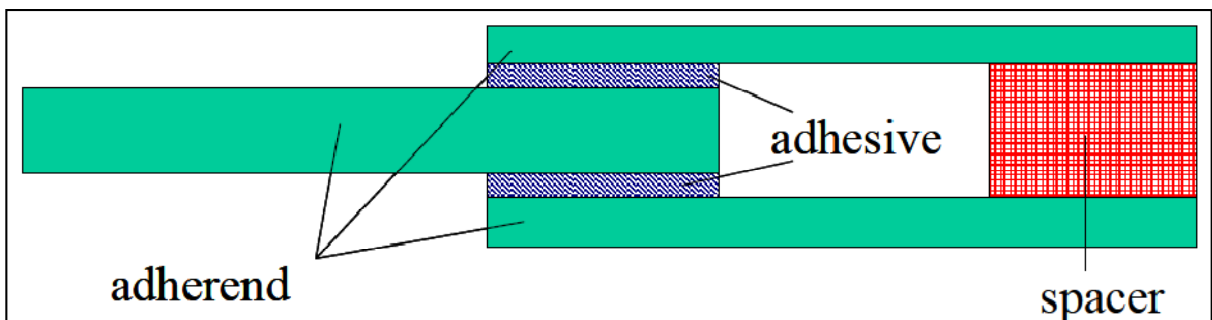

Figure 56: Double lap shear test

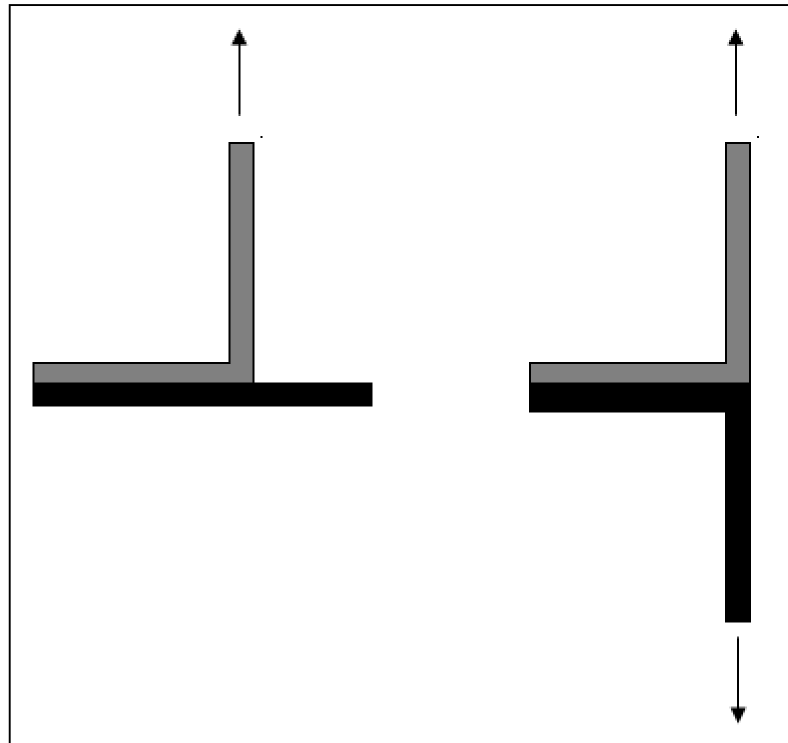

(a) 90° peel test *(b) T-peel test*

Figure 57: Peel test set ups

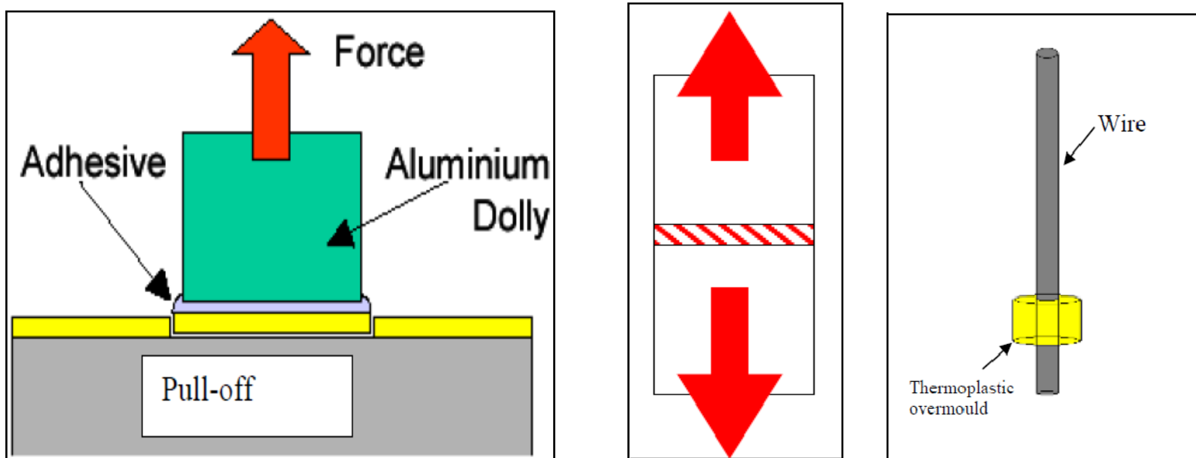

(a) Pull off test *(b) Tensile butt joint* *(c) Pull out test*

Figure 58: Tensile test set ups

7.3 Mechanical Strength Testing of Adhesion in Insert Moulding

Insert injection moulding (IIM) is a well established process in the industry. The joint strength of a composite produced via IIM depends on the material properties and processing conditions. However, there is little data available in the literature on the effect of processing conditions on the joint strength of insert injection moulded samples. Most of the data available is empirical in nature. Grujicic *et.al.* [23] in an overview of the polymer-to-metal direct adhesion technologies classified the work published in the open literature as follows:

1. Micro-scale mechanical interlocking approaches for improvement of adhesion [25]
2. In-coil or stamped-part metal priming with silane or other adhesion promoters for improvement of adhesion [78]
3. Chemical modifications of the injection-moulding thermoplastic material for enhanced adhesion to metal [79] and
4. Other approaches aimed at enhancing polymer-to-metal direct-adhesion

Ramani *et.al.* used tensile butt testing to measure the joint strength of an insert moulded aluminium-polycarbonate composite [25]. They reported that when the insert was maintained at elevated temperature during injection moulding the joint strength increased. They attributed the increased joint strength to lower viscosity of the thermoplastic melt at the interface which results in higher mechanical inter locking. Yeu *et.al.* performed fibre pull out tests on insert moulded fibres in polypropylene [80]. The aim of their study was to establish a pull out test procedure

to ensure specimen failure via interfacial debonding. They observed that the specimen geometry has an effect on the overall pull strength. Chen *et.al.* used aluminium blanks to create insert moulded sheet metal-polymer composites. They were of the opinion that chemical modifications at the metal-polymer interface result in enhancement of the final joint strength of the composite [71]. Fabrin *et.al.* peel tested insert moulded thermoplastic elastomer-aluminium composites [32]. A detailed summary of the few attempts to understand joint strength obtained from the insert moulding process has been presented by Grujicic *et.al.* [23] and Amancio-Filho *et.al.* [24]. Based on all the tests that have been performed, it can be concluded that selection of a test to assess the joint strength of a composite depends upon how well the test mimics the actual manufacturing process for, and in field application conditions of the adhesive joint.

7.4 Methodology

As mentioned in the previous section, there have been few attempts to characterise adhesion obtained at the interface in an insert moulded metal-polymer composite. Hence, there isn't a commonly accepted test procedure in the literature to quantify and compare joint strengths of insert moulded composites. It was therefore necessary to identify a suitable test before characterisation of the material adhesion could begin. As lap shear is one of the most commonly used tests for gauging the mechanical strength of adhesive joints in the laboratory, this was the first method tried in the present study. This was followed by block shear / peel tests and finally shear pull tests as described in the following sections.

7.4.1 Materials and experimental Apparatus

7.4.1.1 Thermoplastics

The polymer samples used for this experiment were granules as received from the manufacturers. The granules were dried before the experiments in a fan oven. The time of drying was as recommended by the manufacturers.

7.4.1.2 Insert materials

For lap shear test samples, the inserts were made by gluing tin foil on an aluminium substrate. The tin foil used for the experiments was from Goodfellow. The thickness of the foil was 0.1mm while its purity was 99.95%. The test sample overlap region was 25 mm wide and 50 mm in length. The same tin foil was used for block shear test samples. The inserts used for pull test were lengths of tinned copper wire from RS electronics. The diameter of the wire was 1.63mm and the thickness of the tin coating was 0.6 μm.

7.4.1.3 Injection Moulding Machine and Mould Tool Manufacture

For all methods of testing, samples were prepared using a vertical plunger type injection moulding machine (Fig. 59). Material was fed from a hopper into the barrel under gravity and the plunger was used to push the pellets in the barrel. The barrel of the unit was heated to the processing temperature of the thermoplastics with the help of band heaters. The plunger was driven by pneumatic drive cylinder. The injection pressure of the machine was calculated to be 900 psi (6.2 Mpa). The details of the injection moulding machine are given in Table 15.

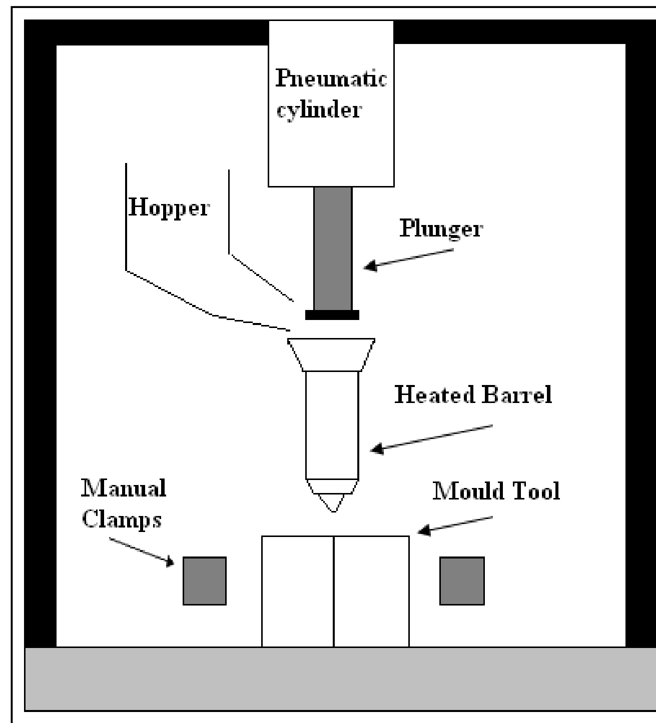

Figure 59: Vertical injection moulding machine set up

Table 15: Details of the vertical injection moulding machine

No	Description	Value
1	Injection Pressure	900 psi (6.2 MPa)
2	Plunger Diameter	20mm
3	Injection stroke	100 mm
4	Heating range	up to 300°C
5	Mould Clamping Unit	Manual

Mould tools were manufactured from aluminium blocks of overall dimensions 90 x 50 x 20 mm. Cavities and gates were machined using milling machines.

7.4.2 Lap Shear Test Method

Initial trials were made with hybrid lap shear test samples produced by insert injection moulding. Fig. 60, 61, 62, and 63 show the design of the tool and placement of the insert in the mould to make the samples.

The adherends / inserts were made up of tin foil glued on aluminium substrates of dimension 25mm x 100mm x 5mm. The aluminium substrate was used to provide the necessary mechanical strength for testing, but the interface to be tested was that between tin and thermoplastic. The thermoplastic layer injected was 1 mm thick.

Although moulding of samples was successful, it was found to be difficult to eject the samples from the tools after moulding without causing damage to them. The reasons for this were:

- As the tin had been glued on the adherends, the mould cavity could not be machined to a close tolerance and there was invariably some clearance between the adherend and the mould wall. During injection moulding, the thermoplastics filled the gaps and made ejection difficult.
- The direction of ejection was normal to the lap shear joint, so that when the mould opened, the two adherends would be pulled away from each other (Fig. 64). This compromised the bond strength during ejection of the sample.

As a result, typically the samples broke on ejection. Fig. 65 is an example of a broken sample.

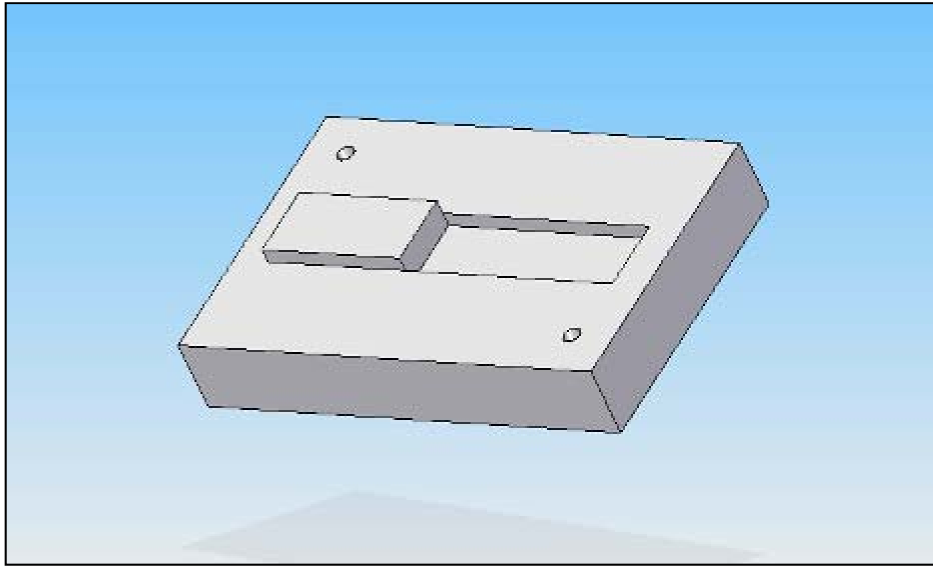

Figure 60: Mould plate side A with cavity for the insert and protrusion

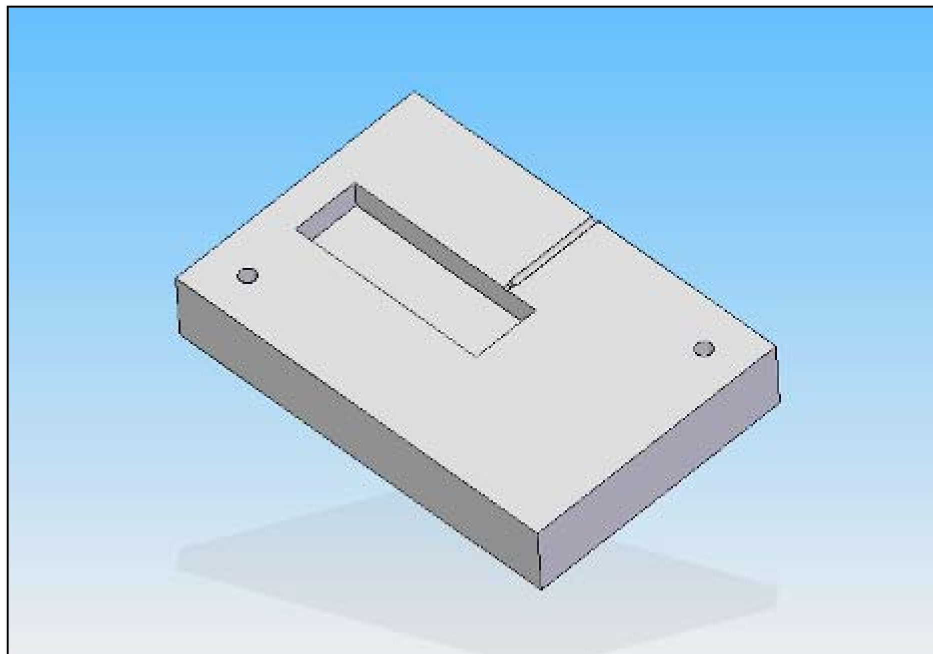

Figure 61: Mould plate side B with runner, gate and cavity

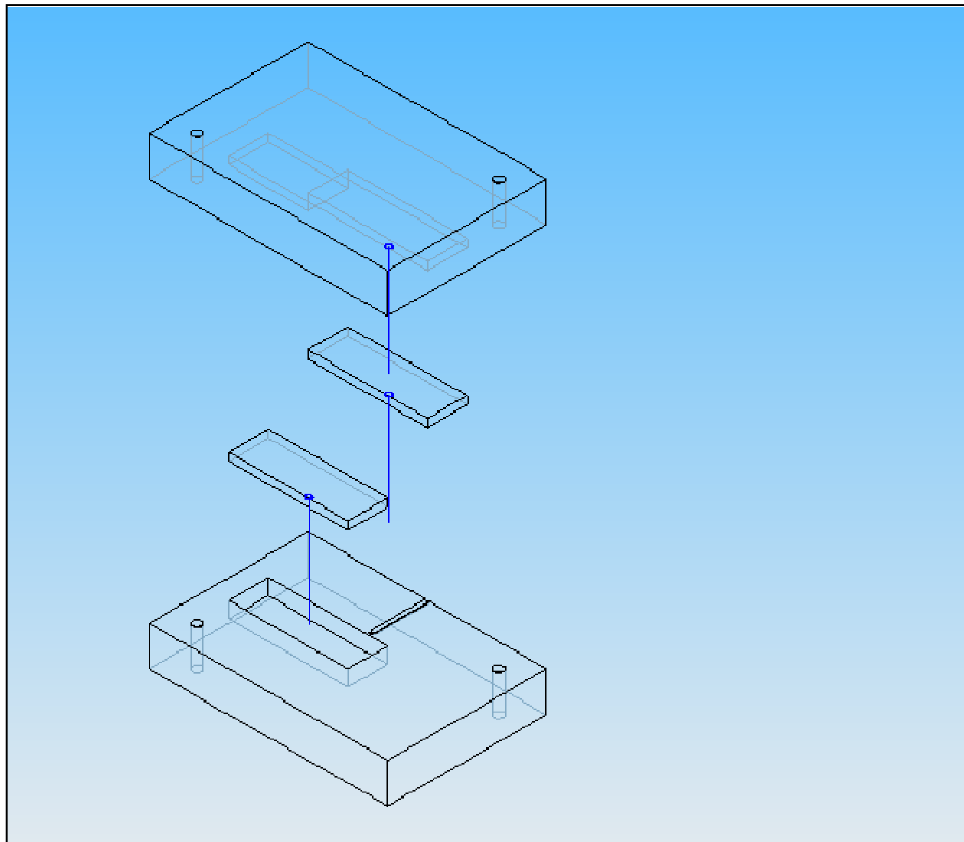

Figure 62: Exploded view of substrate and mould plates' assembly

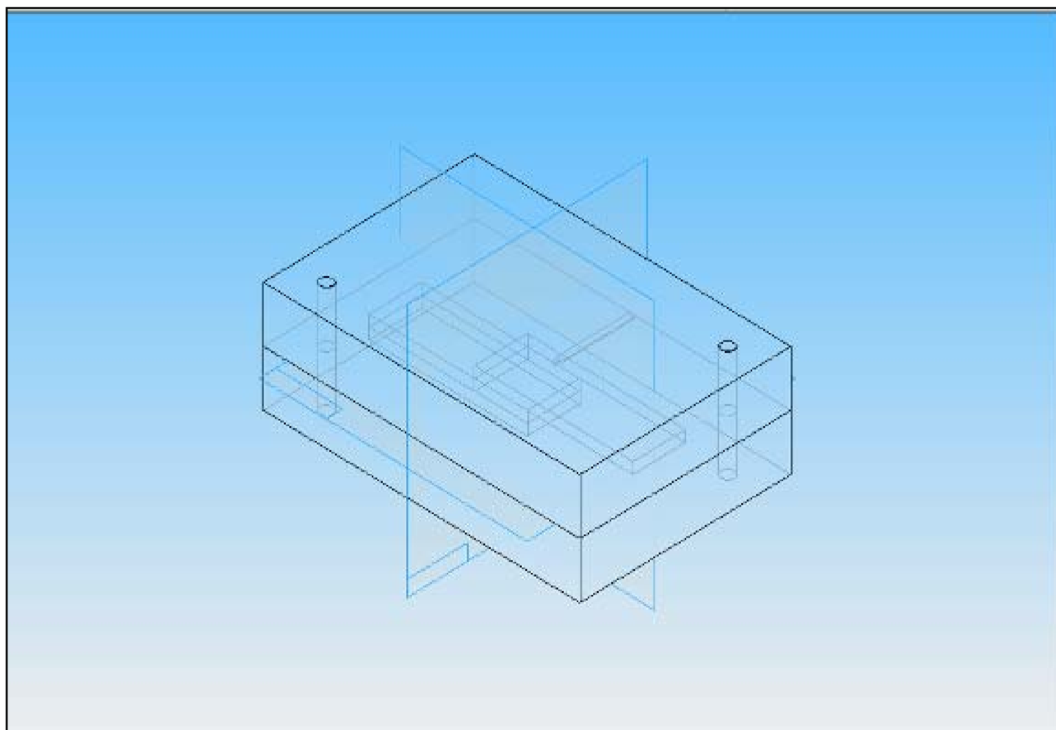

Figure 63: CAD drawing of the mould manufactured for lap shear joint samples (closed).

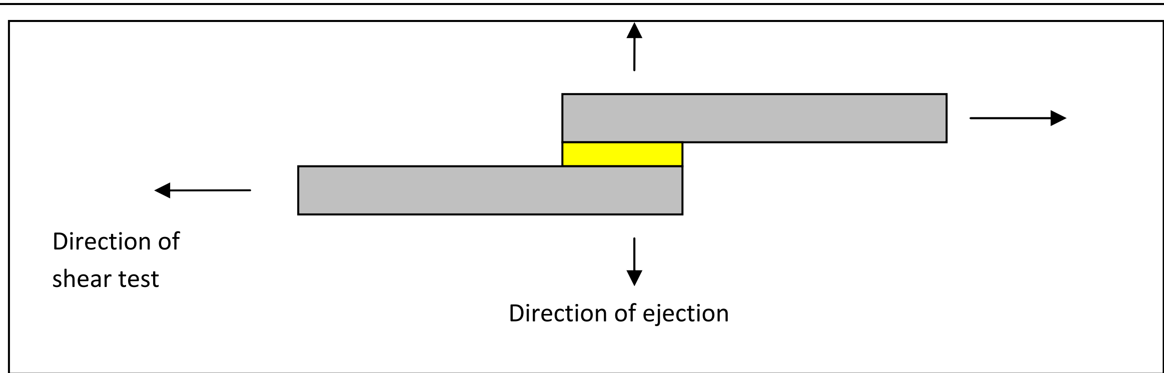

Figure 64: Representation of the directions of forces on the adhesive joint produced during ejection from the mould, and during testing

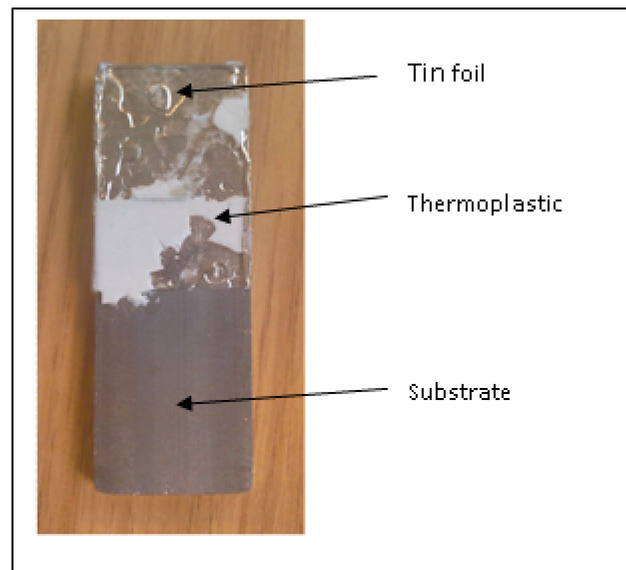

Figure 65: Representative sample of the effect of ejection on the lap shear joint

7.4.3 Block Shear Test / Peel Test

A block shear test design was tried to overcome the ejection force problem. The design is shown in Fig. 66. As this type of test involves the use of only one adherend it was hoped that ejection problems could be avoided. The design also allowed replacement of the glued tin foil aluminium substrate with unsupported tin foil

as the adherend, in which case a peel test would be performed instead of block shear.

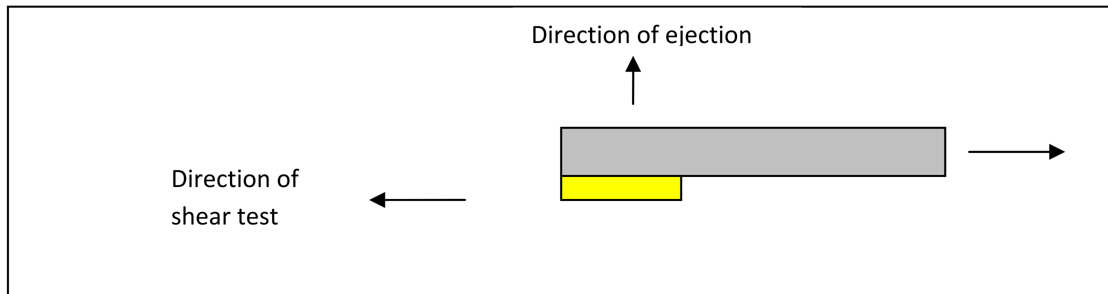

Figure 66: Representation of the directions of forces on the adhesive joint produced

However, even with this design it was found that however little force was applied normal to the direction of shear during ejection, it was still enough to cause any bond formed to rupture. The effect was attributed to shrinkage on solidification that is inherent to thermoplastics, making the bonding area uneven. Although in some cases adhered joints were successfully produced it seemed likely that the strength of the assembly had still been compromised, making strength test results unreliable. Hence, no test results were reported for these samples.

7.4.4 Shear Pull Test

Based on the difficulties encountered in manufacturing the lap shear and peel test samples, it was decided to make samples for a shear pull test. A pull test sample involves a wire (insert) injection overmoulded by a thermoplastic. The sample configuration is shown in Fig. 67. This form of test has the added advantage of better simulating the interaction between electronic components and polymer overmould in service. This is because the joint strength measured in the pull test samples will also be affected by the shrinkage as well as the flow and orientation effects of the

thermoplastics during injection moulding. Pull test samples are therefore more representative of real overmoulded parts.

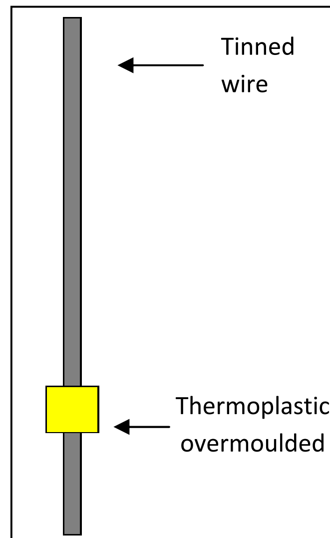

Figure 67: Configuration of a pull test sample

A mould tool was prepared with a channel in each of the cavities with a radius of 0.815mm such that half of the wire diameter fits in each cavity. The dimensions of the cavities forming the overmoulded thermoplastic block were 10mm x 10mm x 10mm.

A jig was made to test this hybrid in-mould overmoulded composite on an Instron 3366 tensile testing machine (Fig. 68). The jig was held in the lower jaw of the Instron tester. The groove of the jig was 3 mm in width. The samples were placed such that the wire passed through the groove of the jig and the thermoplastic overmoulded block was held in place by the jig. The use of the jig was necessary as the thermoplastic block, if held directly in the lower jaw may be crushed or could be squeezed onto the wire. Each tensile test was done at 25mm/min speed. A pre-load of 10 N was set, so that the wire was in tension when the tests started. All flash from the overmoulded sample was removed using a knife. This is because any flash would

result in reduction in the load during testing and could stop the test prematurely. Also, the presence of flash could result in a false engage (pre-load) or slip during testing, resulting in errors. Load vs extension curves were recorded. The tests were programmed to stop when the load reduced by 75% of peak value.

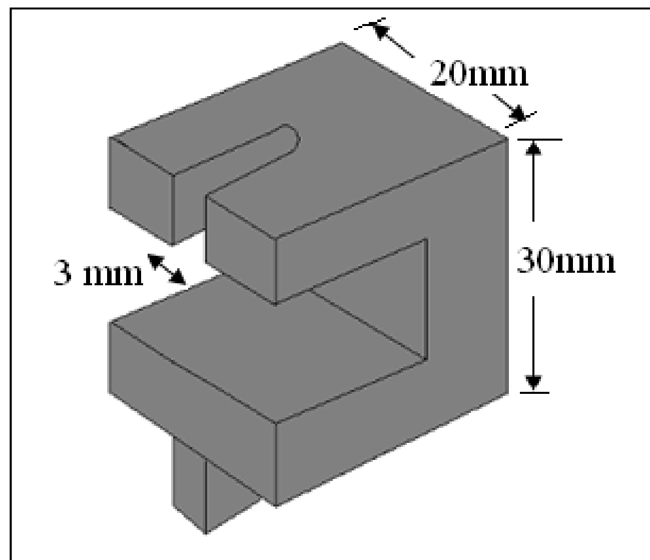

Figure 68: CAD image of the jig produced for the pull test

On visual inspection of the pull test samples after ejection from the mould, the bonded area looked crack free with no signs of bond rupture. However, to ameliorate effects of any compromising of the integrity of the samples during injection, and to improve test statistical validity tensile tests were done on batches of 15 samples. The standard deviation observed was less than 3% for all batches indicating that the preparation method was consistent and repeatable.

7.4.4.1 Insert Temperature

The temperature of the insert plays an important role in deciding the differential cooling rate of the thermoplastic overmould and thus influences the properties of the thermoplastics. Also, the wetting of the insert by the thermoplastic is

influenced by the temperature at the interface. Hence, insert temperature was chosen as the control parameter for the purpose of the mechanical strength tests.

A design of experiment was prepared allowing investigation of the effect of wetting and insert temperature on the ultimate joint strength. Different methods to pre-heat the wire were investigated. The most reliable technique to mimic the effect of a heated insert was found to be to place the entire mould with the wire located in it in an oven, and to pre-heat it to the required temperature immediately before transfer to the injection moulding machine and injection of the melt. Initially it was attempted to verify the temperature of the insert at the instant of moulding thermocouples were attached to the wire. However, this resulted in flash because the thermocouple wire prevented the mould plates from closing, leaving a gap. Generally, flash is not a big problem and is usually shaved off the components. However, the flash due to the thermocouple was considerable. Based on the experiences of the lap shear test, it was felt that any force applied, to remove the flash might compromise the joint strength of the sample, and so excessive flash should be avoided. Also, any residual flash might increase the total area of contact at the interface, resulting in erroneous results. Hence, to avoid flash, a calibration approach was devised in which thermocouples were attached to a wire and the mould was heated in a fan oven. The mould was removed from the oven, the instrumented wire was placed in it and the mould was closed immediately. This experiment was repeated for varying mould temperatures between 80°C and 160°C. It was observed that the mould cooled by about 20°C and the wire reached the temperature of the mould in approximately 20s. It was also found that the mould and the wire remained at the post closure temperature for about 30s before the temperature began again to drop. Thus, it was concluded that insert moulding done in the 21-50s window after the mould is closed

post heating would result in the temperature of the wire being reliably at the chosen insert temperature for the experiment.

7.4.4.2 Experimental Procedure

Based on the initial trials and insert temperature measurements an experimental procedure was established. The steps involved in the making of the shear pull test samples were:

1. The wire was cut to approx. 100 mm length.
2. Lotoxane degreaser and tissue paper were used to degrease the wire.
3. The mould was heated to the desired temperature, i.e. 20°C above the chosen insert temperature in a fan oven.
4. The mould was taken out of the fan oven and the wire was inserted in the channel in the mould.
5. The mould was closed immediately.
6. A timer was started.
7. The temperature of the mating surfaces of the two mould halves was recorded with a thermocouple, 20 seconds after the mould was closed with the wire in it. This temperature was noted as the temperature of the wire. A groove cut into the mould away from the cavity region permitted this.
8. As soon as the mould with the wire in it reached the chosen temperature for the experiment, it was placed in the injection moulding machine and the pull test sample was produced.

Mouldings with insert temperatures 60°C, 80°C, 100°C, 120°C and room temperature (approximately 21°C) were produced.

7.5 Results

Fig. 69-72 show examples of load vs extension curves obtained for a number of different polymers. Considering the curve for PMMA (Fig. 69), it can be seen that at the start of the test there is a linear rise in the load vs extension curve (marked A in Fig. 69). This initial part of the curve is due to the response of the adhesive joint to the tensile load applied. i.e., the stress transfer from the wire to the thermoplastic overmould. The maximum load value obtained (point B) was identified as corresponding to the failure of the bond i.e. complete debonding at the metal thermoplastic interface. The load at this point was therefore taken to be the breaking load. This identification is supported by the extremely low extension values seen as the load increases up to point B on the curve, and was also corroborated through visual observations of bond failure during and after the tensile tests. For all the samples tested, this point occurred at less than 0.5 mm extension. The load decreases sharply after point B. As the test proceeds the load drops until point C. The load vs extension behaviour after bond breaking was interpreted as representing the slipping of the tin coated copper wire through the thermoplastic overmould resisted by frictional forces. For some tests with some materials these loads were relatively steady e.g. PA 6 in Fig. 72, while in for others the frictional load increased with strain e.g. ABS in Fig.70, even to the point of exceeding the breaking load. With the exception of PC and PMMA with insert at room temperature, the nature of the curve for ABS, PC, PMMA and PS was similar to that in Fig. 70. Also, as the insert temperature was varied, the nature of the curve for ABS, PC, PMMA and PS remained the same, the only difference being change in the breaking load value. It is interesting to note that frictional loads exceeding the breaking load were not seen for

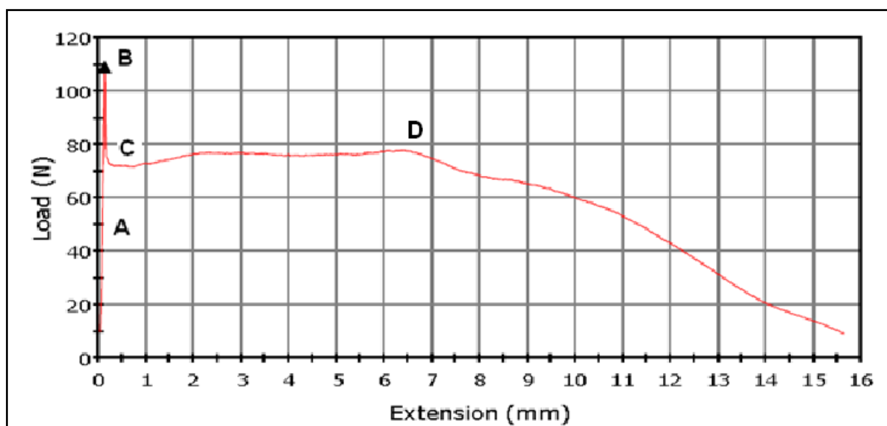

Figure 69: Typical load Vs extension curve for PMMA, insert at room temperature

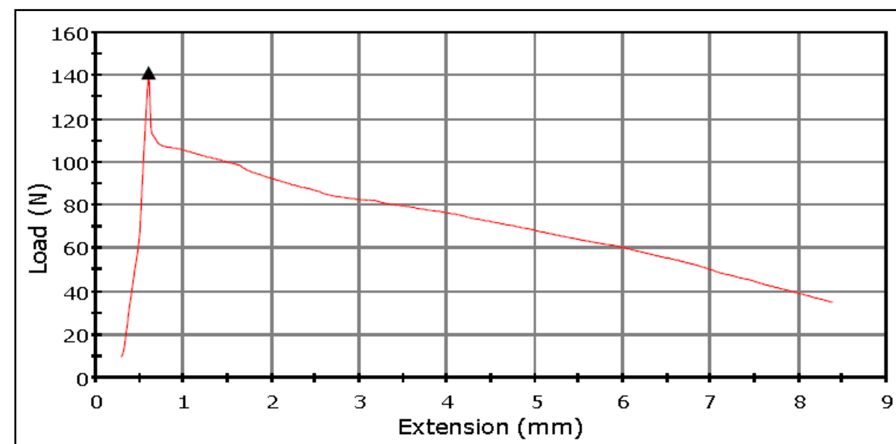

Figure 71: Typical load Vs extension curve for PBT, insert at room temperature.

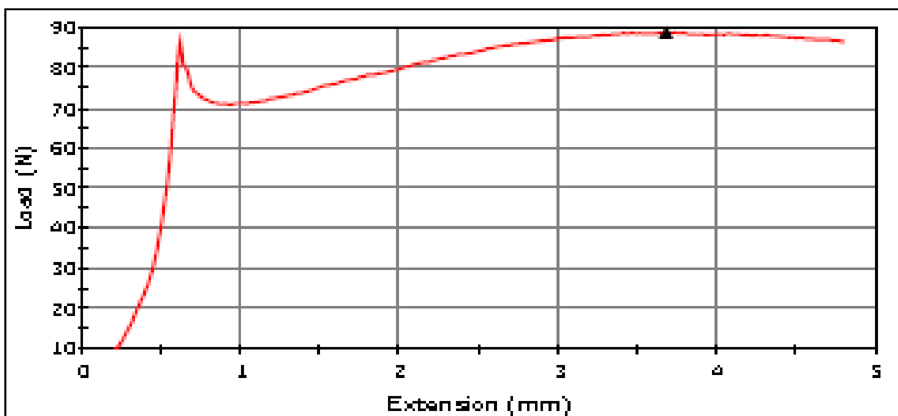

Figure 70: Typical load Vs extension curve for ABS @ insert temperature 60°C

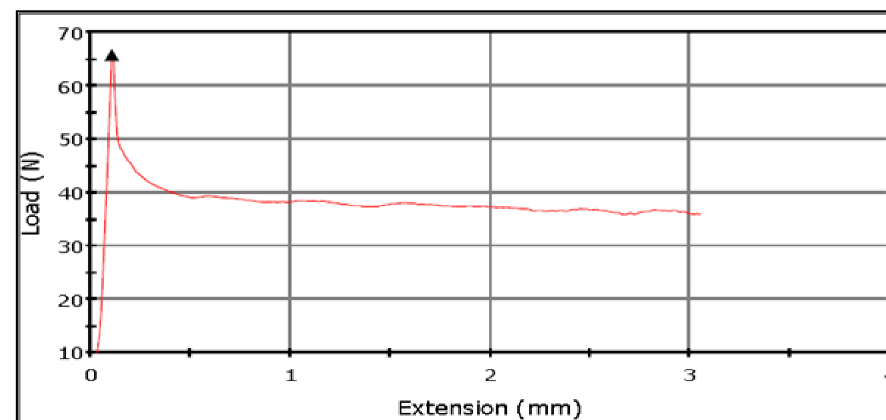

Figure 72: Typical load Vs extension curve for PA 6 insert temperature 80°C

any PBT samples, and not for PA 6 samples with the exception of PA 6 with insert at room temperature. By comparison with the PBT and PA 6 behaviour it was considered justified to identify the short extension peak with the breaking load, whether or not it was the maximum load seen in the test.

Fig. 73 summarises the breaking loads (i.e. point B from the curves) for all the samples tested as a function of insert temperature. Each force value represents an average of 15 measurements. The standard deviation was between 2-3% for all values which is smaller than the differences among most of them. It can be seen that the breaking loads for each material vary with insert temperature, and that the values vary between materials. For the materials tested, PC with insert temperature at 120°C shows the highest breaking load while PA 6 with insert temperature at 120°C shows the lowest. The temperature of maximum breaking load varies among the materials and with the exception of PC, for all the materials tested there is a trend of rise and fall of breaking load with increase in insert temperature. The materials can be ranked by the breaking loads at given insert temperatures e.g. for insert temperature maintained at room temperature the ranking (highest force to lowest) is as follows:

PBT > PC > PMMA > ABS > PS > PA 6

The same hierarchy is maintained when insert temperature is 60°C. However at 80°C, the joint strength hierarchy is

PMMA > PBT > PC> PS > ABS > PA 6

Moreover, when the insert temperature is 100°C

PC > PMMA > PBT > PS> ABS > PA 6

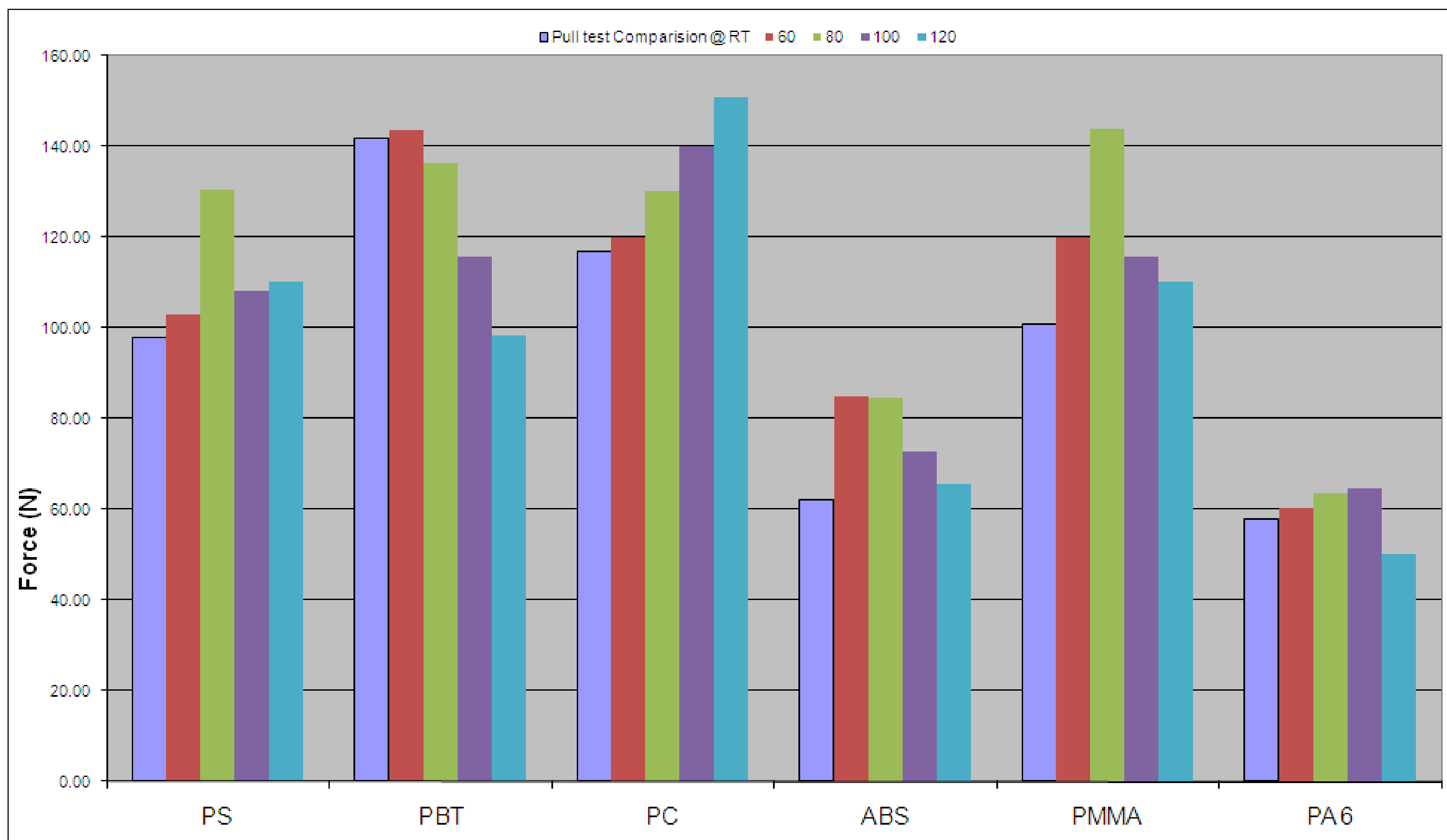

Figure 73: Compilation of data: Averaged breaking load Vs Temperature

And when it is 120°C

PC > PBT> PMMA > PS> ABS> PA 6

Thus changing the insert temperature can change which material exhibits the greatest breaking load. The practical implication of this is that choice of insert temperature is likely to have as strong an influence on the reliability of electronics assembled by the substrateless method as choice of mould material. In fact the maximum strength variation with temperature observed for a single material was 42%, which occurred for PMMA between room temperature and 80°C.

7.6 Discussion

According to Wood *et.al.* the shear strength (breaking load) of an insert moulded fibre-thermoplastic composite (a similar system to the wire / overmould used here) can be attributed to [81]

- Physical and/or chemical bonds and
- The frictional force acting in the radial direction, on account of shrinkage (or lack of it) of the thermoplastic around the insert.

Thus in the simplest case, total shear strength or breaking load (τ) can be described as

$$\tau = \tau_0 + \mu\sigma_{rr} \qquad \text{.................................} \textbf{[10]}$$

where,

τ_0= The adhesive bonding between the fibre and the matrix

μ = The coefficient of friction between the fibre and the matrix

$\boldsymbol{\sigma_{rr}}$ = Radial stress contribution

It is clear from the above equation that interfacial adhesion in insert moulding is a complicated problem that involves interactions of materials at the interface during and after moulding as well as the processing parameters that may influence the material interactions at the interface and result in the radial stress contributions on the insert by the thermoplastic matrix. According to Yue *et.al.* the influence of the interfacial parameters like shear strength, matrix shrinkage pressure and co-efficient of friction on the mechanical properties of composites can readily be understood with reference to their effect on the pull-out curve [80]. According to them for a given system, larger interfacial shear strength results in higher breaking loads. Also, larger matrix shrinkage pressure results in higher breaking loads and higher area under the load vs extension curve while larger coefficient of friction will only result in higher area under the curve. Breaking load signifies the strength of the system while the area under the curve signifies toughness. For substrateless packaging, any loss of contact between the thermoplastic overmould and insert may result in a malfunctioning circuit. Thus, for the purpose of this study, breaking load and matrix shrinkage assume importance.

As stated in the earlier section, a rise and then fall was the observed trend for joint strength / breaking load at various insert temperatures. A study by Ramani *et.al* of polycarbonate bonded to steel and aluminium, reported a continuous rise in joint strength with rise in insert temperature over the range 170-204°C [25]. It has also been well established in the literature that wetting of adherends by adhesives plays an important role in the final bond strength. In Chapter 6, it was shown that wetting of

tin by thermoplastics increases with temperature. Thus it was expected that rise in insert temperature should always lead to improved joint strength, as in fact was observed by Ramani *et al*. The difference between the trend observed here and those of others may be because of the different methods of joint strength testing used by other authors. Ramani *et.al.* performed a tensile butt shear test. Most reports in the literature on adhesive strength at interfaces are for lap shear samples, block shear or peel test samples [26][32][82][83]. Although all these tests are typically used to measure the strengths of joints formed by adhesives, they may not be appropriate for insert moulding as material shrinkage plays a role in all insert moulding processes. The pull test is more representative of the insert moulding process than lap shear test or peel test. Also, as reported in Chapter 6 although wetting improves with rise in temperature at the interface, the work of adhesion at the interface may not always rise with the rise in temperature at the interface.

Yamaguchi *et.al.* investigated the effect of the presence of a polypropylene film on heat flow in film insert moulding, and concluded that the presence of the film caused the injected resin to adopt a higher crystalline content on solidification, due to the slower cooling rate [29]. The rise in insert temperature may have a similar effect on the tin-thermoplastic system, i.e. with hotter inserts the polymer in contact with the tin metal cools down more slowly as compared to cooler inserts, and hence would have a higher crystalline content and comparatively higher shrinkage induced stress, causing changes in the forces acting radially at the insert-thermoplastic interface.

Table 16: Peak loading insert temperatures and Tg of the thermoplastic.

Material	PS	PBT	PC	ABS	PMMA	PA 6
Peak breaking load insert temperature (°C)	80	60	>120	60	80	80
Glass transition temperature (Tg) (°C)	≈89	≈47	≈152	≈110	≈117	≈48

Table 16 gives the glass transition temperatures (Tg) of the thermoplastics and the peak breaking load temperatures of the pull test samples. It can be seen that for the amorphous polymers PS, PC, ABS and PMMA the peak breaking load insert temperature lies below the Tg of the thermoplastics. Thus for the insert temperatures close to or above the Tg of the thermoplastic the breaking loads recorded are lower (Fig. 73). When the temperature of a thermoplastic rises above Tg, it enters the rubbery phase. This transition is accompanied by volumetric expansion, usually explained as the dis-entanglement of the polymer chains. Thus the degree of volumetric expansion experienced by, for example, PS coming in contact with tin at room temperature, vs PS coming in contact with the tin insert at 80°C, is different on account of the different insert temperature. For insert temperatures above the Tg of PS of 89°C, the effect of volumetric expansion is much larger. This change in material properties at the interface, coupled with the slow cooling of the polymer, may have a greater influence on the joint strength than improvement in wetting, resulting in the drop in values seen at insert temperatures around or higher than Tg, due to the effect on stresses developed in the area near the interface. In the case of PC we do not see the characteristic rise and fall pattern as the Tg of PC is greater than the maximum insert temperature used at 152°C.

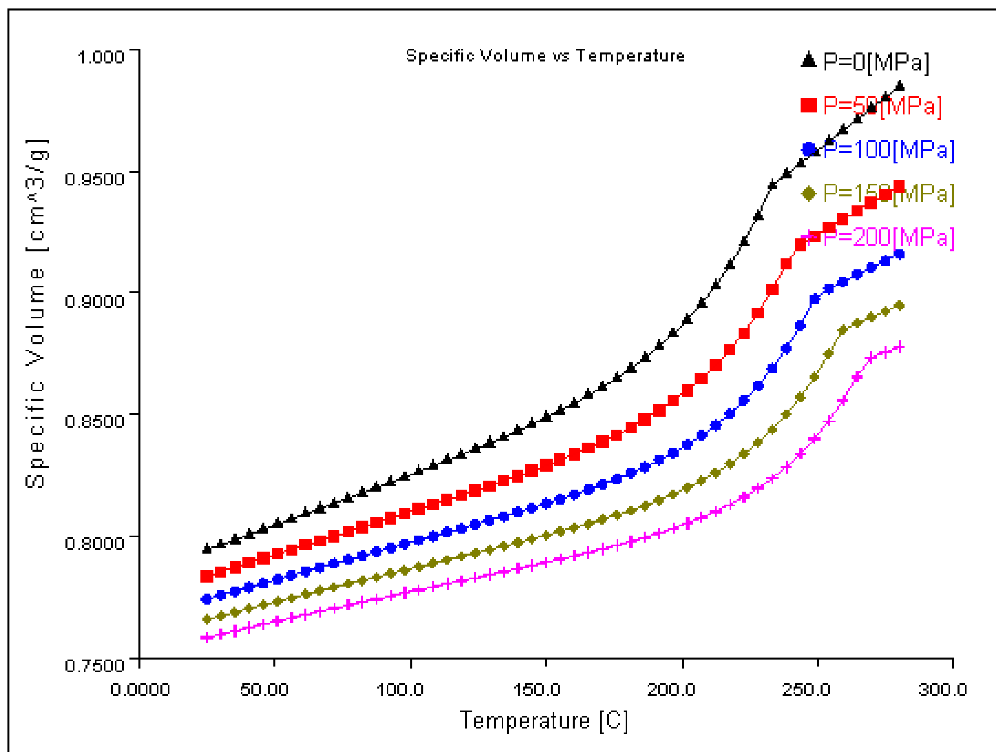

Figure 74: PVT data for PBT

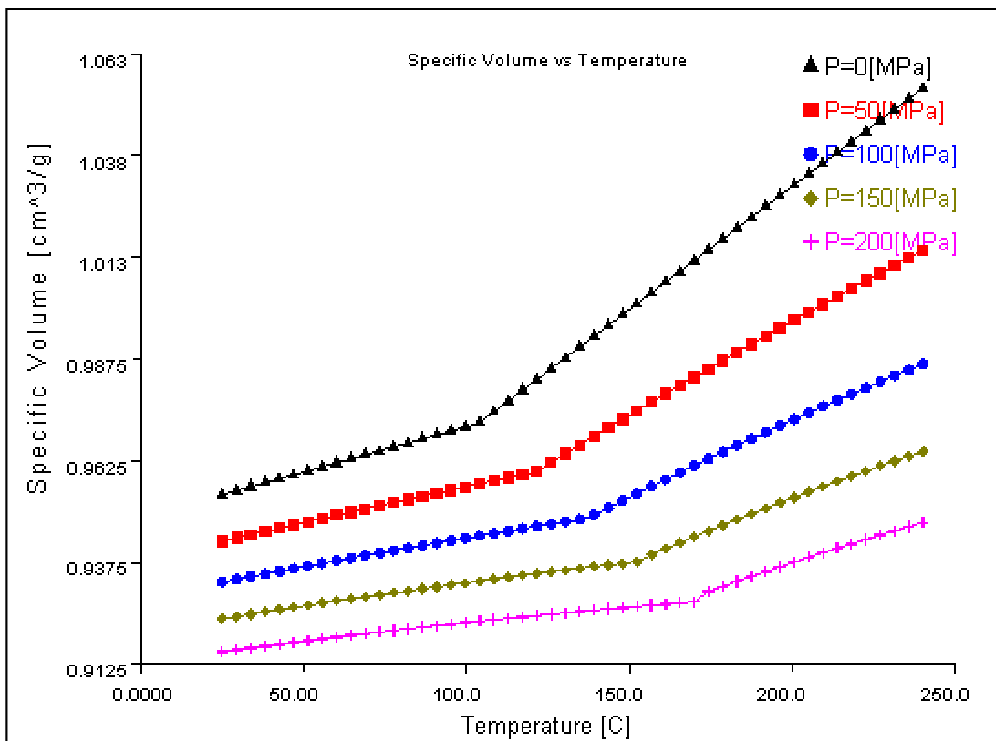

Figure 75: PVT data for PS

For the semi- crystalline polymers PBT and PA 6, the change in specific volume is more around the crystallisation temperature (Tc) than Tg. Fig. 74 and 75 taken from the Moldflow[4] materials data base illustrate the differences in specific volume variation behaviour between the semicrystalline PBT and amorphous PS. Hence the peak breaking loads occur at insert temperature above Tg but drop with subsequent rise in insert temperature.

Table 17 gives the tensile stress at break of thermoplastics (See appendix 2). In general the trend of tensile strength values shows good correlation with the breaking load values in Fig 73. As the bond at the interface comes under load, the stress is transferred from the matrix to the insert. The inherent strength of the matrix may therefore affect the overall bond strength at the interface. This implies choosing thermoplastics with higher strength may result in higher joint strength of the system for substrateless packaging.

Table 17: Tensile stress at break and peak breaking loads

Material	PS	PBT	PC	ABS	PMMA	PA 6
Tensile stress at break (MPa)	51	60	71	31	77	46
Peak breaking loads (N)	129	141	148	83	143	63

[4] See Chapter 8 for the details of Moldflow.

7.7 Conclusions

In this chapter, the use of mechanical strength test for study of bond strength at interface in insert moulding was reviewed. A methodology was devised to test bond strength at interface between tinned copper insert and the thermoplastics selected for this study. A detailed description of the mechanical strength test selection and sample preparation was given. Lap shear test and block shear test sample preparation was attempted but were not tested due to the bond rupture during ejection from the mould after insert moulding. Pull out test samples were prepared by maintaining the insert temperature constant 21, 60, 80, 100 and 120°C and were tested. The standard deviation was less than 3% and hence it was concluded that the sample preparation method was consistent and repeatable. Load vs extension curves were obtained for all the samples manufactured and breaking load was recorded. It was observed that breaking loads varied with insert temperature. Except for PC, for all the materials tested, the breaking loads rise and fall with rise in temperature of the insert. Peak breaking load varied for all the materials. Maximum strength variation observed was 42% for PMMA. Peak breaking load for the amorphous polymers ABS, PS and PMMA were observed for insert temperature maintained just below Tg of the polymer and for semicrystalline polymers PA 6 and PBT it was just above Tg. It was discussed that pull out force variation with insert temperature could be on account of volumetric shrinkage and mechanical properties of the materials.

8 Moldflow Analysis

Contents:

- *Introduction*
- *Reports of Use of FEA for Insert Moulding Analysis*
- *Moldflow*
- *Experimental Method*
- *Results*
- *Conclusions*

8.1 Introduction

Finite element analysis (FEA) is a computational tool that can be used to calculate physical quantities like temperature, deformations, stress and strain throughout a component or structure. Typically the geometry of the structure is divided into smaller finite elements (triangular, quadrilateral or tetras) with nodes at each corner. Once this is done, boundary conditions are set and the loading situation is simulated e.g. the flow of a polymer, or forces at a particular point. The results are calculated by solving equations (constitutive laws) at each node. They are solved for each incremental increase in applied load, displacement etc. across each finite element.

In the case of injection moulding, FEA can be used to simulate the flow induced properties during manufacturing. Moldflow is a commercial software package that is used exclusively to simulate injection moulding process conditions. In this work, the method of building a model in Moldflow for analysis of insert moulding is described and a model of the pull-out test specimen described in Chapter 7 was built. Moldflow was used to simulate the insert moulding process used to produce the test

specimen. The model allowed insight into quantities that are difficult to measure directly, i.e. the melt flow and thermal histories during injection and solidification, and the consequent effects on the degree and spatial distribution of shrinkage throughout the moulding.

8.2 Reports of Use of FEA for Insert Moulding Analysis

Although the use of these software programmes have become a norm in the industry, not many studies have been published covering their use to examine adhesion at the interface in insert moulding analysis. This is because they are mostly used to analyse the stresses and strains developed in the product affecting its service life, and the adhesion at interface is normally accounted for by the use of undercuts and other features. A few of the relevant published studies on the use of FEA in insert moulding analysis are listed below:

1. Zhil'tsova *et.al.* performed a numerical simulation of an insert moulded PBT component. They concluded that pre-heating the insert helps to relax excessive plastic tension on the part insert interface and results in an increase of radial shrinkage of the part [84].
2. Chang performed 3D simulations of insert moulding with ABS as resin and P6- mould steel, beryllium-copper and polymer as inserts. He concluded that the variation in insert properties has an effect on the cycle time. In particular he found that the metal inserts increased the rate of heat flow from the thermoplastic melt on cooling while the plastic insert reduced heat flow rate [85].

3. Thornagel performed 3D moulding simulation by implementing applied crystallization models. He concluded that pre-heating the insert not only affects the properties of the moulding near to the insert, but also in areas downstream of the insert [86].

8.3 Moldflow

Moldflow is a commercial FEA software package used to simulate the injection moulding process. The physical properties of components produced via injection moulding depend on the material properties of the polymers, as well as on the properties induced as a result of the process conditions. Moldflow simulates the flow of polymers from the injection nozzle into the mould cavity. The software can predict the evolution of the flow front, thermal flows and temperatures in the melt, and the degree of shrinkage of the polymer on cooling.

8.3.1 Workflow Sequence for Moldflow Analysis

In general, Moldflow is not used to create CAD models of the parts. CAD models are imported from other CAD programmes for example CATIA or Solid Edge. These models are then meshed (i.e. divided into smaller elements for analysis). There are three mesh options available in Moldflow viz. midplane, dual domain and 3D. In general, the midplane and the dual domain mesh are used for thin wall products. 3D mesh is preferred for products with sudden changes in thickness and for insert moulding analysis. The choice of mesh for a given product is a matter of expertise and experience. Once the model is meshed, the feed system and cooling channels are added. This makes the model ready for analysis. Selection of analysis

sequence depends on the type of data required. As the name suggest, the selection of a sequence of analysis restricts the Moldflow analysis to that stage in injection moulding. E.g.: if “Fill analysis” is selected, Moldflow simulates the flow of the material into the mould cavity and the analysis stops at the stage when the cavity is completely filled. If “Fill + Pack Analysis” is selected, then Moldflow simulates the fill and pack stage of the moulding operation. In all five analysis sequences are available.

- Fill
- Fill + Pack
- Cool
- Fill + Pack + Warp
- Cool + Fill + Pack + Warp

Selection of material type is straight forward. A comprehensive material library is provided with the software and most common grades of thermoplastics are available. The entry in the library for a particular material details its thermal, mechanical and rheological properties. Also, new grades can be created based on the information from material data sheets. Setting of injection location depends on the requirements of the components. Information about the injection moulding machine is provided by the user through the process settings tab. Once the material information and process settings are set, an analysis can be run. The typical Moldflow analysis workflow sequence is as shown in Fig. 76.

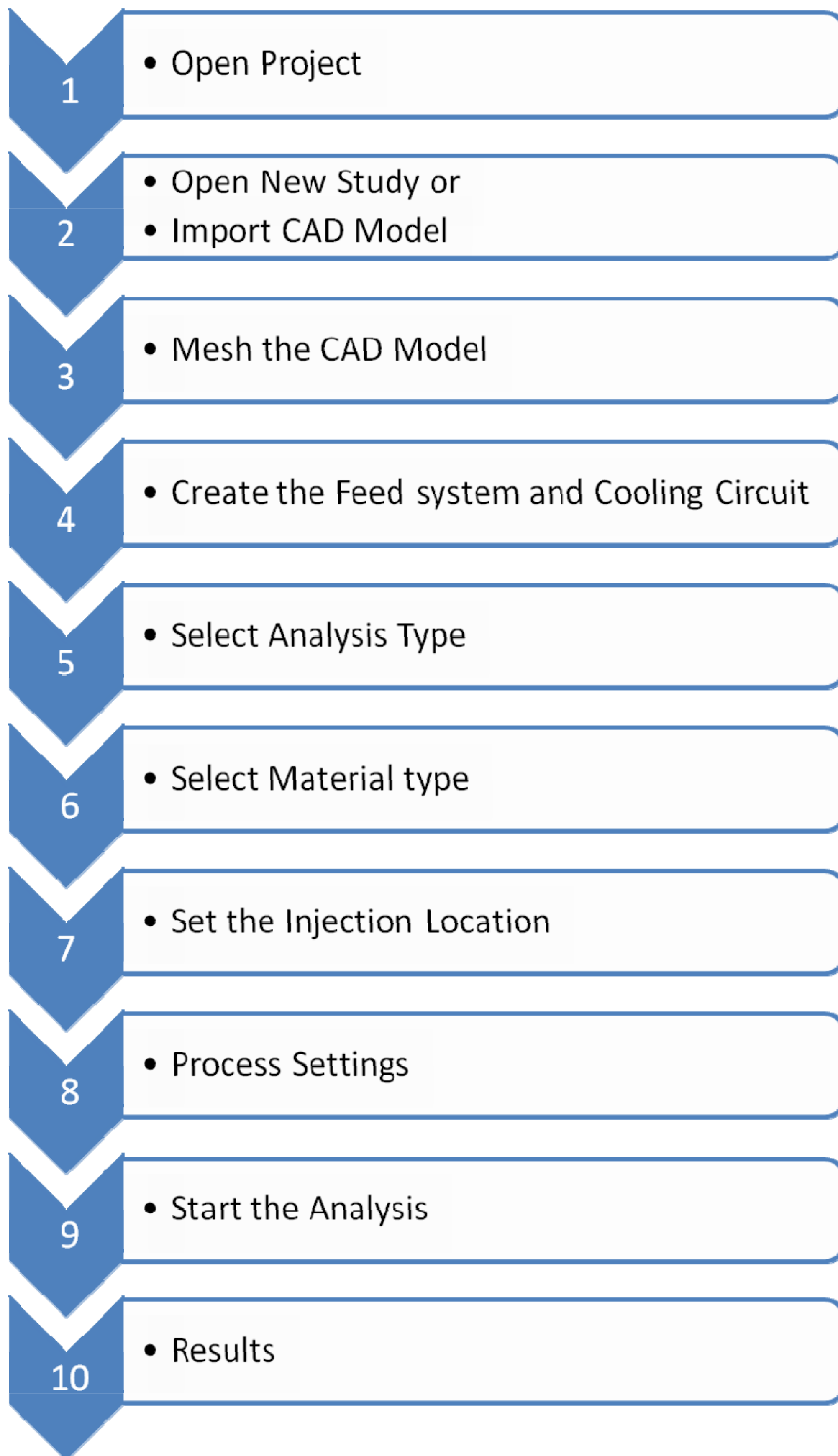

Figure 76: Typical Moldflow analysis workflow sequence

8.4 Experimental Method

The insert moulding analysis was performed to augment the findings of the pull out test from Chapter 7. The CAD model of the pull out test was built using Solid Edge package. The model consisted of a 10 mm on a side cube with an insert wire 100 mm long and 1.63mm in diameter passing centrally through it. However, to properly represent the thermoplastic overmould and insert a special meshing procedure was required as described in the next section.

8.4.1 Meshing Procedure in Moldflow for Insert Moulding Analysis

Insert moulding analysis is usually done to understand the effect of an insert on the flow induced properties of the insert moulded component. The main difference between the insert moulding analysis workflow and the usual Moldflow analysis for injection moulding workflow shown in Fig. 76 occurs after step 2: Importing CAD model and in step 3: Meshing. For the insert moulding analysis, the CAD model for the thermoplastic overmould part and the insert were imported into the study. Then the mesh of the insert was matched node to node with the mesh of the thermoplastic part. The details of the model preparation for insert moulding analysis are as follows

1. A new project was created and the thermoplastic overmould and the insert were imported as independent studies (Fig. 77a, 77b).

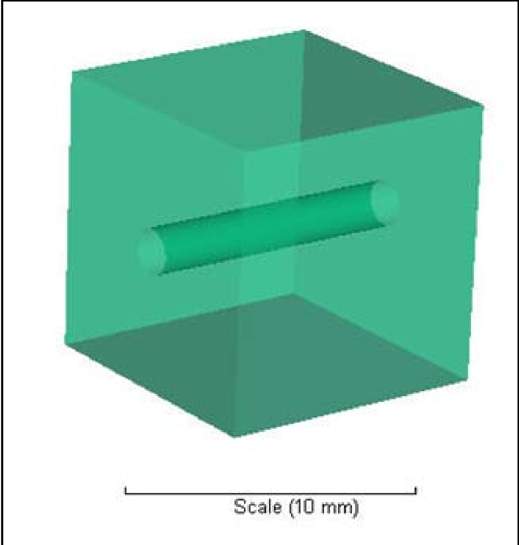

(a) CAD image of the thermoplastic overmould

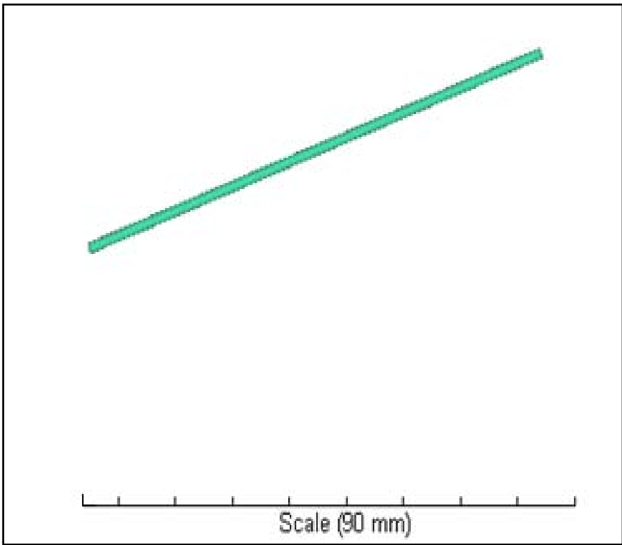

(b) CAD image of the insert

Figure 77: CAD images

2. The overmould and insert studies were separately meshed using the dual domain 2D mesh, which meshes just the outer skin (surface) of the components (fig. 78a, 78b)

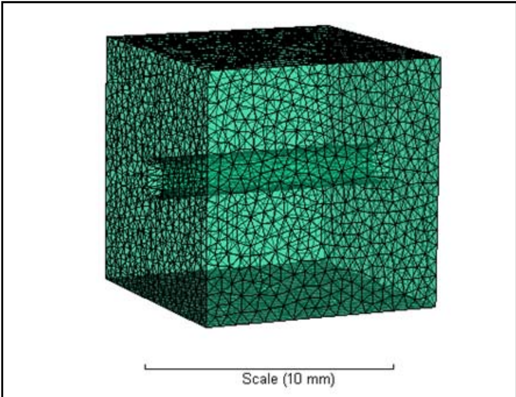

(a) Dual domain mesh for the thermoplastic overmould

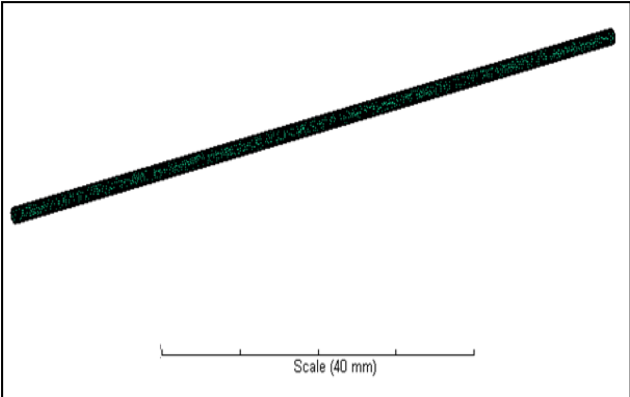

(b) Dual domain mesh for the insert

Figure 78: Dual domain mesh

3. The insert study was added to the thermoplastic overmould study. A cutting plane (i.e. a cross section, section view) was used to observe the mesh-mismatch at the insert-overmould. (Fig. 79a and 79b)

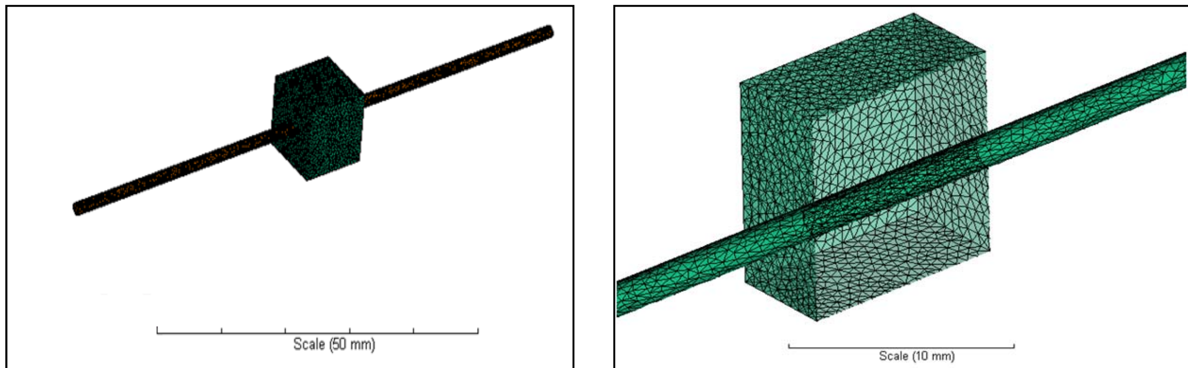

(a) Result of adding the insert study to the thermoplastic overmould study

(b) Use of cutting plane to observe the mesh-mismatch

Figure 79: 'Adding' insert to overmould study

4. In order to get good results at the interface, the insert mesh has to match node to node with the overmould mesh in the region of overlap. This is achieved by copying the mesh pattern of the overmould at the interface and replacing the corresponding region of the insert mesh with it. This way when the two studies are added together, the mesh at the interface of the insert and overmould match node to node. To do this the mesh at the interface was isolated. The areas around the overmould interface were selected and deleted (Fig. 80a) and only the mesh at the interface was obtained (Fig. 80b)

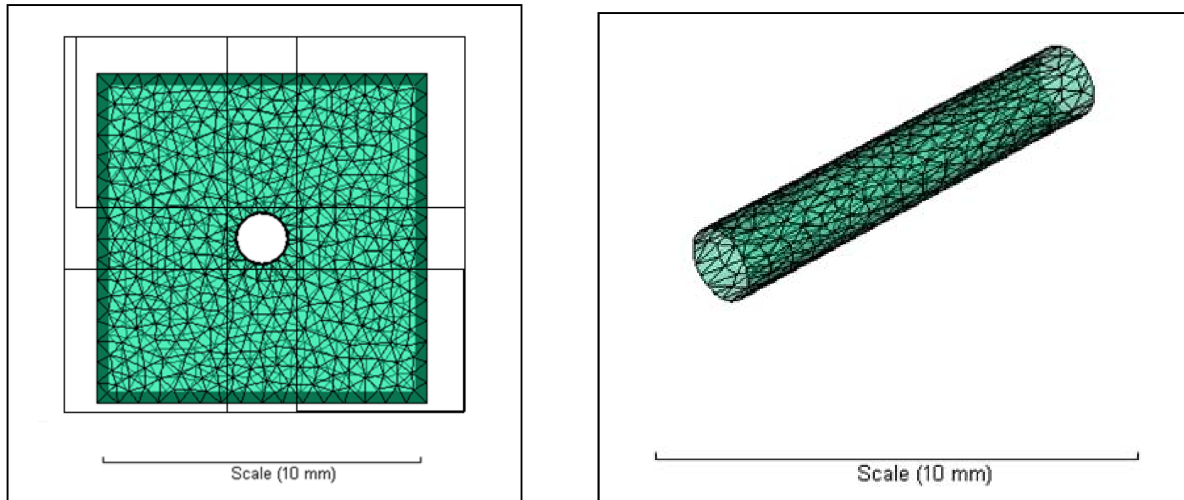

(a) Band select the areas around the interface *(b) Isolated interface area*

Figure 80: Isolation of interface area mesh

5. The temporary study with the isolated mesh was added to the insert study (Fig. 81). Notice the mesh mis-match, which can also be seen in Fig. 79b.

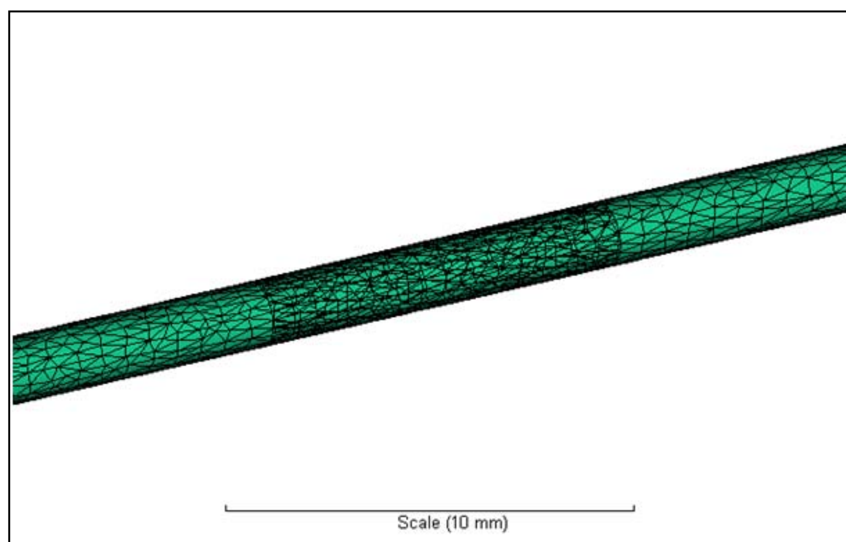

Figure 81: Mis-match of the mesh at interface

6. To delete the overlapped elements of the insert, the elements that were not overlapped have to be isolated. To do this, the elements that were not overlapped were selected (pink elements in Fig. 82a) and assigned to a

different layer (i.e. effectively made invisible). The overmould mesh and the overlapped insert elements were left in the active layer (fig. 82b).

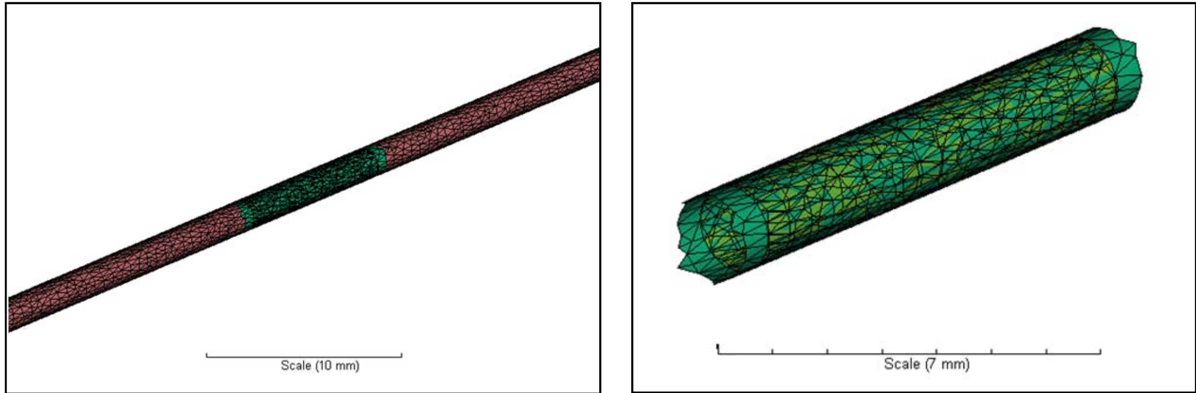

(a) The elements that are not overlapped are band selected

(b) leaving the isolated interface mesh

Figure 82: Isolation of overlapped interface mesh

7. Then the overlapped insert elements were deleted leaving behind the added overmould mesh and the remaining insert elements (Fig. 83).

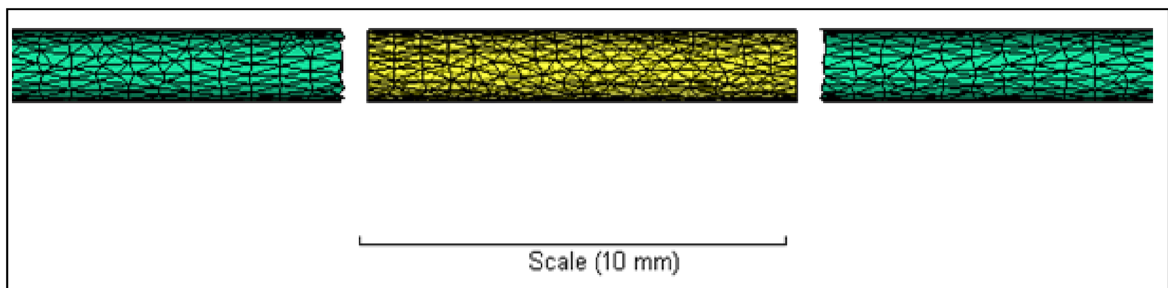

Figure 83: Result of deleting overlapped mesh elements

8. The gap between the remaining insert mesh elements (seen in Fig. 83) and the added mesh was filled by creating new elements to give the new insert mesh.

9. Now that the insert's mesh matched the connector's mesh, both parts were meshed with tetrahedral elements (3D mesh).
10. The 3D insert mesh study was added to the 3D thermoplastic overmould study. A cutting plane was used to verify the mesh-matching. (Fig. 84).

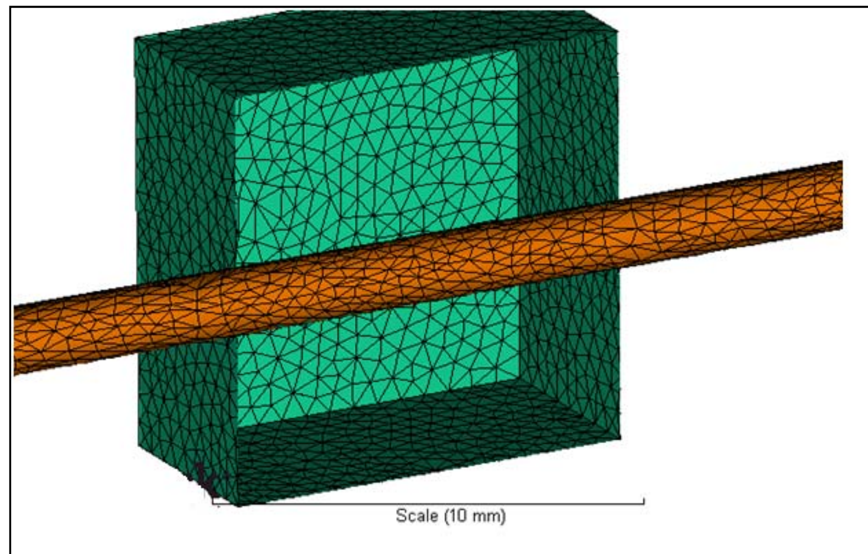

Figure 84: Mesh-match at insert interface

The remaining workflow for insert moulding analysis was similar to the standard workflow shown in Fig. 76 from step 4 onwards.

8.4.2 Selection of Model Parameters

The feed system for the pull test was direct injection from barrel to gate of the mould. The gate location (injection location) was taken to be at the centre of the top surface of the thermoplastic overmould as shown in fig. 85a and 85b.

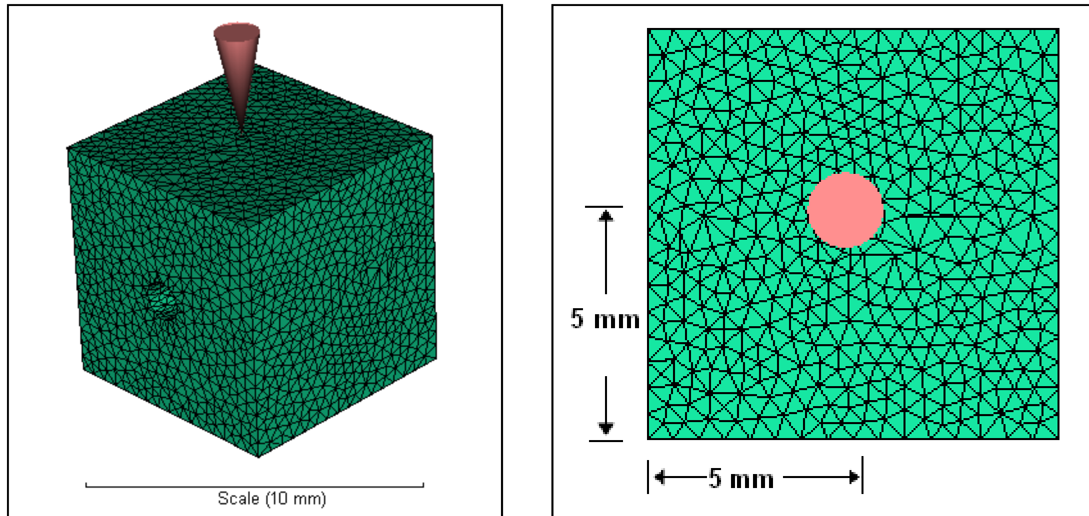

(a) Isometric view of the thermoplastic overmould showing injection location

(b) Top view of the thermoplastic overmould showing injection location

Figure 85: Gate location

The analysis type used was 3D mesh. This was because dual domain analysis cannot be used for insert moulding while the midplane analysis does not allow examination of the critical properties at the insert/ moulding interface.

The material processing parameters chosen were the defaults from the Moldflow materials database. Material files for the exact grades of moulding resins used were selected from the Moldflow library. The default processing parameters were found to be as suggested by the manufacturers in the resin data sheets and so were not changed.

The machine parameters used were default injection moulding settings with

- Filling control: automatic
- Injection pressure: 900psi (6.2 MPa) - representing the estimated pressure used in the pull out experiments, see Chapter 7 Table 15
- Clamping pressure: Manual (max. pressure value used)

The mesh statistics for the Moldflow modelling are listed in Table 18:

Table 18: Mesh Statistics

Number of nodes	19848
Number of Tetras	106805
Aspect ratio	Max 22.4 Average 4.09 Min 1.05
Global edge length	0.49mm

Global Edge Length: In Moldflow, the global edge length decides the mesh density. Generally, at least three layers of tetras through the thickness of the sample are considered good for simulations. The computational time increases exponentially as the mesh density rises. Hence, although fine mesh is desired, it has to be balanced against the time required for simulation. 0.49mm global edge length was considered appropriate for the simulation of pull out test sample.

As this analysis was to simulate the production of the pull test samples, the mould and insert temperatures were set to be equal. The insert temperatures were chosen to match those used in the pull test sample preparations (21, 60, 80, 100 and 120°C). The Fill+Pack analysis sequence was used with a cooling time of 20s. The fill time was approx 1sec.

8.5 Results

The figures in this section are section views made by cutting planes X - Y, Y- Z and Z - X as shown in Fig. 87. The cutting planes pass through the centre of the thermoplastic overmould.

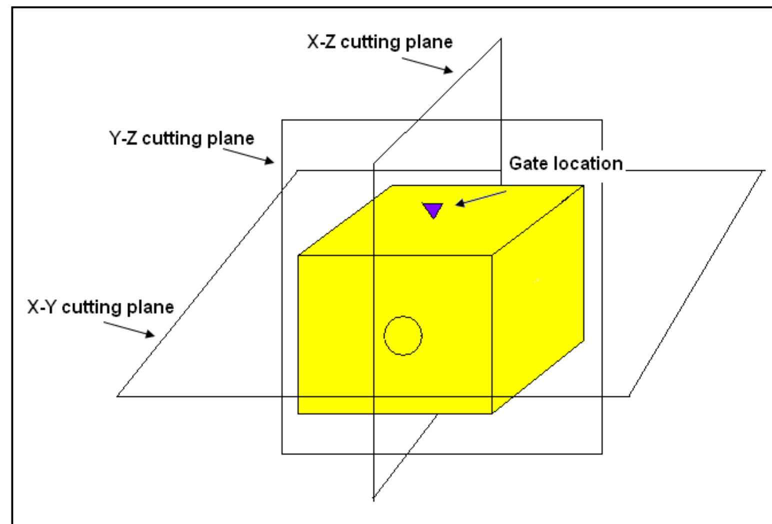

Figure 86: Cutting planes for section views

8.5.1 Temperature at the Flow Front

The Moldflow output mode that tracks the temperature of the thermoplastic melt at the flow front gives the temperature at which the thermoplastic comes in contact with the insert. Fig. 87a-e (X-Y section view) show the temperature at the flow front during injection of PMMA at the given insert temperature. As the melt was injected into the cavity, the temperature at the flow-front varied with flow length in the cavity and dropped below the processing temperature of the thermoplastic. Also, as the melt came in contact with the insert, the temperature of the melt varied depending on the point of contact. From Fig. 87a-e it can be seen that the

temperature of the melt flow front was lowest at the extremities of the part of insert inside the cavity. It is important to note the variation in temperature of melt at flow front. As reported in Chapter 6 the work of adhesion depends on contact angle and surface tension which may vary with the temperature of the melt at the interface. Table 19 summarises the data from all simulations. In general, as might be

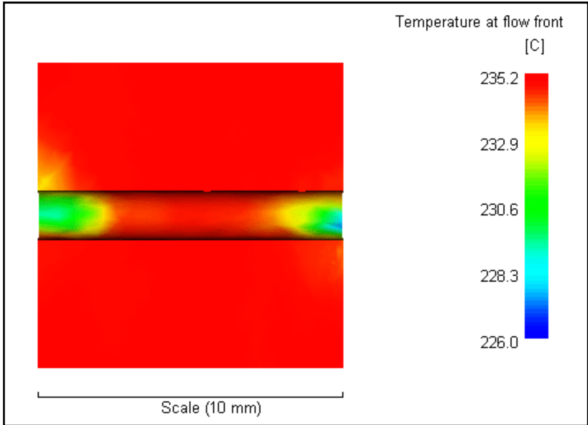

(a) Insert at room temperature

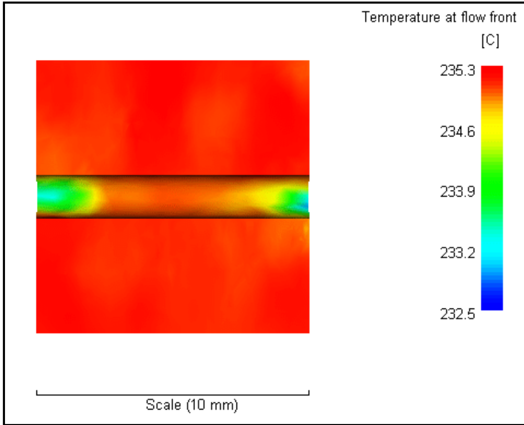

(b) Insert at 60°C

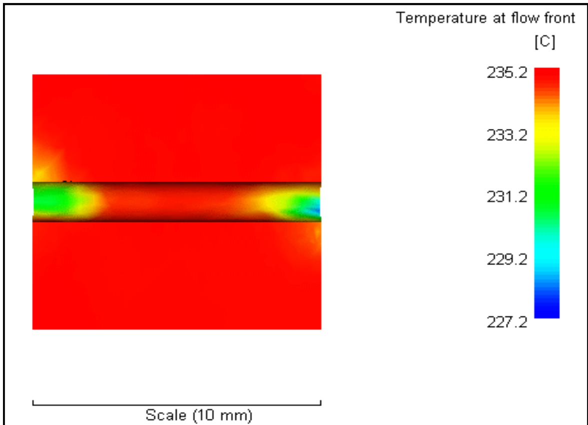

(c) Insert at 80°C

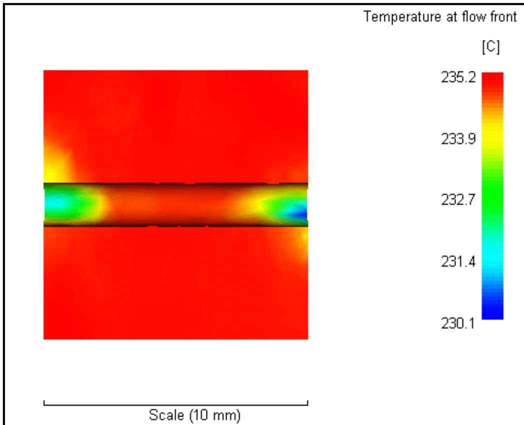

(d) Insert at 100°C

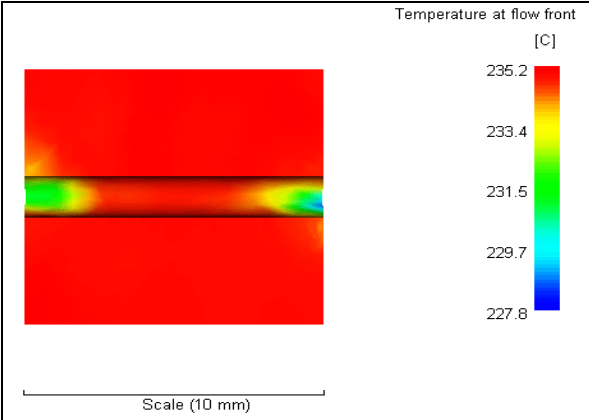

(d) Insert at 120°C

Figure 87: Temperature at melt flow front for PMMA (X-Y section view)

Table 19: Temperature at melt flow front

Material	Temperature at interface	Min. Temp at Flow-front	Melt Temperature	% drop
PMMA	RT	229	235	2.55
	60	229	235	2.55
	80	229	235	2.55
	100	230	235	2.13
	120	230	235	2.13
PS	RT	213	220	3.18
	60	214	220	2.73
	80	215	220	2.27
	100	215	220	2.27
	120	217	220	1.36
PC	RT	291	300	3.00
	60	291	300	3.00
	80	291	300	3.00
	100	292	300	2.67
	120	292	300	2.67
PBT	RT	255.5	260	1.73
	60	256	260	1.54
	80	256.5	260	1.35
	100	256.6	260	1.31
	120	257	260	1.15
PA 6	RT	253	260	2.69
	60	254	260	2.31
	80	254	260	2.31
	100	254	260	2.31
	120	254	260	2.31
ABS	RT	213	220	3.18
	60	214	220	2.73
	80	214	220	2.73
	100	214.5	220	2.50
	120	216.5	220	1.59

expected, the drop in temperature at the melt flow front was lower for the higher insert temperatures. However the differences are quite small. The percentage drop between the minimum temperature seen at the flow front and the processing temperature of the thermoplastic varied between 1 to 3 % for all insert temperatures

8.5.1.1 Discussion

As discussed in Chapter 6 the work of adhesion depends on the surface tension of the thermoplastic melt and the contact angle, both of which in turn are influenced by the temperature at the interface. From the simulation results for temperature at the melt flow front, the insert temperature not only influences the temperature at the insert/moulding interface, but also reduces the drop in temperature at the melt flow front. Hence, temperature at the insert may vary the work of adhesion at the interface. This may have an effect on the bond strength of the joint.

8.5.2 Injection Pressure and Temperature

Fig. 88 a-g (Y-Z section view) show the pressure distribution of the PS melt as it flows into the cavity and around the insert at 21°C (room temperature). Although an injection pressure of 6.2 MPa is applied to cause the melt to flow into the cavity, the pressure at the flow front and through most of the volume of the melt is less than 0.6 MPa, especially in the initial stages. This is in line with the literature on injection moulding process which suggests a gradual rise in cavity pressure during the filling phase [16] and means that the contact of the thermoplastic melt with the insert surface and its subsequent interactions happen at negligible cavity pressure. Looking at the temperature distributions at the same times (Fig. 89a-g, Y-Z section view) it

can be seen that the temperature of the melt drops rapidly to the temperature of the insert (21°C for Fig. 89 a-g) in less than 0.13s after contact with the insert. This was noted for all the simulations for all materials with insert temperature maintained at 21°C. Thus, at least for insert temperatures which are far below Tg of the overmoulding polymer, the packing pressure can have little influence on the wetting of the inserts by the polymer melt. For amorphous polymers ABS, PS and PMMA at or above insert temperatures of 100 °C and for semicrystalline polymers PA 6, PBT at or above insert temperatures of 60°C the temperature of the melt in contact with

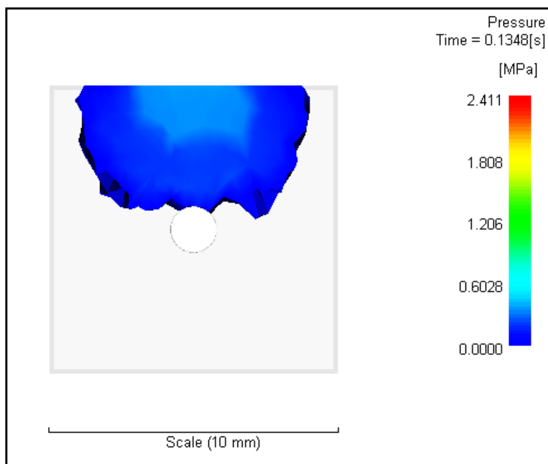

88 (a)

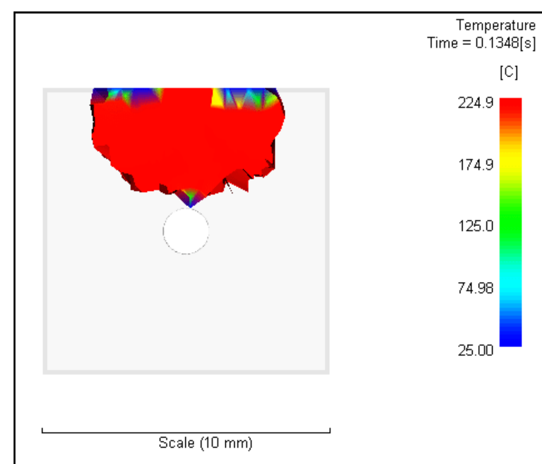

89 (a)

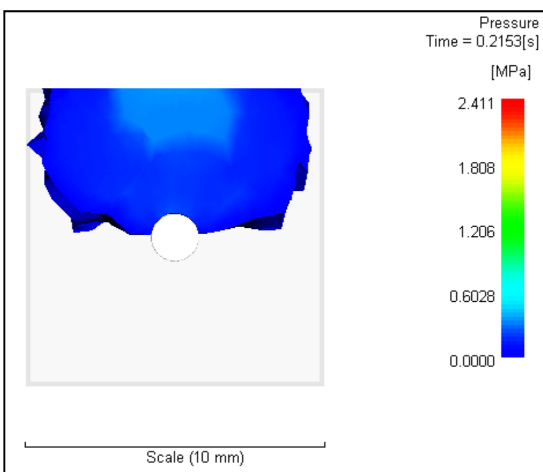

88 (b)

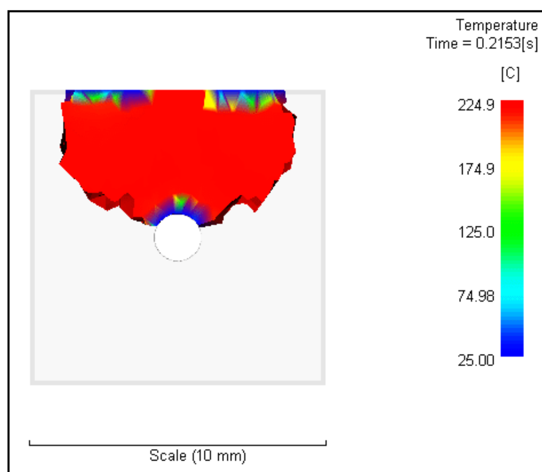

89 (b)

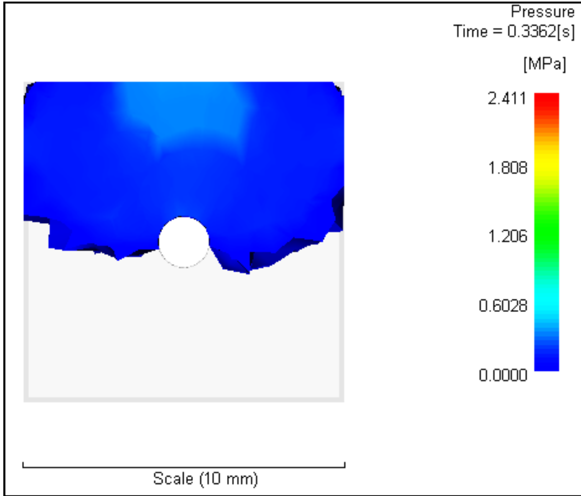

88 (c)

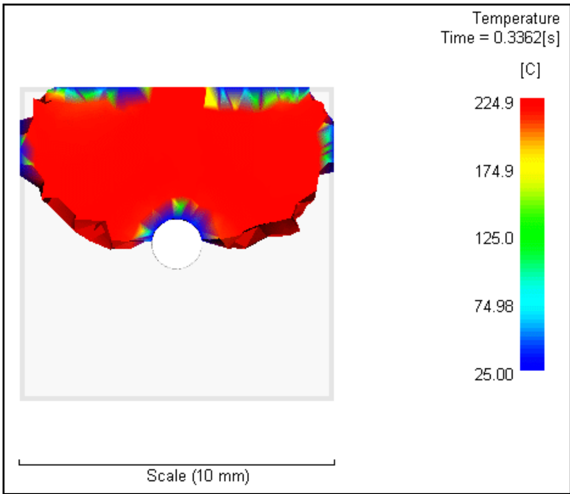

89 (c)

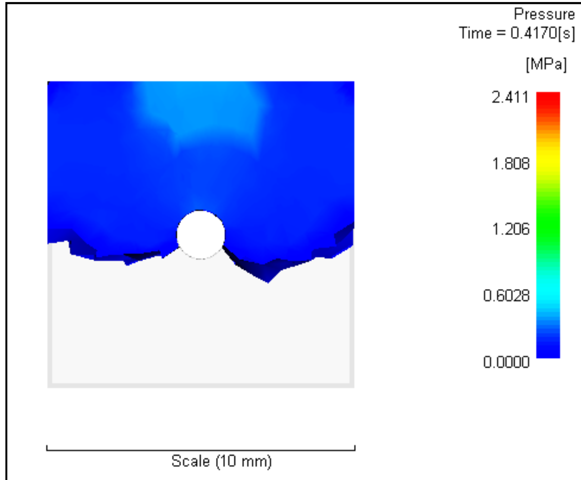

88 (d)

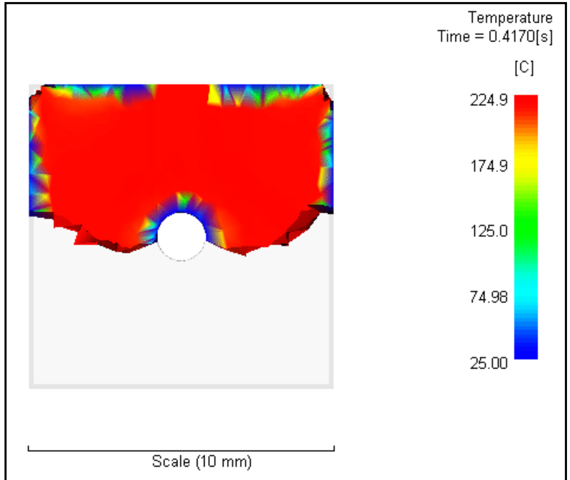

89 (d)

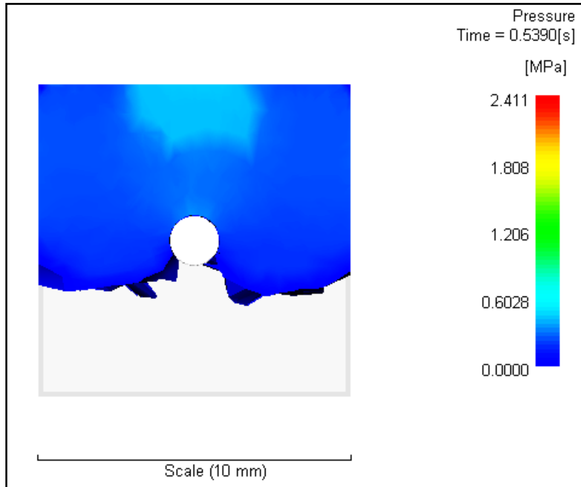

88 (e)

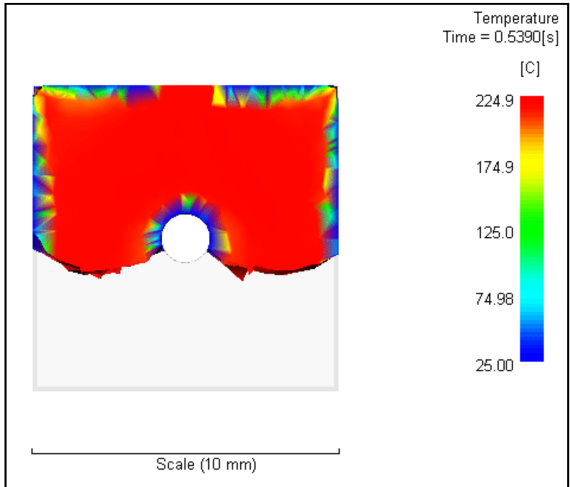

89 (e)

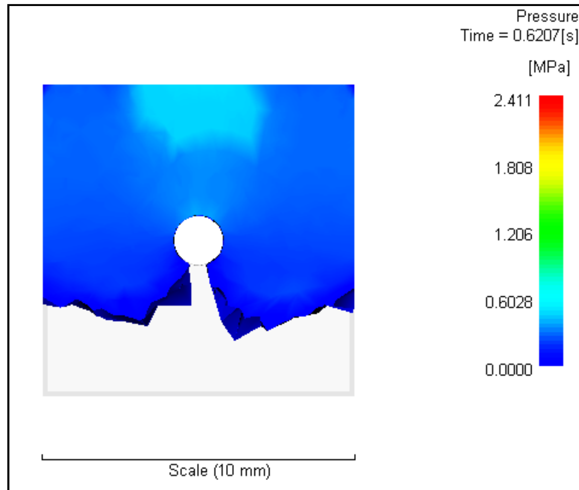

88 (f)

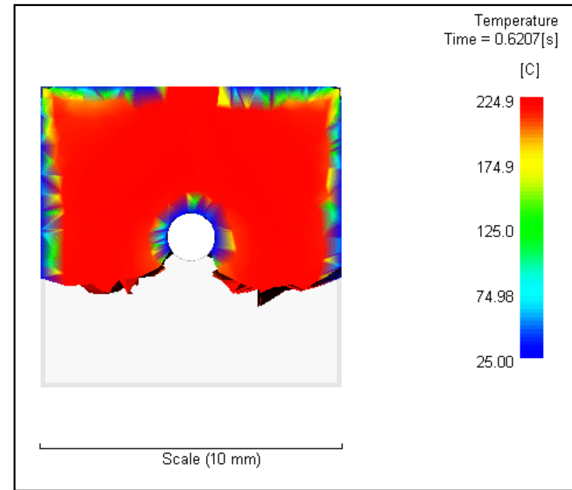

89 (f)

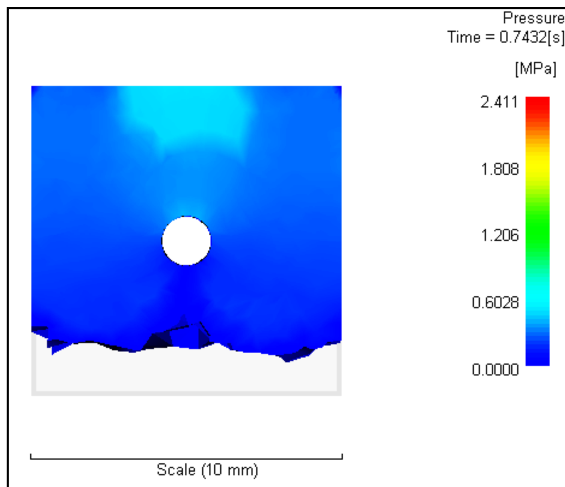

88 (g)

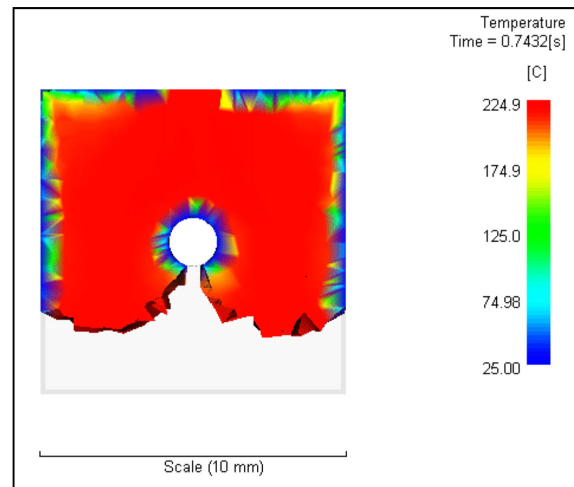

89 (g)

Figure 88 and Figure 89: Pressure and temperature profile for PS (Y-Z section view)

the insert is above Tg and hence high enough that it may still be fluid at the stage when significant cavity pressure is experienced.

8.5.2.1 Discussion

From the results of the simulations presented here (Fig. 88-89 a-g), it seems that injection pressure may not play an active role in bond strength if the temperature of the insert is low (below the Tg of the polymer) as the temperature of the

thermoplastic melt that comes into contact with the insert drops quickly to the temperature at which the insert is maintained. However when the inserts are maintained at temperatures approaching the Tg of the thermoplastics and beyond, the temperature of the thermoplastic melts in contact with the insert drops to the temperature of the insert and hence the thermoplastic molecules at the interface may still be mobile enough to be forced into better contact with the insert surface as a result of the injection pressure i.e. contribute to the 'wetting' of the insert by the thermoplastic. This may result in better adhesion strength for amorphous polymers ABS, PS and PMMA at or above insert temperatures of 100°C, and semicrystalline polymers PA 6 and PBT at or above insert temperatures of 60°C.

8.5.3 Volumetric Shrinkage

Fig. 90 a-e show the volumetric shrinkage distribution for a cross section perpendicular to the insert axis (cutting plane Y-Z) for overmoulding with polycarbonate samples. The volumetric shrinkage experienced by the thermoplastics varies from the surface of the mould to the surface of the insert. From the pattern that emerges from these simulations, volumetric shrinkage is similar in concentric rings around the insert. The volumetric shrinkage at the interface is lower compared to the volumetric shrinkage away from the interface. This trend was observed at all the insert temperatures and materials simulated. Table 20 summarises the results of the volumetric shrinkage plots for values of shrinkage at the insert thermoplastic interface and in the interior of the moulding. The values of volumetric shrinkage at the interface for PA 6, PBT and PC remained almost constant at all the insert temperatures. They vary slightly in the interior. Volumetric shrinkage at the interface for PS, PMMA and ABS shows an increase of 0.86%, 0.30 % and 1.19% at temperatures of 120°C,

100°C and 120°C respectively compared to 25 °C. This increase in volumetric shrinkage at the interface means that the difference in shrinkage between the surface and bulk decreased. These results therefore indicate that for PA, PMMA and ABS maintaining the inserts at high temperature may have a profound effect on the stress state at the interface. It must be noted that the change in volumetric shrinkage at the interface was not accompanied by similar change in the volumetric shrinkage in the interior, i.e.: the effect of the temperature of the insert was limited to the material at the interface.

8.5.3.1 Discussion

In general all thermoplastic melts experience volumetric shrinkage on cooling. However the amount and microscopic origin of volumetric shrinkage varies depending on the type of thermoplastic viz. amorphous or semicrystalline. The volumetric shrinkage in semicrystalline thermoplastics results from the densification upon crystallisation (with crystals being of higher density than the amorphous phase) in addition to the shrinkage due to the temperature drop (coefficient of thermal expansion (CTE)) [87]. In case of amorphous polymers volumetric shrinkage is mainly due to the drop in the temperature (not crystal densification). In general, the phase change from an amorphous melt to a partially ordered semicrystalline morphology leads to higher volumetric shrinkages in semicrystalline thermoplastics in comparison to amorphous thermoplastics. In the PVT diagrams in Fig. 74 and 75 in Chapter 7 it can be seen that for the amorphous thermoplastic (PS) the rate of decrease in specific volume with temperature decreases as the temperature falls below the Tg of the polymer. However, as noted by Malloy, the PVT diagram for the

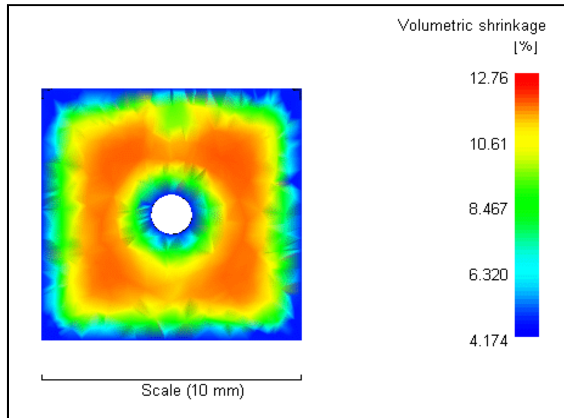

(a)Insert at 21°C

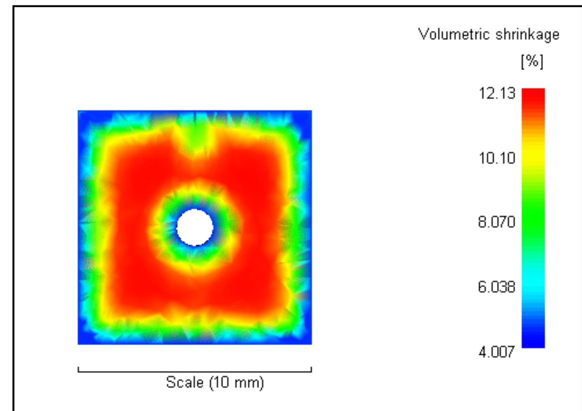

(b) Insert at 60°C

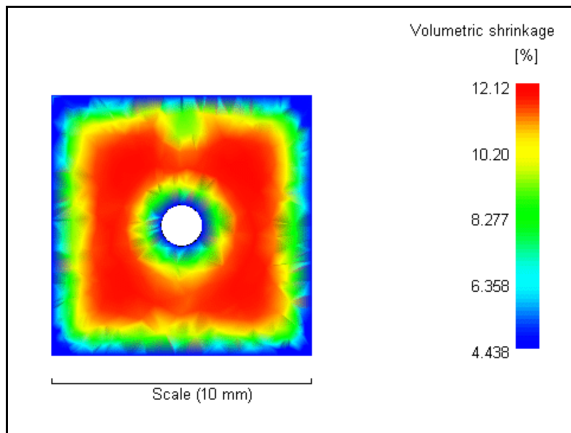

(c)Insert at 80°C

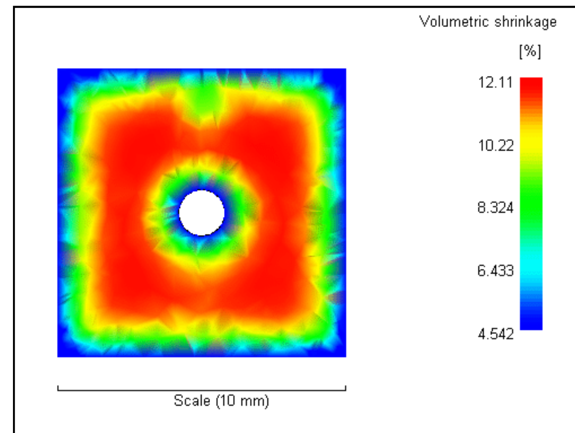

(d) Insert at 100°C

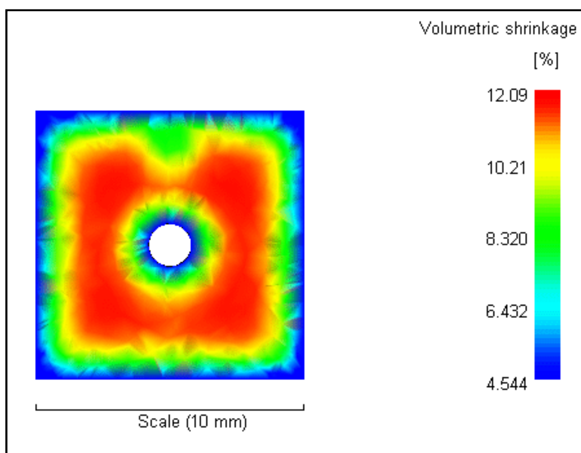

(e)Insert at 120°C

Figure 90: Volumetric shrinkage distribution for PC (cutting plane Y-Z)

Table 20: Volumetric shrinkage

Material	Temperature of insert	%volumetric shrinkage at interface	% volumetric shrinkage in interior	Difference
PBT	Room temperature (25)	13.93	17.65	3.72
	60.00	13.93	17.67	3.74
	80.00	13.93	17.65	3.72
	100.00	13.93	17.65	3.72
	120.00	13.93	17.57	3.64
PS	Room temperature (25)	2.19	8.13	5.94
	60.00	2.19	8.11	5.92
	80.00	2.19	8.13	5.94
	100.00	2.19	8.13	5.94
	120.00	3.05	8.09	5.04
PMMA	Room temperature (25)	1.79	9.32	7.53
	60.00	1.77	9.30	7.53
	80.00	1.79	9.20	7.41
	100.00	2.11	9.14	7.03
	120.00	1.79	9.15	7.36
PC	Room temperature (25)	4.65	11.76	7.11
	60.00	4.64	11.82	7.18
	80.00	4.65	11.77	7.12
	100.00	4.65	11.74	7.09
	120.00	4.65	11.67	7.02
PA6	Room temperature (25)	7.48	15.43	7.95
	60.00	7.48	15.44	7.96
	80.00	7.48	15.42	7.94
	100.00	7.48	15.42	7.94
	120.00	7.48	15.41	7.93
ABS	Room temperature (25)	2.61	8.09	5.48
	60.00	2.60	8.04	5.44
	80.00	2.61	8.06	5.45
	100.00	2.61	8.06	5.45
	120.00	3.80	8.12	4.32

semicrystalline polymer PBT shows a more rapid ‘step like change’ in specific volume at its melting temperature [88], while the rate of change in specific volume at Tg is more gradual than that of the amorphous polymer. The higher shrinkage values of PS, PMMA and ABS in Table 20 can thus be attributed to their being amorphous polymers, with Tgs of 89°C, 117°C and 110°C respectively. By contrast the Tg of PC, which is also amorphous, is higher than the maximum insert temperature at 152°C and hence no discernable change in volumetric shrinkage was observed. For the semicrystalline polymers PA 6 and PBT a step volume change would only be expected at even higher temperatures (closer to their Tm). Thus no discernable change in volumetric shrinkage at the insert interface for these materials is observed.

The amount of volumetric shrinkage also depends on the rate of cooling [87]. The temperature of the thermoplastic melt at the insert or the mould walls drops a lot faster than in the interior of the moulding, and therefore the cooling rate in the interior is much lower, so the shrinkage of all mouldings in the interior is higher than that at the insert and is also insensitive to insert temperature. The volumetric shrinkage around the insert has been described as one of the mechanisms responsible for the matrix gripping the insert [87]. However, the difference in shrinkage between bulk and interface regions may lead to residual stress in the component which would add to failure of the bond at the interface at lower levels of externally applied stress. Thus the increased levels of shrinkage for PS, PMMA and ABS at the insert interface at higher insert temperature and hence reduced difference in degree of shrinkage compared to the interior may be expected to be associated with reduced residual stress and hence lower pull out strength.

Refer to Appendix 1 for results of weld line and air traps.

8.6 Conclusions

In this chapter, the use of FEA in general and Moldflow in particular, for insert moulding analysis was reviewed. Insert moulding analysis was performed to support the findings of the pull out test. A detailed description of the meshing procedure in Moldflow for insert moulding analysis was presented. Boundary conditions were applied and Fill + Pack analysis was performed. The results of the Moldflow analysis with regards to the temperature at flow front, injection pressure and volumetric shrinkage were discussed in detail. It was observed that the temperature at flow front varies with flow length of the thermoplastic melt and drops rapidly to the temperature of the insert upon contact. The thermoplastic melt comes in contact with the insert at low (less than 0.6 MPa) pressure. Volumetric shrinkage of the overmould varied from insert interface to the interior. Variable shrinkage leads to residual stresses. It was also observed that volumetric shrinkage at the interface for PS, PMMA and ABS shows an increase of 0.86%, 0.30 % and 1.19% at temperatures of 120°C, 100°C and 120°C respectively. These results along with the results from the previous chapters will be put together to understand the effect of materials and processing conditions on the adhesion at interface in an insert moulded sample.

9 Discussion

Contents:

- *Introduction*
- *AFM Force-distance and Pull Test*
- *Wetting and Pull Test*
- *Moldflow Analysis and Pull Test*
- *General Discussions*
- *Selection of Materials*
- *Selection of Materials for Substrateless Packaging*

9.1 Introduction

For substrateless packaging to be the technology of choice for electronics manufacture it has to overcome all the technological bottlenecks and deliver products that are at par on quality and reliability with the current products. Out of all the areas of research that come to fore this study concentrated on understanding the adhesion between legs of electronic components and the thermoplastic overmould at material and macro (system) level, and on identifying thermoplastics that can be used to manufacture substrateless electronics.

Based on the theories of adhesion, it was surmised that at the material level, interatomic forces between solids and wetting processes at the interface between overmould and insert would play an important role in adhesion at the interface. Hence, as reported in Chapter 5 AFM force-distance experiments and in Chapter 6 wetting experiments, were performed. The mechanisms of adhesion at the interface depend not only on the materials interacting at the interface but also the processing parameters involved in the insert injection moulding process. Hence, mechanical strength tests were performed as reported in Chapter 7. In order to fully interpret the

results of the mechanical strength tests, and to assess the contribution to the results obtained of material interactions at the insert interface, numerical simulations were done using Moldflow as reported in Chapter 8.

The results of these experiments were discussed in isolation from each other in the respective chapters. In this chapter, the results from the previous chapters are compared and discussed to help build a complete picture of the interactions among the various influences on system level adhesion, and to identify what might be the ideal conditions for optimum adhesion at the insert-overmould interface.

9.2 AFM Force-Distance and Pull Test

In Chapter 5 AFM measurements to measure the solid-solid interaction force between tin and the thermoplastics at room temperature were reported. The observed trend in interaction force magnitude was

PC > PMMA > PBT > ABS > PS > PA 6

This can be compared with the trend in pull-out strengths at room temperature reported in Chapter 7 which was

PBT > PC > PMMA > ABS > PS > PA 6

The trend observed in mechanical strength tests is very similar to the one obtained from AFM force distance experiments with the notable exception of PBT. However, for higher insert temperatures, the trend for mechanical strength test changes and is not at all comparable to the trend observed by AFM force distance measurements. As has been seen from the Moldflow results in Chapter 8 the change

in insert temperature affects the thermo-mechanical history of the overmould, viz temperature at interface, rate of cooling etc. However as all the mechanical strength tests are done at room temperature, if interatomic forces were a dominant factor (as opposed to the thermo-mechanical history) the mechanical strength test results would be expected to always follow the trend seen in AFM force distance measurements.

Schirmeisen *et.al.* Wong *et.al.* and Han *et.al.* compared AFM force-distance measurements to mechanical strength tests [55-57]. Schirmeisen *et.al.* concluded that the adhesion strengths obtained from mechanical strength test (stud pull test) results were much lower than the theoretical adhesion strengths calculated from the AFM results. They concluded that AFM measures ideal maximum bond strength, which can be greatly different from the obtained bond strength. Wong *et.al.* used an atomic force microscope in characterizing the nanoscale adhesion force in a copper – self assembled monolayer (SAM) adhesion promoter - epoxy moulding compound encapsulant system. The results were used as the criteria in selecting a SAM candidate. They compared the nanoscale AFM results with button shear tests and found them to be consistent with the result of button shear tests. Han *et.al*. used AFM pull-off measurements to predict adhesion at the solid–solid interface formed by materials used in the seat-membranes of microvalves. The results were compared to tests on microvalves that had been fabricated with different surfaces at the seat⁄membrane interface. They found good correlation between the micro and macro level adhesion. It is interesting to note that Schirmeisen *et.al.* reported that the mechanical strength test yields strengths much less than that for theoretical adhesion forces at the interface while Wong *et.al.* and Han *et.al.* found good correlation between the AFM and the mechanical strength test results.

Some of the results in the literature show an agreement between trends in AFM force distance measurements and in mechanical strength tests. These trends were used as selection criteria for materials at the bond interface. By contrast in the current work it can be concluded that although interatomic factors are one of the mechanisms involved in adhesion at interface, they cannot be used in isolation for material selection.

9.3 Wetting and Pull Test

As discussed in Chapter 6, the importance of wetting for adhesion at the interface in insert injection moulding has been well debated over the years. With a few exceptions, the popular opinion is that the better the wetting the higher the adhesion at the interface. Also, as discussed in detail in Chapter 6, the conventional view in the literature on the effect of rise in temperature at the interface during joint formation is that contact angles decrease (improved wetting) with rise in temperature. However, there is not much literature available on the wetting by thermoplastics of low melting point substrates (i.e. where the melting point is within the range of processing temperatures of most thermoplastics). Imachi in his work saw a decrease in the wetting of low melting point solids by thermoplastics at temperatures beyond the melting temperature of the substrate [70]. In Chapter 6 high temperature contact angle experiments to ascertain the wetting characteristics of the thermoplastics used in this study on tin were reported. Contact angle data was obtained at various steady state temperatures. It was found that contact angle decreased with rise in temperature, and there was no increase in contact angles at or above the melting temperature of tin (≈232°C). Based on the classical theories of adhesion, lower contact angle corresponds to better wetting and hence should result in higher

adhesion at interface. Thus if wetting played a major role in adhesion at interface, the pull strength results for a thermoplastic-tin pair would be expected to rise continuously with insert temperature. However, in the work reported in Chapter 7 the adhesion strength was seen to increase until the insert temperature reached around Tg for amorphous polymers, and just above Tg for semicrystalline polymers, and then decreased.

From the ranking of contact angles made by the thermoplastics on tin at a fixed temperature, the ranking of adhesion strengths would be expected to be

PS > PMMA > PA 6 > PBT > PC

The trend from the pull tests was almost opposite to the trend from contact angle data. This result is very important as using materials that wet the surface of the insert to improve adhesion strength has been a well accepted approach in adhesive joint optimisation. However, just using contact angle as a surrogate for degree of wetting may not be the right approach as the surface tension of the adhesive, in this case the thermoplastic melts, varies with temperature. Taking account of the surface tension by calculating the work of adhesion yields a modified expected adhesion strength ranking at 240°C (see Chapter 6) of:

PC > PA 6 > PBT > PS > PMMA

The trend observed through the work of adhesion calculations is also not replicated by the pull out tests. It is however interesting to note that the work of adhesion calculations for PMMA-tin reported in Chapter 6 Table 13 show that the work of adhesion may rise or fall with increasing temperature, in spite of continuously

falling contact angles. This effect may contribute to the rise and fall in bond strengths which was observed during the pull tests.

From the discussion above, it can be concluded that contact angle analysis also cannot be used in isolation for material selection, as the ultimate bond strength of an insert moulded joint may not correspond to the trends exhibited in contact angle analysis.

9.4 Moldflow Analysis and Pull Test

As was seen in the Moldflow results in Chapter 8 when the thermoplastics come in contact with the insert at insert temperatures below Tg, they solidify almost instantaneously forming a skin. As shown in Table 20 of Chapter 8 in the first column the skin formed at the insert interface shrinks around the insert at all insert temperatures. However the volumetric shrinkage in the skin layer is higher at temperatures above the Tg for the amorphous. Parlevliet *et.al.* in their review on residual stresses in thermoplastic composites have cited research that suggests the volumetric shrinkage of the skin layer around the fibre results in radial compressive forces that 'grip' the fibre and allow stress transfer [87]. From these results it would be expected that pull strength test results at all insert temperatures should remain fairly constant or rise as the volumetric shrinkage increases. However, as reported in Chapter 7, Fig. 73 the pull strength in fact increased with increase in insert temperature up to Tg of the thermoplastic and then decreased with further rise in the temperature.

It has been reported in the literature that the volumetric shrinkage at the insert interface results in formation of moulded-in stresses at the thermoplastic-insert

interface [16]. Zhil'tsova *et.al.* through their study of insert moulded PBT components concluded that rise in insert temperature resulted in lower thermal residual stresses in the component [84]. Kulkarni *et.al.* studied thermal stresses in aluminium 6061 and nylon 66 long fibre thermoplastic (LFT) composite joint and reported that on account of the difference in co-efficient of thermal expansion (CTE) of the thermoplastics and metals insert (factor of 4 and above) residual stress is generated as the thermoplastic cools below its Tg [28]. Thus, although the volumetric shrinkage of the thermoplastic around the insert may be a gripping mechanism that provides shear stress transfer, the moulded in stress in the component and residual stress at the interface that are a direct consequence of the volumetric shrinkage and cooling of the thermoplastic may weaken the interface thus reducing the bond strength.

9.5 General Discussion

In the previous sections, the relative extent of material and processing factors contributing to the measured adhesion were discussed. It is clear from the discussions that adhesion at interface depends on a combination of material and processing conditions. The adhesion strength of the tin-thermoplastic joint varies with thermoplastic metal combination as well as the temperature at which the insert is maintained. A possible explanation for this may be a combination of the material and processing parameters. From Eqn. 10 the shear strength of a joint depends on the adhesion at the interface and the radial compressive stress generated on account of thermal residual stress and moulded in stress.

As discussed in Chapter 8, during insert moulding, when the thermoplastic melt comes in contact with the insert its temperature drops rapidly to end up close to

the temperature of the insert. Thus the rate of cooling of the thermoplastic melt at the insert interface from its processing temperature to room temperature depends on the temperature of the insert. When the insert is at room temperature, the rate of cooling is much higher as compared to when the insert is at 120°C

The effect of rate of cooling varies from amorphous thermoplastics to semicrystalline thermoplastics. Kim *et.al.* and DiLandro *et.al.* studied the effect of rate of cooling of amorphous polymers and found that the formation of residual stresses depends mainly on the rate of cooling through the Tg range of the amorphous polymer [89] [90]. The faster the rate of cooling through the Tg range the higher the residual thermal stresses. Therefore, when the insert is maintained at room temperature, the thermoplastic melt comes in contact with the insert and solidifies rapidly, limiting the effect of injection pressure to force the thermoplastic in better contact with the insert. The thermoplastic melt shrinks around the insert gripping it. This also leads to formation of moulded in stress. As mentioned earlier, the rate of cooling of the thermoplastic melts at the insert interface through their Tg range generates thermal residual stress at the interface which may result in compressive forces on the insert. For higher insert temperatures (but below the Tg of the thermoplastic) the rate of cooling of the thermoplastic melt at the interface reduces marginally. This may reduce the thermal stress generated at the interface. However, with the slower rate of cooling through the Tg range of the thermoplastic, the influence of injection pressure in forcing the melt in better contact with the insert may rise. This may be responsible for the increase in bond strength. Thus the bond strength increases initially when with increase in insert temperature up to near Tg. As the insert temperature is increased through and beyond the Tg of the thermoplastic, it can be assumed that the effect of the injection pressure on forcing the polymer and

insert surface together does not increase further. However, there will be an appreciably slower cooling rate through the Tg range of the thermoplastic of the material at the interface of the insert. This will lead to the thermal residual stress generated at the interface being much lower. This may account for reduction in bond strengths observed above Tg.

Unlike the amorphous thermoplastics, in case of semicrystalline thermoplastics, the generation of thermal residual stress at varying cooling rates can be unpredictable with two competing mechanisms. On fast cooling higher residual stresses can be generated due to the amorphous phases as described in the previous paragraph, while lower residual stresses would result from reduction in crystal fraction and hence less crystallisation shrinkage [87]. The crystallisation kinetics for every semicrystalline thermoplastic is different and therefore the balance between the two mechanisms will vary as well. For PA 6, the variation in bond strength with insert temperature is not as big that observed with PBT. It can therefore be surmised that the residual stresses generated at the insert interface with PBT reduce at lower cooling rates while those with PA 6 remain fairly constant. Both PA 6 and PBT have Tg's well below 60°C. The initial rise in the bond strength when the insert is maintained at higher temperature may be due to the injection pressure forcing the polymer into better contact with the insert interface.

9.6 Selection of Materials

The results from Chapters 5 - 8 and the discussion above suggest that selection of material for an insert moulding process cannot be decided solely based on the interactions of the materials at the interface. Process induced properties need

to be considered. Also, as discussed in Chapter 7, the adhesion strength of a joint at the interface in an insert moulded component may be dominated by the mechanical properties of the thermoplastics.

Considerations other than bond strength must be taken into account in recommending a material for future substrateless packaging assemblies. For the thermoplastics tested for this study, the highest practical adhesion strengths were seen with, in descending order of strength, PC, PMMA and PBT. However it must be noted that most thermoplastics are processed with mould temperatures maintained in the range of 40-90°C [16]. Choosing a material that allows the insert to be maintained in this range would therefore be the most manufacture friendly option, as it would be easiest to heat mould and insert together instead of trying to maintain the insert at a temperature significantly higher than that of the mould. In general during injection moulding of PC and PBT, the mould temperature is maintained at 90 and 60°C respectively. While PC showed the highest bond strength at the interface when the insert was maintained at 120°C, at 90°C, the bond strength would be expected to be lower than that for PBT system at 60°C. Thus, based on bond strength at the interface for realistic moulding conditions, PBT should be selected over PC.

9.7 Selection of Materials for Substrateless Packaging

Substrateless Packaging technology was at the heart of this research. In the original work done by *Webb et.al.* there were gaps noticed at the interface of the legs of the electronics and the thermoplastic overmould [9]. These gaps were thought to be the result of lack of adhesion at interface and were considered detrimental to the development of the product and would detrimentally affect long term reliability of

interconnections. One of the aims of this study was to select better material for future trials of this process. Webb *et.al.* used ABS to manufacture the first prototypes for substrateless packaging. The choice of material was influenced by the plating requirements for the interconnections. The results of this work show that ABS was not the best choice of material for substrateless packaging amongst the typical commercial polymers available. In fact based on this study, it is advised to not use ABS for substrateless packaging. The use of commercial thermoplastics like PBT, PMMA or PC would be a much better option. As seen in the literature survey, these thermoplastics have already been used in applications like MIDs. They can also be plated for interconnections.

10 Conclusions

Contents

- *Future Work*

PCB technology is central to modern electronics manufacturing. However, the inherent non-recyclability of the thermoset polymers used to manufacture PCBs has created end of life disposal problems. The substrateless packaging process was developed at Loughborough University as an alternative method of manufacturing electronics. The process involves injection moulding to overmould electronic components in thermoplastic polymers. Initial prototype samples were manufactured by Webb *et.al.* [9]. They observed that intimate contact between the overmoulded thermoplastic resin, and the legs of the electronic components, was crucial for the integrity of the electrical interconnection. Small gaps were found to occur around the embedded components after solidification, which could either act as weak points in the electrical interconnect pattern, or prevent electrical interconnect being achieved at all. These gaps were thought to be the result of adhesion problems the thermoplastic overmould and the tin surface metallisation of the electronic components. This problem, unique to the process of substrateless packaging, is not covered in the literature and hence formed the basis of this study.

The original objectives of the study were:

1. *To understand adhesion between legs of electronic components and the thermoplastic overmould at the material level*

2. *To understand the effects of the insert injection moulding process conditions on interfacial adhesion, i.e. adhesion at the interface between the legs of the electronic components and thermoplastic overmould*

3. *To identify thermoplastic polymers that may be used for overmoulding electronic components.*

A literature survey on insert moulding in general was done that identified mechanisms contributing to adhesion at the metal-thermoplastic interface as material properties, interfacial forces between the materials, wetting at the interface, temperature of the insert (consequently temperature at the interface) and insert moulding parameters. The chosen methodology was designed to allow investigation of all these factors. A subsequent literature survey was done on materials used in electronics and in particular thermoplastics used as substrates. As a consequence PS, PBT, PC, ABS, PMMA and PA 6 were chosen as overmould materials, and tin as the insert material, for the study. The achievements of and conclusions drawn from the investigation can be summarised as follows:

- *Analysis of interfacial forces between tin and thermoplastics*

AFM force-distance curves were used for analysis of interfacial forces between tin and the thermoplastic materials. A FIB / SEM based method was developed to attach a tin particle on an AFM cantilever. Highly consistent cantilever deflections were obtained (maximum error less than 8%). PA and PMMA interatomic interactions with tin were found to be noticeably stronger than the other polymers. Cantilever deflections were ranked in the order of the interatomic interactions between the thermoplastic and tin (from higher to lower) as follows:

PC > PMMA > PBT > ABS > PS > PA 6

From consideration of the different possible contributions to the measured forces it was concluded that the trend of interatomic interactions obtained is due to a combination of electrostatic forces, capillary forces and dispersion forces acting between the materials tested.

- *Analysis of wetting by thermoplastics at high temperature*

Contact angle analysis was used as a proxy to study the wetting interactions of thermoplastic melts on tin substrates. Sessile drop analysis over a range of temperatures embracing the processing temperatures of the polymers used and the melting point of tin was used to obtain contact angles. ABS was found to degrade on prolonged exposure to high temperature and didn't form an equilibrium shape. Highly consistent readings were recorded for all the other materials tested (range of less than 1% from mean). It was observed that contact angles decreased for all the other polymers monotonically with rise in temperature at interface. The order of the thermoplastics by contact angle (greatest to smallest) at 220°C was

PC > PBT > PA 6 > PMMA > PS

Values for work of adhesion at interface from the Young-Dupre equation were calculated at 240°C and it was found that the materials ranking changed significantly. The new ranking was (highest to lowest work):

PC > PA 6 > PBT > PS > PMMA

It was further found that when the work of adhesion was calculated similarly for PMMA at various temperatures, a monotonic trend was no longer seen.

- *Analysis of mechanical strength at the interface*

Pull out test samples were prepared at insert temperatures of 21, 60, 80, 100 and 120°C. Load vs extension curves were recorded in pull out tests for all the samples manufactured and breaking load for each test determined. The standard deviation in the breaking load for all sample batches was less than 3% and hence it was concluded that the sample preparation method was consistent and repeatable. The magnitude of breaking load varied among the materials. Except for PC, for all the materials tested, the breaking loads rise and fall with rise in temperature of the insert. The maximum strength variation with temperature observed was 42% for PMMA. It was observed that peak breaking load for the amorphous polymers ABS, PS and PMMA occurred for insert temperature just below Tg of the polymer, and for semicrystalline polymers PA 6 and PBT it was just above Tg. The ranking of materials by maximum pull out strength was found to be consistent with the ranking by mechanical strength (tensile strength at yield) of the thermoplastics.

- *Numerical simulations*

Insert moulding analysis was performed using Moldflow to aid in interpretation of the findings of the pull out test. A detailed description of the meshing procedure in Moldflow for insert moulding analysis was presented. The temperature at flow front, injection pressure, temperature distribution in the melt and volumetric shrinkage were analysed. It was observed that the temperature at flow front varies with flow length of the thermoplastic melt, and drops rapidly to the temperature of the insert upon contact. The thermoplastic melt comes in contact with the insert at relatively low pressure (less than 0.6 MPa). Therefore it was concluded that the efficacy of holding pressure on assisting wetting of the insert by the thermoplastic melt may depend on

the temperature of the insert interface. Volumetric shrinkage of the overmould varied between the insert interface and the interior, which would be expected to lead to residual stresses in the moulding. It was also observed that volumetric shrinkage at the interface for the amorphous thermoplastics PS, PMMA and ABS shows an increase of over that for insert at room temperature of 0.86%, 0.30 % and 1.19% at insert temperatures of 120°C, 100°C and 120°C respectively, while the shrinkages at interface for the semicrystalline thermoplastics showed little temperature sensitivity.

The results in terms of material rankings from both the material level tests (AFM force distance experiment and wetting at high temperature) did not correspond to the mechanical strength test results. It was therefore concluded that the choice of material for thermoplastic overmould cannot be made purely based on the material interactions at interface between tin and thermoplastics in solid or melt phase. It was also concluded that the observed variation in the pull-out strengths with temperature of the insert maintained during overmoulding, must be largely due to the thermo-mechanical properties of the material at the interface.

One of the objectives of this study was to suggest a thermoplastic polymer that may be used for manufacturing overmoulded electronics. Based on the results of this study, PC, PBT and PMMA were recommended as being likely to give superior performance to the ABS which was used in early trials of the substrateless packaging process. Of these, from a process economics point of view, PBT would be the most suitable.

10.1 Future Work

In this study, it was suggested that the that the variation in bond strength with the variation in insert temperature was on account of the injection and packing pressure along with the thermo-mechanical history of the material at the interface. This suggests future experiments on adhesion at insert moulded components in which the injection and packing pressure are varied along with the insert temperatures. Such experiments will help in understanding the role of insert temperature and processing conditions on the quality of the component/overmould interface.

In this study, it was suggested that although the volumetric shrinkage of the thermoplastic around the insert provides a 'gripping' mechanism the effect of residual stress at the interface due to differential volumetric shrinkage between the interface and bulk of the moulding, and CTE mismatch between the insert and the thermoplastic materials decreases the bond strength at the interface. Future research should address the development of residual stresses and their exact role in adhesion at interface in an insert moulded joint. This would be particularly appropriate as according to Parlevliet *et.al.* few studies are available that investigate the effects of residual stress formation in thermoplastic composites [87].

Webb *et.al.* manufactured substrateless packaging prototypes using ABS as the overmould material [9]. In light of the new information available from this study, it is suggested that future substrateless packaging experiments should be carried out using the recommended materials PC, PBT or PMMA, and in particular PBT, at the recommended mould temperatures. Also, as the results from the mould flow analysis

performed in this study suggest that the temperature of the melt flow front may vary depending on the flow length, there may be variable thermo-mechanical properties at the mould material interface with the electronic components, depending on their location in the mould. Hence a finite element analysis similar to the one done in this study is suggested for all future substrateless packaging.

11 References

[1] B. R. I. H. Simon Cunnington, “Electronic 2015,” 27-Feb-2010. [Online]. Available: http://webarchive.nationalarchives.gov.uk/+/berr.gov.uk/whatwedo/sectors/electronicsitservices/publications/electronics2015/page20099.html. [Accessed: 27-Mar-2011].

[2] R. R. Tummala, *Fundamentals of Microsystems Packaging*. McGraw-Hill Professional, 2001.

[3] “UN outlines global e-waste goals,” *BBC*, 06-Mar-2007.

[4] C. Weiss and H. Muenstedt, “Surface modification of polyether ether ketone (peek) films for flexible printed circuit boards,” *The Journal of Adhesion*, vol. 78, no. 6, pp. 507-519, Jun. 2002.

[5] P. Glendenning, I. Annergren, T. J. Lett, and W. Xincai, “Moulded Interconnect Device Technology Development.” SIMTech Technical Report, 2001.

[6] A. Paproth, K.-J. Wolter, J. Friedrich, and R. Deltschew, “Metal-polymer composites for molded interconnect devices (MID),” in *Proceedings Electronic Components and Technology, 2005. ECTC ’05.*, Lake Buena Vista, FL, USA, pp. 1891-1894.

[7] A. Paproth, K.-J. Wolter, and R. Deltschew, “Adhesion of polymer/metal bonds for molded interconnect devices (MID),” in *28th International Spring Seminar on Electronics Technology: Meeting the Challenges of Electronics Technology Progress, 2005.*, Wiener Neustadt, Austria, pp. 313-318.

[8] K. Gilleo and D. Jones, “INJECTION MOLDED & MICRO FABRICATION ELECTRONIC PACKAGING,” presented at the Molding 2005, New Orleans, LA, USA, 2005.

[9] D. P. Webb, D. A. Hutt, D. C. Whalley, and P. J. Palmer, “A substrateless process for sustainable manufacture of electronic assemblies,” in *2008 2nd Electronics Systemintegration Technology Conference*, Greenwich, 2008, pp. 511-516.

[10] J. Fjelstad, “Environmentally friendly assembly of robust electronics without solder,” *Circuit World*, vol. 34, no. 2, pp. 27-33, 2008.

[11] F. Sarvar, D. C. Whalley, D. A. Hutt, P. J. Palmer, and N. J. Teh, “Thermal and thermo-mechanical modelling of polymer overmoulded electronics,” *Microelectronics International*, vol. 24, no. 3, pp. 66-75, 2007.

[12] E. Petrie, *Handbook of adhesives and sealants*, 2nd ed. New York: McGraw-Hill, 2007.

[13] D. Packham, *Handbook of adhesion*, 2nd ed. Hoboken N.J.: John Wiley, 2005.

[14] A. Pizzi, *Handbook of adhesive technology*, 2nd ed. New York: M. Dekker, 2003.

[15] J. Frados and Society of the Plastics Industry., *Plastics engineering handbook of the Society of the Plastics Industry, inc.*, 4th ed. New York: Van Nostrand Reinhold, 1976.

[16] D. Rosato, D. Rosato, and M. Rosato, *Injection molding handbook.*, 3rd ed. Boston: Kluwer Academic Publishers, 2000.

[17] R. Crawford, *Plastics engineering*, 3rd ed. Oxford ;;Boston: Butterworth-Heinemann, 1998.

[18] V. Goodship and J. Love, *Multi-material injection moulding*. Shrewsbury, U.K. :: Rapra Technology,, 2002.

[19] R. M. Gouker, S. K. Gupta, H. A. Bruck, and T. Holzschuh, “Manufacturing of multi-material compliant mechanisms using multi-material molding,” *The International Journal of Advanced Manufacturing Technology*, vol. 30, no. 11-12, pp. 1049-1075, Feb. 2006.

[20] L. S. Gyger, “Thermal and Thermomechanical Behavior of Multi-Material Molded Modules with Embedded Electronic Components for Biologically-Inspired and Multi-Functional Structures.” [Online]. Available: http://drum.lib.umd.edu/handle/1903/3966. [Accessed: 28-Mar-2011].

[21] H. A. Bruck, “Using Geometric Complexity to Enhance the Interfacial Strength of Heterogeneous Structures Fabricated in a Multi-Stage, Multi-Piece Molding Process,” *Experimental Mechanics*, vol. 44, no. 3, pp. 261-271, Jun. 2004.

[22] A. G. Banerjee, X. Li, G. Fowler, and S. K. Gupta, “Incorporating manufacturability considerations during design of injection molded multi-material objects,” *Research in Engineering Design*, vol. 17, no. 4, pp. 207-231, Feb. 2007.

[23] M. Grujicic et al., “An overview of the polymer-to-metal direct-adhesion hybrid technologies for load-bearing automotive components,” *Journal of Materials Processing Technology*, vol. 197, no. 1-3, pp. 363-373, Feb. 2008.

[24] S. T. Amancio-Filho and J. F. dos Santos, “Joining of polymers and polymer-metal hybrid structures: Recent developments and trends,” *Polymer Engineering & Science*, vol. 49, no. 8, pp. 1461-1476, Aug. 2009.

[25] K. Ramani and B. Moriarty, “Thermoplastic bonding to metals via injection molding for macro-composite manufacture,” *Polymer Engineering & Science*, vol. 38, no. 5, pp. 870-877, May. 1998.

[26] H. Sasaki, I. Kobayashi, S. Sai, H. Hirahara, Y. Oishi, and K. Mori, “Adhesion of ABS resin to metals treated with triazine trithiol monosodium aqueous solution,” *Journal of Adhesion Science and Technology*, vol. 13, no. 4, pp. 523-539, Jan. 1999.

[27] M. Grujicic et al., “Computational analysis of injection-molding residual-stress development in direct-adhesion polymer-to-metal hybrid body-in-white components,” *Journal of Materials Processing Technology*, vol. 203, no. 1-3, pp. 19-36, Jul. 2008.

[28] R. R. Kulkarni, K. K. Chawla, U. K. Vaidya, and J. M. Sands, “Thermal stresses in aluminum 6061 and nylon 66 long fiber thermoplastic (LFT) composite joint in a tailcone,” *Journal of Materials Science*, vol. 42, no. 17, pp. 7389-7396, Jun. 2007.

[29] S. Yamaguchi, Y. W. Leong, T. Tsujii, M. Mizoguchi, U. S. Ishiaku, and H. Hamada, “Effect of crystallization and interface formation mechanism on mechanical properties of film-insert injection-molded poly(propylene) (PP) film/PP substrate,” *Journal of Applied Polymer Science*, vol. 98, no. 1, pp. 294-301, Oct. 2005.

[30] Ananthanarayanan. A, H. Bruck, and S. Gupta, “Interfacial Adhesion in Multi-stage Injection Molded Components,” presented at the 2006 SEM Annual Conference & Exposition on Experimental and Applied Mechanics, 2006.

[31] N. Mahmood, K. Busse, and J. Kressler, “Investigations on the adhesion and interfacial properties of polyurethane foam/thermoplastic materials,” *Journal of Applied Polymer Science*, vol. 104, no. 1, pp. 479-488, Apr. 2007.

[32] P. A. Fabrin, M. E. Hoikkanen, and J. E. Vuorinen, “Adhesion of thermoplastic elastomer on surface treated aluminum by injection molding,” *Polymer Engineering & Science*, vol. 47, no. 8, pp. 1187-1191, Aug. 2007.

[33] T. Peltola, P. Mansikkamaki, and E. O. Ristolainen, “3D integration of electronics and mechanics,” in *Proceedings. International Symposium on Advanced Packaging Materials: Processes, Properties and Interfaces, 2005.*, Irvine, California, USA, pp. 5-8.

[34] N. J. Teh, S. Prosser, P. P. Conway, P. J. Palmer, and A. Kioul, “Embedding of electronics within thermoplastic polymers using injection moulding technique,” in *Twenty Sixth IEEE/CPMT International Electronics Manufacturing Technology Symposium (Cat. No.00CH37146)*, Santa Clara, CA, USA, pp. 10-18.

[35] T. Peltola, “Integration of Multilayer PWB into Plastic Covers by Injection Moulding,” in *2006 1st Electronic Systemintegration Technology Conference*, Dresden, Germany, 2006, pp. 1342-1346.

[36] K. Gilleo and D. Jones, “Thermoplastic Injection Molding: New Packages and 3D Circuits,” presented at the IPC Printed Circuits Expo, Anaheim, CA, February 20.

[37] M. Jawitz, *Printed circuit board materials handbook*. New York: McGraw-Hill, 1997.

[38] “IPC 4101B- Specification for BaseMaterials for Rigid andMultilayer Printed Boards.” IPC-Association Connecting Electronics Industry, Jun-2006.

[39] E. Bradley, C. Handwerker, J. Bath, R. Parker, and R. Gedney, *Lead-free electronics : iNEMI projects lead to successful manufacturing*. Hoboken N. J. ;Piscataway N. J.: Wiley;IEEE Press, 2007.

[40] E. Suhir, *Micro- and Opto-Electronic Materials and Structures: Physics, Mechanics, Design, Reliability, Packaging*. [New York]: Springer Science Business Media LLC, 2007.

[41] M. Biron and ScienceDirect (Online service), *Thermoplastics and thermoplastic composites technical information for plastics users*. Oxford :: Butterworth-Heinemann,, 2007.

[42] J. Brydson, *Plastics materials*, 7th ed. Oxford ;;Boston: Butterworth-Heinemann, 1999.

[43] B. Cappella and G. Dietler, “Force-distance curves by atomic force microscopy,” *Surface Science Reports*, vol. 34, no. 1-3, pp. 1-104, 1999.

[44] Y. Gan, “Invited Review Article: A review of techniques for attaching micro- and nanoparticles to a probe’s tip for surface force and near-field optical measurements,” *Review of Scientific Instruments*, vol. 78, no. 8, p. 081101, 2007.

[45] Digital Instruments Veeco Metrology Group, “Attaching Particles to AFM Cantilevers.” Digital Instruments, 2001.

[46] J. K. Eve, N. Patel, S. Y. Luk, S. J. Ebbens, and C. J. Roberts, “A study of single drug particle adhesion interactions using atomic force microscopy,” *International Journal of Pharmaceutics*, vol. 238, no. 1-2, pp. 17-27, May. 2002.

[47] E. Bonaccurso, M. Kappl, and H.-J. Butt, “Hydrodynamic Force Measurements: Boundary Slip of Water on Hydrophilic Surfaces and Electrokinetic Effects,” *Physical Review Letters*, vol. 88, no. 7, Feb. 2002.

[48] O. Sqalli, I. Utke, P. Hoffmann, and F. Marquis-Weible, “Gold elliptical nanoantennas as probes for near field optical microscopy,” *Journal of Applied Physics*, vol. 92, no. 2, p. 1078, 2002.

[49] I. U. Vakarelski and K. Higashitani, “Single-Nanoparticle-Terminated Tips for Scanning Probe Microscopy,” *Langmuir*, vol. 22, no. 7, pp. 2931-2934, Mar. 2006.

[50] H.-J. Butt, B. Cappella, and M. Kappl, “Force measurements with the atomic force microscope: Technique, interpretation and applications,” *Surface Science Reports*, vol. 59, no. 1-6, pp. 1-152, Oct. 2005.

[51] J. Ralston, I. Larson, M. W. Rutland, A. A. Feiler, and M. Kleijn, “Atomic force microscopy and direct surface force measurements (IUPAC Technical Report),” *Pure and Applied Chemistry*, vol. 77, no. 12, pp. 2149-2170, 2005.

[52] G. Willing, T. Ibrahim, F. Etzler, and R. Neuman, “New Approach to the Study of Particle–Surface Adhesion Using Atomic Force Microscopy,” *Journal of Colloid and Interface Science*, vol. 226, no. 1, pp. 185-188, Jun. 2000.

[53] D. M. Schaefer and J. Gomez, “Atomic Force Microscope Techniques for Adhesion Measurements,” *The Journal of Adhesion*, vol. 74, no. 1, pp. 341-359, Dec. 2000.

[54] M. A. Lantz et al., “Quantitative Measurement of Short-Range Chemical Bonding Forces,” *Science*, vol. 291, no. 5513, pp. 2580-2583, Mar. 2001.

[55] A. Schirmeisen, D. Weiner, and H. Fuchs, “Measurements of metal-polymer adhesion properties with dynamic force spectroscopy,” *Surface Science*, vol. 545, no. 3, pp. 155-162, Nov. 2003.

[56] C. K. Y. Wong, Hongwei Gu, Bing Xu, and M. M. F. Yuen, “A new approach in measuring Cu-EMC adhesion strength by AFM [electronics packaging applications],” in *Electronic Components and Technology Conference, 2004. Proceedings. 54th*, 2004, vol. 1, pp. 491-495 Vol.1.

[57] J. Han, J. Yeom, G. Mensing, D. Joe, R. I. Masel, and M. A. Shannon, “Surface energy approach and AFM verification of the (CF)n treated surface effect and its correlation with adhesion reduction in microvalves,” *Journal of Micromechanics and Microengineering*, vol. 19, no. 8, p. 085017, Aug. 2009.

[58] C. Harper, *Modern plastics handbook*. New York: McGraw-Hill, 2000.

[59] G. Hearn and J. Ballard, “The use of electrostatic techniques for the identification and sorting of waste packaging materials,” *Resources, Conservation and Recycling*, vol. 44, no. 1, pp. 91-98, Apr. 2005.

[60] A. F. Diaz and R. M. Felix-Navarro, “A semi-quantitative tribo-electric series for polymeric materials: the influence of chemical structure and properties,” *Journal of Electrostatics*, vol. 62, no. 4, pp. 277-290, Nov. 2004.

[61] N. Eustathopoulos, N. Sobczak, A. Passerone, and K. Nogi, “Measurement of contact angle and work of adhesion at high temperature,” *Journal of Materials Science*, vol. 40, no. 9-10, pp. 2271-2280, May. 2005.

[62] B. Duncan, R. Mera, D. Leatherdale, M. Taylor, and R. Musgrave, “Techniques for characterising the wetting, coating and spreading of adhesives on surfaces.” NPL, Mar-2005.

[63] M. Wouters and B. Ruiter, “Contact-angle development of polymer melts,” *Progress in Organic Coatings*, vol. 48, no. 2-4, pp. 207-213, Dec. 2003.

[64] J. A. DeVore, “Practical quantitative solderability testing,” in *Proceedings of the IEEE National Aerospace and Electronics Conference*, Dayton, OH, USA, pp. 2027-2034.

[65] J. Y. Park, C. S. Kang, and J. P. Jung, “The analysis of the withdrawal force curve of the wetting curve using 63Sn-37Pb and 96.5Sn-3.5Ag eutectic solders,” *Journal of Electronic Materials*, vol. 28, no. 11, pp. 1256-1262, Nov. 1999.

[66] K. Grundke, P. Uhlmann, T. Gietzelt, B. Redlich, and H.-J. Jacobasch, “Studies on the wetting behaviour of polymer melts on solid surfaces using the Wilhelmy balance method,” *Colloids and Surfaces A: Physicochemical and Engineering Aspects*, vol. 116, no. 1-2, pp. 93-104, Sep. 1996.

[67] D. Yang, Z. Xu, C. Liu, and L. Wang, “Experimental study on the surface characteristics of polymer melts,” *Colloids and Surfaces A: Physicochemical and Engineering Aspects*, vol. 367, no. 1-3, pp. 174-180, Sep. 2010.

[68] B. Sauer and N. Dipaolo, “Surface tension and dynamic wetting on polymers using the Wihelmy method: Applications to high molecular weights and elevated temperatures,” *Journal of Colloid and Interface Science*, vol. 144, no. 2, pp. 527-537, Jul. 1991.

[69] N. Lee, Y.-K. Kim, and S. Kang, “Temperature dependence of anti-adhesion between a stamper with sub-micron patterns and the polymer in nano-moulding processes,” *Journal of Physics D: Applied Physics*, vol. 37, no. 12, pp. 1624-1629, Jun. 2004.

[70] M. Imachi, “Hot-melt adhesion and wettability of polyethylene/metal in the vicinity of the metal melting point,” *Journal of Polymer Science: Polymer Letters Edition*, vol. 26, no. 3, pp. 129-133, Mar. 1988.

[71] M. Chen, X. Zhang, Q. Lei, and J. Fu, “Finite element analysis of forming of sheet metal blank in manufacturing metal/polymer macro-composite components via injection moulding,” *International Journal of Machine Tools and Manufacture*, vol. 42, no. 3, pp. 375-383, Feb. 2002.

[72] H. Erbil, *Surface chemistry of solid and liquid interfaces*. Oxford UK ;;Malden MA: Blackwell Pub., 2006.

[73] B. Cherry, *Polymer surfaces*. Cambridge [Eng.] ;;New York: Cambridge University Press, 1981.

[74] E. N. Ito, M. M. Ueki, R. E. S. Bretas, and E. Hage Junior, “Interfacial tension of PBT/SAN blends by the drop retraction method,” *Materials Research*, vol. 11, no. 2, Jun. 2008.

[75] X. Shen, “Microplastic embossing process: experimental and theoretical characterizations,” *Sensors and Actuators A: Physical*, vol. 97-98, no. 1-2, pp. 428-433, Apr. 2002.

[76] E. Taghizadeh, G. Naderi, and C. Dubois, “Rheological and morphological properties of PA6/ECO nanocomposites,” *Rheologica Acta*, vol. 49, no. 10, pp. 1015-1027, Aug. 2010.

[77] B. Duncan and L. Crocker, “Review of Tests for Adhesion Strength.” NPL Report MATC(A)67, Dec-2001.

[78] P. Shah, “Adhesion of Injection Molded PVC to Silane Primed Steel,” University of Cincinnati, 2005.

[79] D. Berry and A. Namkanisorn, “Fracture Toughness of a Silane Coupled Polymer-Metal Interface: Silane Concentration Effects,” *The Journal of Adhesion*, vol. 81, no. 3-4, pp. 347-370, Mar. 2005.

[80] C. Yue, H. Looi, and M. Quek, “Assessment of fibre-matrix adhesion and interfacial properties using the pull-out test,” *International Journal of Adhesion and Adhesives*, vol. 15, no. 2, pp. 73-80, Apr. 1995.

[81] J. R. Wood and G. Marom, “Determining the interfacial shear strength in the presence of transcrystallinity in composites by the ‘single-fibre microcomposite compressive fragmentation test’,” *Applied Composite Materials*, vol. 4, no. 4, pp. 197-207, Jul. 1997.

[82] F. J. Boerio and P. Shah, “Adhesion of Injection Molded PVC to Steel Substrates,” *The Journal of Adhesion*, vol. 81, no. 6, pp. 645-675, Jun. 2005.

[83] M. Honkanen, M. Hoikkanen, M. Vippola, J. Vuorinen, and T. Lepistö, “Metal–Plastic Adhesion in Injection-Molded Hybrids,” *Journal of Adhesion Science and Technology*, vol. 23, no. 13, pp. 1747-1761, Sep. 2009.

[84] T. Zhil'tsova, V. Neto, A. Fonseca, and M. Oliveira, "Numerical Simulation of a PBT Component with Molded-in Metal Insert," presented at the PMI 2008, University College Ghent, Belgium, 2008.

[85] R. Chang, Y. Peng, D. Hsu, and W. Yang, "Three-dimensional insert molding simulation in injection molding," presented at the Antec 2004, Chicago, 2004, vol. 1, pp. 496-500.

[86] M. Thornagel, *Enhanced 3D Injection Molding Simulation by Implementing Applied Crystallization Models*. Wiley-VCH Verlag GmbH & Co., 2007.

[87] P. P. Parlevliet, H. E. N. Bersee, and A. Beukers, "Residual stresses in thermoplastic composites—A study of the literature—Part I: Formation of residual stresses," *Composites Part A: Applied Science and Manufacturing*, vol. 37, no. 11, pp. 1847-1857, Nov. 2006.

[88] R. A. Malloy, *Plastic part design for injection molding: an introduction*. Hanser Verlag, 1994.

[89] K.-S. Kim, H. Hahn, and R. Croman, "The Effect of Cooling Rate on Residual Stress in a Thermoplastic Composite," *Journal of Composites Technology and Research*, vol. 11, no. 2, p. 47, 1989.

[90] L. DiLandro and M. Pegoraro, "Evaluation of residual stresses and adhesion in polymer composites," *Composites Part A: Applied Science and Manufacturing*, vol. 27, no. 9, pp. 847-853, 1996.

12 Appendix-1

Weld Line

A weld line is formed when two flow fronts meet. Moldflow simulations can show the probable locations of the weld lines. Unlike the Moldflow output for 2D mesh, weld lines cannot be mapped for 3D mesh. However, the analysis of the fill time data can give a good idea of the location of the weld line. Fig.I (a-d) show the filling of the mould leading to the formation of the weld line. It is clear that the weld line is formed where the two melt flow fronts come in contact with each other after flowing around the insert. Similar results were observed for all the materials at all the insert temperatures (room temperature, 60, 80, 100, 120°C). The pink line in Fig I (d) is the approximate location of the weld line for the pull test samples.

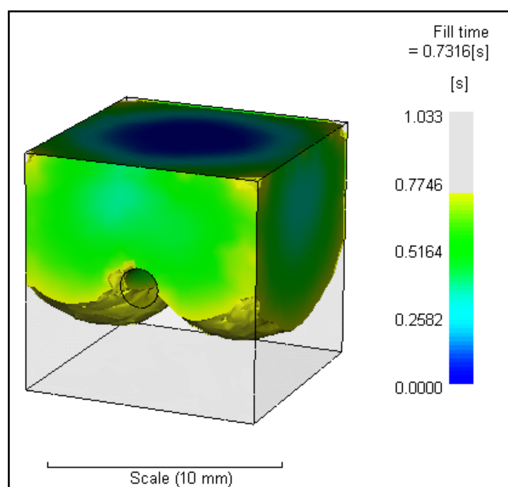

(a)

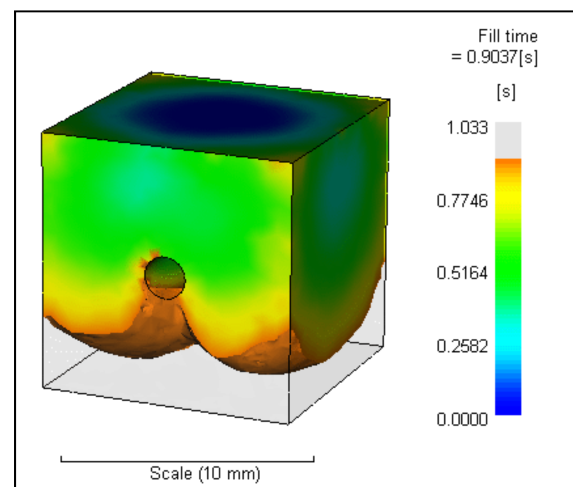

(b)

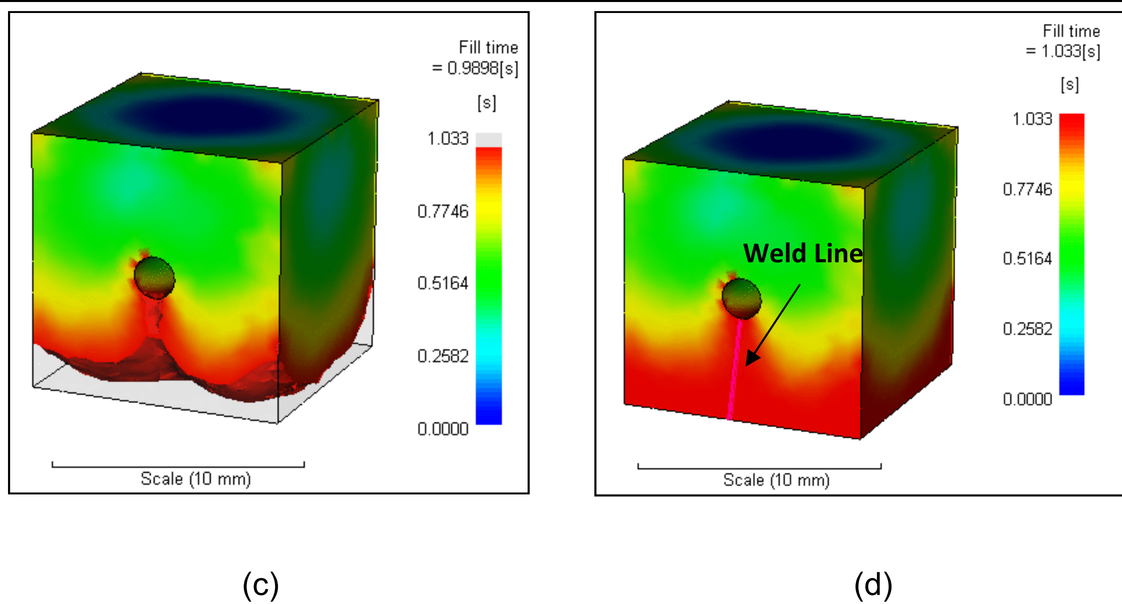

(c) (d)

Figure XCI: Formation of weld line for PA 6 with insert at room temperature

Air Trap

An air trap is an air or gas bubble that has been trapped by converging flow fronts or trapped against the cavity wall. Air traps are often prevented by changing the gate location or part thickness. Moldflow simulations predict the possible locations of air traps. However, it must be noted that the results of actual moulding can vary significantly on account of the mould parting line or vents. Fig. II shows the Moldflow output for air traps. The results for all the simulations for all insert temperatures (room temperature, 60, 80, 100, 120°C) were similar. It must be noted that none of the air traps indicated by Moldflow were observed during any of the pull test sample mouldings.

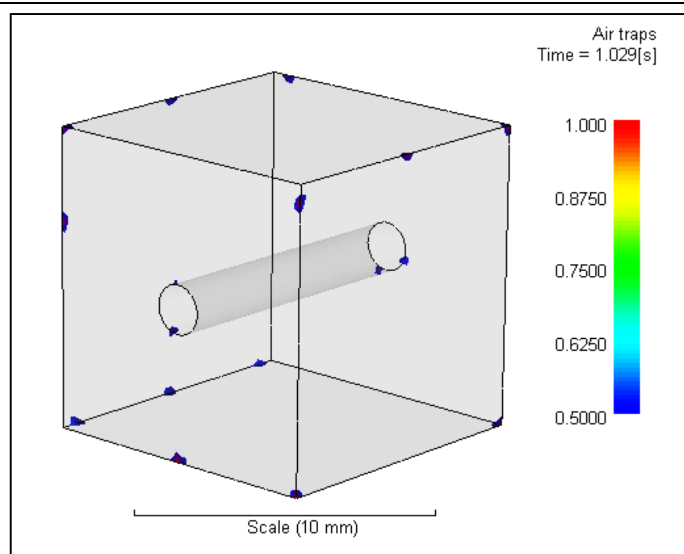

Figure II: Probable air traps (shaded blue areas) for PBT with insert at 100°C

13 Appendix – 2

Content removed due to copyright